A novel co-culture model of human bronchial epithelial cells and *Pseudomonas aeruginosa* biofilms to mimic chronic lung infections in cystic fibrosis

Dissertation

zur Erlangung des Grades

des Doktors der Naturwissenschaften

der Naturwissenschaftlich-Technischen Fakultät

der Universität des Saarlandes

von

Jenny Juntke

Saarbrücken

2018

Tag des Kolloquiums: 08. April 2019

Dekan: Prof. Dr. Guido Kickelbick

Berichterstatter: Prof. Dr. Claus-Michael Lehr

        Prof. Dr. Thorsten Lehr

Vorsitz: Prof. Dr. Marc Schneider

Akad. Mitarbeiter: Dr. Jessica Hoppstädter

Die vorliegende Arbeit entstand im Zeitraum

von April 2013 bis November 2016

unter Betreuung von Herrn Prof. Dr. Claus-Michael Lehr

am Lehrstuhl für Biopharmazie und Pharmazeutische Technologie

an der Universität des Saarlandes

und am Helmholtz-Institut für Pharmazeutische Forschung Saarland.

Für meine Familie

"When you are face to face with a difficulty,
you are up against a discovery."

I. Table of contents

II. Short Summary

Cystic fibrosis is a genetic disease, which manifests mainly in the lungs of the affected patients. Despite early, aggressive antibiotic treatment the patients sooner or later develop chronic bacterial lung infections.

In vitro models can be useful tools in terms of getting a better understanding of this disease. Furthermore, they can be advantageous to evaluate safety and efficacy of novel drugs and drug delivery systems against the pathogens, the most prominent one being *Pseudomonas aeruginosa*.

Aim of this work was to development a model of human bronchial epithelial cells in co-culture with *P. aeruginosa* biofilms in order to mimic chronic lung infections as they occur in cystic fibrosis.

The here used human cell line CFBE41o- was characterized thoroughly for morphology, barrier properties, permeability and mucus production. Since the cell line does not produce mucus, which however plays a major role in the development of chronic CF infections, the application of external human mucus was successfully implied.

Since direct infection with *P. aeruginosa* and biofilm development on the human cells did not lead to a stable model, the application of a preformed biofilm was utilized.

This model was subsequently used to evaluate safety and efficacy of antibiotic-loaded nanoparticles against *P. aeruginosa*. These particles where nebulized on the co-culture and proved to be efficient not only against planktonic but also against the much more resistant biofilm grown bacteria.

III.   Kurzzusammenfassung

Die angeborene Krankheit Mukoviszidose macht sich vor allem in der Lunge der betroffenen Patienten bemerkbar. Trotz frühzeitiger, aggressiver Antibiotikabehandlung leiden die Patienten irgendwann an einer chronischen Lungenentzündung.

In vitro Modelle sind äußerst hilfreich um diese Krankheiten besser zu verstehen. Sie können außerdem dazu genutzt werden neue Arzneistoffe und Wirkstoffträger auf ihre Sicherheit und Wirksamkeit gegen Problemkeime zu untersuchen, allen voran sei hier *Pseudomonas aeruginosa* genannt.

Ziel dieser Arbeit war es ein solches Modell, bestehend aus humanen Bronchialepithelzellen in Co-Kultur mit *P. aeruginosa* Biofilmen, welches die chronische Lungenentzündung bei Mukoviszidose widerspiegelt, zu entwickeln.

Die verwendeten Zellen wurden eingehend charakterisiert. Da sie keinen Mukus produzieren und dieser eine wichtige Rolle bei der Manifestation der chronischen Lungenentzündung spielt, wurde externer humaner Mukus für das Modell verwendet.

Eine direkte Infektion der Zellen mit *P. aeruginosa* und anschließender Biofilmentwicklung, führte zum vorzeitigen Tod der humanen Zellen. Daher wurde ein vorgeformter Biofilm auf die Zellen aufgebracht, um ein stabile Co-Kultur zu erhalten.

Dieses Modell wurde nun genutzt um die Sicherheit und Effektivität antibiotika-beladener Nanopartikel gegen *P. aeruginosa* zu testen. Die auf die Co-Kultur vernebelten Partikel erwiesen sich sowohl gegen planktonische als auch gegen im Biofilm gewachsenen Bakterien als äußerst wirksam.

1 Introduction

1.1 Cystic fibrosis and how it effects the respiratory tract

1.1.1 Genetic backround

More than 80,000 people worldwide are affected by the genetic disease cystic fibrosis (CF) [1]. It can be considered as the severest autosomal recessive disorder in Caucasians with an incidence of about one in 3500 live births. CF is also found in other ethnic groups but to a much lower extent [2, 3]. Despite huge improvements in disease management and treatment, life expectancy is still below 50 years [4].

CF was first described in 1938 [5] but it took over half a century until the responsible gene was identified in 1989 [6]. Mutations in this gene result in malfunction of the cystic fibrosis transmembrane conductance regulator (CFTR) protein. The CFTR is a cAMP-regulated chloride and bicarbonate ion channel [7, 8]. It can be found in the apical plasma membrane of different epithelial cells in the body. In addition, the CFTR regulates other ion channels and thus, has a crucial role in fluid homeostasis. Today around 2,000 different mutations have been identified since the gene was first discovered [7]. However, just a small fraction of these mutations are accountable for the clinical symptoms of CF [8]. The known mutations can be categorized in functional classes, whereas each class marks mutations that affect the protein synthesis or function at different stages [7, 9]. Today a distinction between seven different classes is made. Mutations belonging to class I-III result in defective synthesis, defective maturation and processing or blocked regulation of the CFTR, respectively [9, 10]. Mutations found in the classes IV, V and VI are responsible for decreased conductance, decreased abundance or increased turnover of the CFTR, correspondingly [9]. In light of gene therapy a new class VII was added to the system by De Boeck and Amaral [1]. Here mutations of class I that per se cannot be rescued with gene therapy (e.g., large deletions) are categorized [1]. However, since this subdivision approach of class I would require precise knowledge of the molecular pathology it's discussed controversial [11, 12]. Nonetheless, the classes I-III and the new class VII are associated with severe disease and classic phenotypes of CF [9]. Gene therapy options for patients with such mutations are very limited to none. Thus, class I-III and VII should be closely related in any kind of system [12, 13].

The most common mutation occurring in almost 90% of CF cases is F508del [7]. It belongs to category II and results in a misfolding of the protein. The immature mutant

is retained in the endoplasmatic reticulum and degraded prior to reaching the apical cell surface [1]. This in turn severely reduces the CFTR function and leads to the typical CF hallmarks.

1.1.2   Hallmarks of cystic fibrosis

Cystic fibrosis is a multi-organ disease. The lacking CFTR activity causes ion, pH, and fluid imbalances. The dilatation of exocrine glands and there abnormally viscous mucosal secretions lead to obstruction in the pancreatic ducts (exocrine pancreatic insufficiency results in fat maldigestion), intestine (e.g., meconium ileus, fatal if left untreated) and bile canaliculi (leading to hepatic damage). Male patients are often infertile [2, 14, 15]. In addition secondary diseases like diabetes mellitus, distal intestinal obstruction syndrome, and CF-related bone disease (e.g., osteoporosis) can manifest [2].

However, the thick and sticky secretions (i.e., mucus) obstructing the airways are the major hallmark of CF. The accumulating mucus offers good growth conditions for bacteria and thus, leads to persistent and recurrent lung infections, the major cause for morbidity and mortality in patients [16, 17].

Usually, in the lungs of healthy individuals inhaled pathogens and particles get entrapped in the pulmonary mucus secreted by goblet cells [18, 19]. Another secretory cell type contributing to the respiratory lining fluid (mucus) are the club cells (formerly known as Clara cells). These non-ciliated cells secrete a number of anti-inflammatory and immunomodulatory substances (e.g., the club cell secretory protein). Furthermore, they have a high xenobiotic metabolism, and a regenerative role as progenitor cells for ciliated cells and themselves [19].

These two cell types (i.e., goblet and club cells) are ubiquitous in the epithelial surface of the lung. The mucus secreted by them gets subsequently cleared from the lungs by cilia-generated forces. This process, also called mucociliary clearance (MCC) is the primary defense mechanism protecting our airways. An important component of this innate defense mechanism is the airway surface liquid (ASL). It consists of two layers: the already mentioned mucus layer on top of the cilia (varying in height) and the periciliary liquid layer (PCL), which has roughly the height of the outstretched cilia [20, 21]. The PCL can be found in the mucus-free area at the epithelial cell surface. It has a lower viscosity than the mucus, thus allowing for rapid beating of the enclosed cilia.

Furthermore, the PCL keeps the mucus layer at distance from the underlying epithelial cells [20, 21].

In addition, the ASL contains antibacterial substances (e.g., lysozyme), cells of the immune system (e.g., macrophages), signalling molecules, and cytokines [20]. The CFTR facilitates ASL. The chloride ions secreted by the CFTR draw water from the epithelial cells and therefore hydrated the PCL and mucus. In CF-lung the hydration of the ASL is altered resulting in viscous, "dehydrated" airway mucus. Also the PCL is less hydrated and has a depleted volume, which in turn impedes cilia beating, compresses them and eventually stops mucus clearance completely [21]. The now resulting immobile mucus offers perfect conditions for inflammation and bacterial infection, leading to chronic lung disease typical for CF [18]. In addition, several studies imply that the excessive pulmonary inflammatory responses seen in CF patients might be related to a defect in the adaptive immune responses [22]. The differences of ASL composition in healthy and CF lung are shown in Figure 1.1.
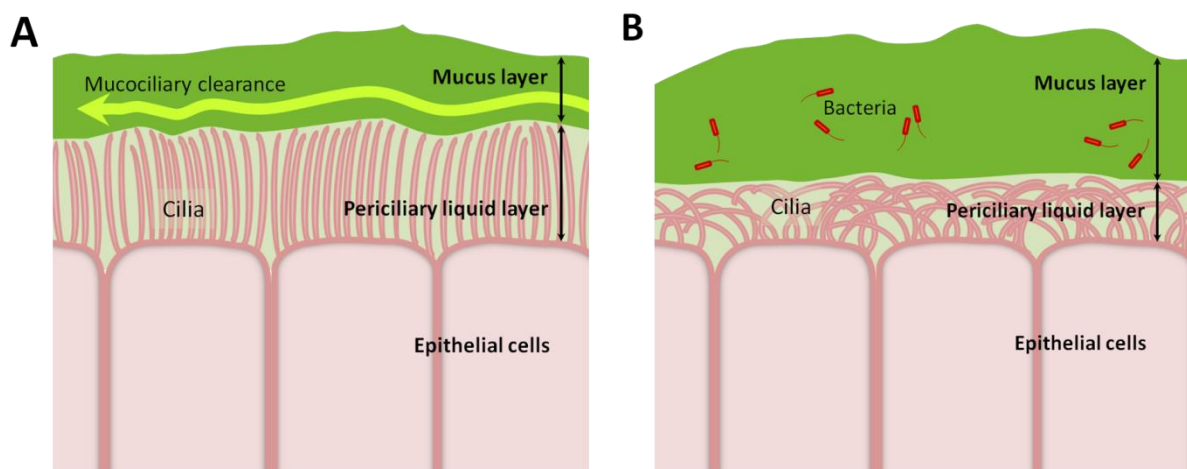
Figure 1.1: Airway surface liquid composition in healthy and CF lung. In the healthy lung (**A**) the cilia can beat freely in the periciliary liquid layer (PCL), and thus clear inhaled particles and pathogens from the lungs (mucociliary clearance, MCC). In the CF lung (**B**) the mucus layer is less hydrated and therefore more viscous. Also, the PCL has a higher viscosity and ciliary beating is inhibited. The MCC is coming to a stop. Inhaled pathogens cannot be cleared from the lungs and the accumulating mucus offers good growth conditions for them. This leads to the chronic colonization of the lungs with bacteria.

1.1.3   Lung infections in cystic fibrosis

The infections occurring in the airways of CF patients are polymicrobial and complex [23, 24]. Characteristic pathogens found in the lungs of CF patients are *Pseudomonas aeruginosa*, *Burkholderia cepacia complex*, *Staphylococcus aureus*, *Stenotrophomonas maltophilia*, *Achromobacter xylosoxidans*, *Haemophilus influenza* and nontuberculous mycobacteria. Interestingly, the microbiota changes in the lifetime of a CF patient (see Figure 1.2) [24, 25]. Typically, *H. influenza* and *S. aureus* are found in the lungs of young children. The increasing number of methicillin-resistant Staphylococcus aureus (MRSA) infections can be explained by the rising number of hospitalizations throughout the life of CF patients since the infection with MRSA is primarily healthcare associated [25].
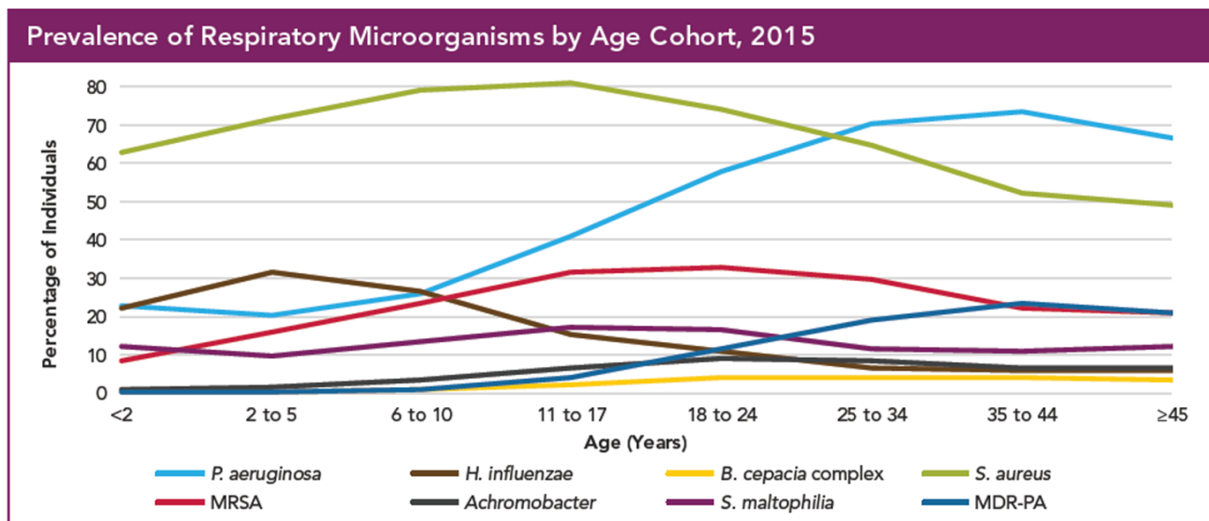
Figure 1.2: Prevalence of respiratory microorganisms by age. Prevalence of different pathogens changes during the lifetime of a CF patient. While in children *S. aureus* is most prominent, *P. aeruginosa* is the major microorganism in adult patients. Reprinted with permission of [25].

However, incidence of *S. aureus* and MRSA decline later in life and infections with the facultative anaerobe Gram-negative pathogen *P. aeruginosa* become more prominent in adolescence. More than 70% of adult CF patients are chronically infected with this pathogen [26]. The occurrence of multidrug-resistant *P. aeruginosa* (MDR-PA) infection is most prominent in older adolescents and adults with CF. These findings are most likely related to the cumulative exposure to antibiotics of those patients. However, the clinical significance of this drug resistance is unclear [25]. The main reason current

therapies against bacterial infection in CF patients fail, is *P. aeruginosa'*s ability to build antibiotic-resistant biofilms [27, 28].

1.1.4   Biofilm development

P. aeruginosa is one of the most extensively studied biofilm formers [29], however, our ability to eradicate infections with this pathogen are still insufficient. This is also due to the fact that bacteria living in biofilms can be up to thousand-fold more resistant to antibiotics than their planktonic counterparts [30]. The stages of such a biofilm development are shown in Figure 1.3.

Biofilms are dense microbial aggregates. The bacteria are attached to a surface or each other and are surrounded by a self-produced matrix of highly hydrated extracellular polymeric substances (EPS) [31, 32]. This matrix is primarily composed of exopolysaccarides, proteins, extracellular DNA (eDNA), lipids and the main component water [32]. The EPS matrix has various functions in a biofilm. It allows the adhesion of the biofilm to a surface (i.e., biotic or abiotic) and enables the aggregation of the bacteria to each other. It is the structural element determining the mechanical stability and architecture of the biofilm. The EPS maintains a hydrated microenvironment around the bacteria even allowing survival in water-deficient surroundings. Though the sorption of organic and inorganic compounds the EPS also serves as a nutrient source for the bacteria residing in it [32]. The eDNA allows genetic information to be exchanged between biofilm cells via horizontal gene transfer. The EPS is not a solid structure. Proteins (i.e., enzymes) in the EPS can degrade parts of the structural EPS and thus allowing cell release from the biofilm. In the light of treating biofilm infections, the function of the EPS as a protective barrier seems most important. It not only serves as protection from specific and nonspecific host defence mechanisms during an infection, the EPS also allows for more tolerance to numerous antimicrobial agents (e.g., antibiotics, disinfectants) [32, 33]. This barrier represented by the EPS can also lead to low diffusion rates or even failing penetration of antibiotics into the biofilm. One example in *P. aeruginosa* biofilms is the interactions of positively charged antibiotics (e.g., Tobramycin) and negatively charged exopolysaccharide (e.g., alginate) resulting in hindered penetration of the antibiotic [34, 35]. Furthermore, the enzymatic activity of the EPS can cause the inactivation of antibiotic drugs [36, 37]. However, the main reason for failure of antibiotic therapies is the changed metabolism of

P. aeruginosa in parts of the biofilm. The low metabolic activity in these subpopulations of the biofilm is due to low oxygen concentration and nutrient supply in the inner parts of the biofilm [34, 38]. These conditions result in slow cell division rates and/or anaerobic growth. This in turn, can limit the efficiency of antibiotics like ß-lactams or aminoglycosides, which target actively dividing bacteria or aerobically growing pathogens, respectively [39].
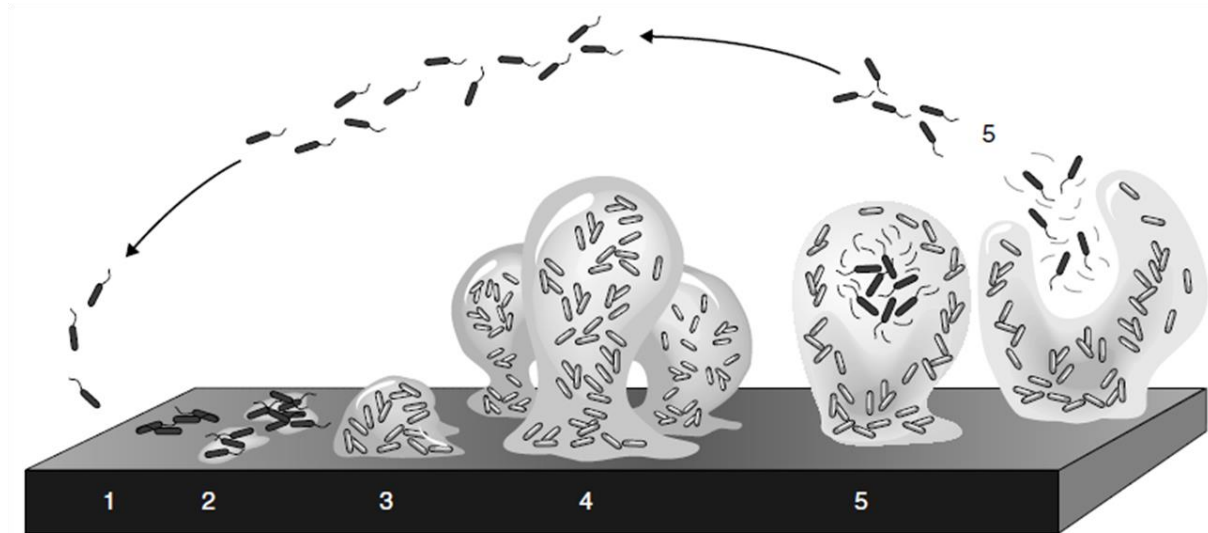
Figure 1.3: Development of a biofilm. At stage 1 the bacteria attach reversibly to a surface. At stage 2 they are already attached irreversibly to the surface and they lose their flagellar motility. This step is mainly mediated by the EPS. In the third stage first biofilm maturation visible by the development of early biofilm architecture is evident. In the subsequent stage (4) the maturation is complete and the biofilm exhibits a complex architecture. In the further development (stage 5) single motile cells (dark bacteria in image) can detach from the biofilm and can start new microcolonies somewhere else. This biofilm development step is also called dispersion stage. Adapted with permission from [40].

The differentiation of a biofilm is related to bacterial cross-talk, the so-called *quorum sensing* (QS). These signals control the expression of several genes in a cell-density-related manner [41]. In addition, the production of several virulence factors (e.g., extracellular enzymes and cellular lysins like rhamnolipids) is coordinated by the QS system. These virulence factors play a major role for the pathogeneses of infections as they protect the bacteria from phagocytes [31, 37].

The best described QS molecules of Gram-negative bacteria like *P. aeruginosa* are the *N*-acyl-*l*-homoserine lactones (AHL). These AHL molecules vary among bacteria, and some bacteria exhibit several AHL molecules. However, they all display the same

essential structure, an acyl chain of variable length. When the AHL molecules bind to their specific receptor (i.e., R receptor) they form an activated complex. This complex in turn binds to specific regulator upstream of the promoter region and subsequently regulates the target gene transcription in a positive or negative way (e.g., upregulation of virulence factor) [42].

The major QS systems in *P. aeruginosa* are the AHL systems encoded by *las* and *rhl* [42, 43]. On top, *P. aeruginosa* also expresses a quinolone signal pathway [44]. This Pseudomonas quinolone signal (PQS) encoded by *pqs* genes offers an additional QS regulatory pathway. These three systems are hierarchically arranged. The *las* system controls the *rhl* system, while the *pqs* system functions as a mediator between the two, but is also regulated from *las* system [43, 45].

All three systems (i.e., *las*, *rhl* and *pqs*) play an important role in the initiation and coordination of biofilm formation. *P. aeruginosas* ability to build such a self-produced matrix can be compromised when the QS system is defective [46, 47], thus, making this a promising target for the treatment of the *P. aeruginosa* biofilm infections [47].

Recently, a fourth QS system was discovered in *P. aeruginosa*, the integrated quorum sensing system (IQS) and its corresponding signal [48]. Via this system the integration of environmental changes and stress into the bacterial QS signaling is possible (e.g., the phosphate depletion that the pathogens often come upon during the establishing of infections [48, 49]). Furthermore, it can regulate the *pqs* system and contributes to bacterial virulence in host animal models (e.g., mouse and zebrafish). However, its role in *P. aeruginosa* infections and biofilm formation are not fully understood yet and need further investigation [48, 50].

1.2 Treatment of cystic fibrosis

Thanks to huge treatment improvements median survival of CF patients has increased steadily. While patients rarely reached the age of 2 in 1938 [5] and in 1989, when the genetic background of the disease was revealed, barely turned 30 years, nowadays the median predicted survival age is almost 48 years [4, 25]. This increase in median survival age results mainly from early disease diagnosis (i.e., newborn screening programs), as well as timely screening for common CF associated comorbidities (e.g., diabetes or distal intestinal obstruction syndrome). In addition, also the establishment of dedicated CF care centers and evidence-based guidelines, and the implementation of therapies in order to improve pulmonary function and nutrition have contributed to that success [4, 51]. The routine care should examine CF patients at the least 4 times per year and determine the pulmonary function and microbiology as well as the nutritional status (e.g., growth and body weight in children or body mass index in adults). In addition, specific blood tests (e.g., for inflammatory markers) should be performed once a year [52].

As mentioned earlier, CF is a disease mostly affecting the lungs. However, since also malnutrition due to pancreatic insufficiency and diabetes are very common in CF patients, an optimized nutritional status in addition to a therapy maintaining pulmonary function are key factors to improve the survival with this disease. Furthermore, a good nutritional status is associated with better pulmonary function and survival in CF patients [51]. In general, a high caloric and fat enriched diet, supplementation of fat-soluble vitamins and the pancreatic enzyme replacement therapy are the standard care to improve the nutritional status. CFTR modulators like the CFTR potentiator ivacaftor (Kalydeco®) can further increase that. Treatment with this modulator can enhance pancreatic function and bodyweight, helps to control diabetes in addition to reducing pulmonary exacerbations and improving respiratory function [51, 52].

For the pulmonary manifestation the enhancement of the mucociliary clearance (MCC), prevention of *P. aeruginosa* infections, suppression of chronic colonization, and treatment of the airway inflammation are the major goals [53]. In order to increase the MCC and clear the lung of the thick mucus, inhaled mucolytics (e.g., recombinant human DNase, dornase alfa, Pulmozyme®) are administered [53, 54]. Also, the

rehydration of the ASL and viscous mucus via inhalation of hypertonic saline, often preceded from a bronchodilator, can improve the MCC and lung function [54-56]. In addition, physiotherapy is an important component of treatment. It usually consist of airway clearance techniques, especially after administering inhaled mucolytic substances, and physical exercise [52].

As shown in Figure 1.2, bacterial burden changes during the life of a CF patient. However, the major pathogen in adult patients is *P. aeruginosa*, the leading cause of morbidity and mortality in CF patients [57, 58]. Once a biofilm is established by these bacteria eradication is almost impossible. Therefore, prevention of *P. aeruginosa* infections is mandatory in CF disease management [53]. With an early aggressive antibiotic treatment, as conducted now in many cystic fibrosis centers around the world, this is trying to be achieved [59, 60]. This treatment usually consists of inhaled antibiotics like tobramycin and colistin, oral and intravenous antibiotics like ciprofloxacin and combinations of aminoglycosides and beta-lactams, respectively [61, 62]. Even though patients receive these preventive and aggressive therapies and usually are monitored on a frequent basis for bacterial infections, the chronic colonization with *P. aeruginosa* is often inevitable once a biofilm is formed [62]. These bacterial biofilms causing the chronic infections show increased tolerance to the innate and adaptive immune system, phagocytosis and the administered antibiotics [53, 63]. Nonetheless, high doses and long-term administration of inhaled and intravenous antibiotics like tobramycin, aztreonam, and colistin in combination with mucolytics and physiotherapy can at least suppress the chronic infection temporarily [64, 65].

The exaggerated inflammatory response occurring in acute and chronic infections are an additional challenge in CF therapy. Here, the use of anti-inflammatory agents (i.e., macrolides like azithromycin or high doses of ibuprofen) can at least decrease respiratory exacerbations and slightly improve pulmonary function [53, 66]. Interestingly, common anti-inflammatory drugs used in asthma care like corticosteroids lack efficacy in CF [64, 67].

All taken together, even though enormous progress has been made in the last decades, treatment of CF and the resulting infection with *P. aeruginosa* is far from optimal. For that reason, novel drugs and treatment approaches are mandatory.

1.3 Novel treatment approaches

1.3.1 Gene therapy

With the discovery of the CFTR gene in 1989 [6], the idea to treat CF right at its genetic basis arose. Due to the fact that only a single gene disorder is involved in CF, no specifics about the patient's genotype are necessary for gene therapy, and treatment via the pulmonary route being noninvasive and comparatively easy, raised hopes in academia, industry, and patients to have gene therapy options before long. But quite soon it became clear, that CF gene therapy was far more complex than initially anticipated [7]. The gene transfer to the lungs proofs to be rather difficult due to effective intra- and extracellular barriers like the nuclear membrane, airway mucus, MCC and immune responses [7, 9]. In addition, the selection of suitable gene transfer agents (i.e., viral or nonviral) is not trivial. Nevertheless, several approaches are currently under investigation and to some extent already in clinical trials [9, 54]. For CFTR modulation it can be distinguished between the potentiators, opening the defective CFTR channel at the cell membrane, and CFTR correctors, which can increase the trafficking of CFTR protein to the cell surface. In addition, read–through agents can help to suppress premature termination codons as they occur in class I mutations [68]. The actual gene therapy, trying to deliver functional DNA to the nucleus of lung cells in order to get a functional CFTR protein transcribed, has also made it to clinical trials. A modest increase in lung function could be noted in the verum group twelve months after the treatment with liposomes loaded with plasmid DNA encoding the CFTR gene (pGM169/GL67A gene–liposome complex) [69]. Furthermore, with Eluforsen (QR-010) an aerosolized RNA oligonucleotide intended to repair CFTR-encoded mRNA in patients with the F508del mutation is in clinical phase 1b [9, 54].

Even though CF therapy via correction of the CFTR gene is still in its infancy, with the recently approved CFTR potentiator, ivacaftor (Kalydeco®), at least a modulation of the defective CFTR protein at the cell surface is possible. Unfortunately, only around 5% of CF patients with mutations belonging to class III and IV benefit from this therapy [68]. However, with lumacaftor/ivacaftor (Orkambi®) and tezacaftor/ivacaftor (Symdeko™) two combinations of a CFTR corrector/potentiator were approved. These combinations are also helpful to patients with mutations belonging to other classes, most importantly the most common CF mutation F508del [54]. But further research is ongoing and

necessary, since still only 55% of the people with CF profit from these CFTR modulators and clinical benefits are modest [68, 70]. At the moment combinations of tezacaftor/ivacaftor and VX-445 or VX659 are in phase three of clinical trials. Similar to Symdeko™ these combinations (CFTR correctors) aim to restore the CFTR function [54]. Furthermore, several other CFTR modulators are in phase two at the moment (e.g., QBW251, a potentiator, just completed phase 2a) [54].

1.3.2 Nanocarriers

Another innovative approach to treat bacterial biofilms in CF is with anti-infectives encapsulated in nanocarriers [71]. These nanostructured carriers can be composed of biocompatible and biodegradable polymers (e.g., PLGA), solid lipids, or a mixture of solid and liquid lipids [72, 73]. Nanocarriers can be administered as inhalation aerosols, and thus minimize the systemic exposure and the related side effects. Furthermore, with this administration route the local drug concentration in the lungs can be increased [59]. Drug loaded nanocarriers could offer a better penetration into the biofilm compared to the free drug due to their size and surface properties. In addition, the nanoformulations can protect their anti-infective cargo until it reaches the site of action and promise a controlled release of the anti-infective agents [36].

1.3.3 Aerodynamic properties of inhaled formulations

In order to achieve a controlled release of the anti-infective cargo, nanoformulations must first be deposited in the lungs by means of inhalation. Thereby, particles can be deposited via five different mechanisms. While interception and electrostatic precipitation are related to particle shape and electrostatic charges, respectively, the other three mechanisms (i.e., inertial impaction, sedimentation and diffusion) are related to particle size [74]. However, not only size and shape, but also density determines the aerodynamic behaviour of inhaled particles. Thus, the aerodynamic diameter combing all three parameters is often referred to. It is defined as the diameter of a spherical particle with a density of 1 g/cm³ having the same aerodynamic behaviour as the characterized particle [75].

Bigger particles (> 1-10 µm) deposit for the most part through impaction and sedimentation, while the smaller particles (< 0,1 µm) get deposited mainly via diffusion in the deep lung. Of note, particles with a size between 100 nm and 1 µm show the

lowest deposition. In view of the fact that particles of that size (0.1 μm-1 μm) are too small for impaction and only show a slow diffusion, they are usually exhaled before they can deposit [74]. However, most nanocarriers are in that critical size range and for that reason not suitable for inhalation as a dry powder. Yet, by formulating a nanosuspension of the nanocarriers and applying them with a nebulizer, droplets of the right size can be achieved (i.e., ~1 μm) [76]. However, nebulization devices are not well accepted from patients due to long administration times, portability of the device, complex cleaning procedures, rather higher costs compared to dry powder devices and need for maintenance. Furthermore, nebulization often has a low efficiency and suffers from poor reproducibility [59, 77]. By means of reformulating the nanocarriers into microparticles (e.g., through spray drying, nanoparticle flocculation), a deposition of the particles can be achieved. Since the reformulated nanoparticles attain an aerodynamic particle size of 1 – 5 μm, which enables them to reach the lung periphery [76].

These microparticles can now be applied via a dry powder inhaler and as a result the drawbacks of nebulization can be circumvented. Such powders for inhalation are typically characterized with the mass median aerodynamic diameter (MMAD) and the corresponding geometric standard deviation (GSD). The MMAD is the cut off size at which 50% off particles are bigger and 50% are smaller than this median value [74]. Furthermore, also the fine particle fraction (FPF) is an important parameter when characterizing pharmaceutical formulations for inhalation. The FPF is defined as the mass fraction of an inhaled dose with an aerodynamic diameter smaller than 5 μm, and thus the amount of powder expected to reach the lung [78]. Typically, these parameters (i.e., MMAD, GSD and FPF) are determined with cascade impactors like the Next Generation Impactor or the Andersen Cascade Impactor [74].

1.3.4 Quorum sensing inhibitors

Targeting the QS system with quorum sensing inhibitors (QSI) has been proposed recently as new anti-virulence strategy. By using such QSIs a reduced production of virulence factors, and thus a possible prevention of biofilm formation or other virulence mechanisms associated with *P. aeruginosa* infections can be accomplished [79, 80]. However, also several useful bacterial species living in the human body use such QS systems. Targeting the QS could therefore lead to unknown side effect. On the other

hand, the *pqs* system is only employed by *P. aeruginosa* and some Burkholderia species making inhibitors for this QS system a promising approach [79, 81]. In order to successfully deliver such QSIs to the lungs they can be encapsulated in nanocarriers [73].

1.3.5 Bacteriophage therapy

Bacteriophages also showed promising results as potential treatment option against antibiotic–resistant bacteria like *P. aeruginosa* [82]. Phages are viruses targeting and infecting only specific bacteria. For that reason, phage therapy can minimize the side effects on the natural flora of the patient [83]. Bacteriophages can replicate themselves at the infection site, infect the pathogenic bacterium and lyse it. In addition, phages are able to evolve, when bacteria develop resistance, and thus are able to regain effectiveness [82-84]. Even though antibacterial effects and their specificity are well known, their safety to mammalian organisms has not been fully investigated yet [82]. Since *in vivo* studies are time consuming, as well as limited due to ethics and costs, the use of suitable animal *in vivo* models and much more important *in vitro* models to evaluate the safety of these novel nanocarrier and phage therapies are necessary.

1.4 *in vivo* models of CF

Animal models have been widely used to study cystic fibrosis and disease pathogenesis. Several animal models have been described such as pig, ferret, rabbit, rat, and mouse [85]. However, not all are equally suited to study all aspects of CF. Only the pig and the ferret show all organ specific disease markers present in human CF patients (e.g., lung infection, impaired growth, intestinal disease, pancreatic and hepatic insufficiency, gallbladder failure) [85]. Even though CFTR-knockout mice were engineered 3 years after the gene was discovered in 1989 [86, 87], these widely used animal models lack the spontaneous lung infection so typical for CF [85]. Thus, alternative mouse models exhibiting inflammation and mucus obstruction were developed. They showed symptoms of CF lung disease like reduced MCC, mucus accumulation, immune responses, a decreased lifespan and the increased susceptibility to bacterial infections [85, 88, 89]. Furthermore, mouse and rat models that can mimic the infected lung were developed by infecting CFTR knock out animals either intravenously or intratracheally with CF relevant pathogens like *P. aeruginosa* [90]. However, infection of the murine

lung can on the one hand easily result in acute sepsis and death of the animal when the administered bioburden is too high. On the other hand also a fast clearance of the pathogen is possible, since rodents are resistant to *P. aeruginosa* lung infections by nature [91-93]. In both cases, a chronic infection cannot be mimicked for more than a few weeks. Yet, by immobilizing the bacteria for example with agar, agarose, seaweed or alginate produced by the pathogen itself, also chronic infections can be simulated [91, 93, 94].

These rodent models helped to study the efficacy and pharmacokinetics of several antimicrobials (e.g., azithromycin) [95]. In addition, they were helpful to gain more insight in the pathogenesis of biofilm development [90].

However, the need for animal models that fully exhibit the human CF phenotype was still unsatisfied. Therefore, CF ferret and pig models were developed in 2008 not least by implementing the knowledge gained from creating the knockout mice in 1992 [90]. These two species show a much closer resemblance to the human lung cell biology than mouse, rat, or rabbit, since they contain submucosal glands (SMG) important for mucus production. These SMG are not present in rabbits and are limited to the trachea region in mouse and rat. The similarity of the ferret and pig models to the human lung phenotype enables a fast translation of novel therapies like gene therapy to the human situation. However, these two animal models are more resource intensive than for example rodent models, and consequently not as widely used [85, 96].

Nonetheless, alternative testing methods for novel therapies should be implemented in research in order to replace, reduce, and refine animal experiments according to the 3R principle of Russell and Burch [97].

1.5   *in vitro* models of CF

In the last three decades extensive efforts have been made to develop *in vitro* models in order to better understand the molecular and cellular pathophysiology of CF and the accompanying infection processes [98]. Since the major problem in CF are the recurring and chronic lung infections caused from the biofilm formation of the pathogens, *in vitro* models of different complexity were established to better understand biofilm development and to overcome the lack of adequate treatment option. Some of these models could already be used to develop and investigate new treatment options for cystic fibrosis. In addition, such *in vitro* models help to reduce animal experiments in

preclinical trials and are therefore suitable tools to effectively implement the 3R principle.

A good overview of exicisting *in vitro* and *in vivo* biofilm models is given in the review by Lebeaux et al. [90] The described models are useful tools to understand the development of such complex bacterial communities of one or even more pathogens (e.g., *P. aeruginosa* and *S. aureus*). Furthermore, they can be used to get a first hint of the efficacy of a new drug.

1.5.1 Biofilm models

Typically, biofilms grown *in vitro* are produced in flow cells, spinning-disk reactors, drip flow reactors or tube biofilm reactors. Even though these models allow for the growth of high density biofilms in continuous and controlled culture conditions, they are limited by the small amount of biofilm produced at the same time in order to use them as new compound screening tools [99]. Two models offering this high throughput option have been developed. One option is to grow the biofilms directly in 96-well microtiter plates [100, 101], or the other to cultivate them on peg lids as in the Calgary biofilm device [102]. These biofilm models can be utilized with different pathogens (e.g., *P. aeruginosa*) and were already described in 1998. They allow a high throughput of test compounds by producing 96 equivalent biofilms and therefore offer the opportunity to choose antibiotics effective against biofilm growing bacteria on a rational basis [102].

However, abiotic grown biofilms (i.e., on glass or plastic like microtiter plates) differ significantly from biofilms grown on living tissue. Such biotic grown biofilms can be over one hundred times more resistant to antibacterial treatments than biofilm grown on an abiotic surface [103]. In addition, abiotic biofilm models do not allow to observe any (patho)physiological changes that might occur in the epithelium during the infection and some antibiotic therapy, such as cellular viability and epithelial barrier function. Thus, *in vitro* models that offer both, a living lung epithelium and a developing biofilm offer huge advantages for the susceptibility testing of novel antibiotic compounds.

1.5.2 Human lung anatomy

The human lung epithelium is generally divided into two anatomical regions: the central lung (conducting airways) and the deep, peripheral lung (alveolar region) [104].

The thin alveolar epithelium has a squamous nature and is to the most part composed of the alveolar type I cells (96%). The cuboidal alveolar type II cells, although greater in number, only make up 3% of the alveolar surface area. The extremely thin morphology and extensive surface area (140 m²) of the peripheral lung epithelium allows for a rapid gas exchange. The apical membranes of the two cell types are connected by tight junctions (TJs, also see chapter 3.3.1) resulting in a tight barrier, the air-blood barrier [104, 105].

Yet, for the treatment of CF, the central lung is the target region of the inhaled antibiotics. The pseudostratified airway epithelium has a much smaller surface area (1-2 m²). Besides transporting air to the deep lung, the most important function of the tight airway epithelium is the mucociliary clearance. The airways are composed of ciliated cells, mucous goblet cells, basal cells, serous cells, brush cells, club cells (former Clara cells) and neuroendrocrine cells [104, 105]. The cellular composition varies at different levels of the airways (starting with nasal epithelium, followed by trachea, large and small bronchi and the terminal bronchioles). However, most of the epithelium is covered by ciliated cells (most abundant cell type), mucus-producing goblet cells and club cells [104]. A mixed primary culture of these human airway epithelial cell types would closely resemble the central lung epithelium *in vitro* [104].

1.5.3 Human airway cell culture models

However, even though human primary cells (e.g., from CF patients) are irreplaceable to understand the underlying mechanisms of CF, they have several drawbacks. Due to the limited availability of tissue, their elaborate handling, risk of contamination, and additionally the terminal differentiation and the limited lifespan of primary cells make the use of cell lines a much more convenient alternative as basis for *in vitro* models (e.g., co-culture models of human epithelial cells and typical CF pathogens) [106]. Transformed airway epithelial cells can overcome these shortcomings and, in comparison to carcinoma cell lines, the original cell type of the transformed cells is known. Starting out with engineering cells that exhibit the typical CF mutations, several cell lines were generated already in 1995 [106] and over 40 cell lines were available for CF research just 10 years later [107]. Even though cell lines can be a result of a carcinomas like the widely used bronchial epithelial cell line Calu-3, typically, the immortalization of airway epithelial cells is achieved through transformation for

example with a simian virus 40 (SV40) based system. One of these cell lines resulting from such a transformation is the CFBE41o- cell line [107]. These cells have a human bronchial epithelial origin and are homozygous for the most common mutation in CF, the ΔF508 mutation. The CFBE41o- cells were systematically characterized and found to be useful for example CF gene transfer studies or as screening tool for alternative treatments [108]. For this reason, they have been used in several studies with CF background (NCBI PubMed database listed 131 studies with these cells in 2018) [109].

While subcultures of primary cells and some of the transformed cell lines may lose certain differentiated features (e.g., ion transport, secretion, formation of tight junctions), a measure to induce differentiation in both primary cells and cell lines, is to grow the cells at an air-liquid interface (ALI) [106]. By culturing the cells on permeable inserts, and thus providing them with medium from the basolateral side and exposing them to air on the apical side, can model the *in vivo* situation as found in the lung much better then submersed cultures (see Figure 1.4 for comparison of culture condition). Epithelial cells grown in that way (i.e., ALI) form polarized cell layers. Furthermore, it allows to measure their epithelial barrier properties (see also chapter 3.3.1) and apply pulmonary drugs in form of aerosols for example with the Pharmaceutical Aerosol Deposition Device On Cell Cultures (PADDOCC) system [106, 110].
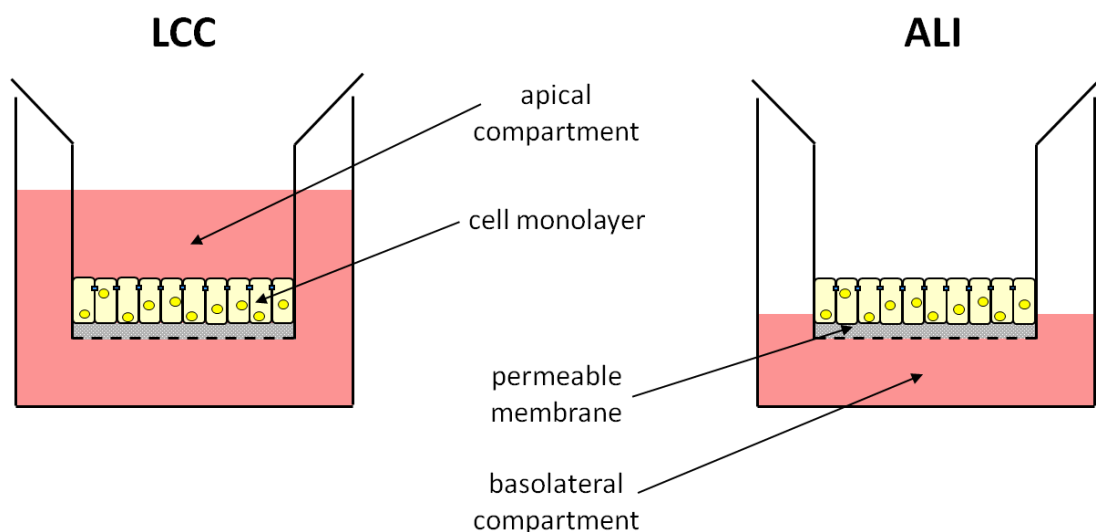
Figure 1.4: Schematic of culture conditions in a Transwell® system. For liquid-covered conditions (LCC) cells are fed with medium from apical and basolateral side. For air-liquid interface (ALI) conditions cells receive medium only through the permeable membrane from the basolateral compartment. They are exposed to air on the apical side.

Alongside primary cells or other cell lines (e.g., Calu-3, A459) the CFBE41o- cells have also been used for co-culture models of human epithelial cells and *P. aeruginosa* biofilms. Such *in-vitro* models have been described previously by several groups [82, 103, 111-113]. Partially, these models were cultivated at air-liquid interface conditions, but in some cases not during the whole experiment [27, 111]. In addition, the rapid bacterial overgrowth of the cultures after the infection with *P. aeruginosa* resulted in a model not viable for more than 8 h [111, 112].

Also, organoids as *in vitro* systems to study the CFTR function might be mentioned here. These advanced three-dimensional (3-D) structures are useful tools for disease modelling and to screen drugs for their CFTR corrective function (e.g., with the help of CRISPR-Cas9) and model regeneration after CFTR repair [85, 114]. In this context the widely used lung adenocarcinoma cell line A549 was exploited. These cells seem rather unsuitable for an *in vitro* co-culture model of CF since they lack barrier properties due to insufficient expression of tight junction proteins and moreover do not produce mucus when grown as monolayers. However, when grown as 3-D aggregate model in a rotating-wall vessel, the cells showed increased expression of tight junction proteins (e.g., occcludin, ZO-1, E-Cadherin) and polarity. Furthermore, the cells produced mucopolysaccharides and antibodies against mucus proteins MUC1 and MUC5A bound with higher affinity, when cells were grown as 3-D aggregates in contrast to cells grown as monolayers [115]. These findings emphasize the importance of not only choosing a suitable cell line but also the right culture conditions for an *in vitro* model.

Nonetheless, the properties of the above described models make them unsuitable for testing aerosolized medicines. However, inhalable formulations are of the utmost importance when treating infections occurring due to CF pathophysiology. *In vitro* models valid to test such formulations for their safety and efficacy are therefore still needed.

2 Aim of this work

Even though *in vitro* models of different complexity mimicking cystic fibrosis can be found in the literature, a model cultivated at an air-liquid interface, which exhibits the typical infection with *P. aeruginosa* biofilms in cystic fibrosis, does not exist yet. A model reflecting this complex situation and at the same time allowing to test new aerosolized pharmaceutical formulations would therefore be of great value.

This thesis was part of the project "cystic Fibrose Delivery" (FiDel). FiDel's aim was to develop and proof the concept of a nano-scaled drug delivery system in order to treat chronic *P. aeruginosa* biofilm infections in cystic fibrosis. Thus, part of this project was the establishment of *in vitro* models of the air-blood barrier of different complexity. These models should then be used to evaluate drug delivery systems, also generated in this project, for their safety and efficacy.

As discussed previously, the reproducibility of such a model would benefit from using cell lines. Therefore, two cell lines, one as model for the healthy bronchial epithelium, and a second one as model cell line for the diseased epithelium were scrutinized. Especially their ability to form a tight barrier at liquid-covered conditions, but more importantly, when grown at an air-liquid interface were inspected. Mucus is a significant non-cellular barrier and could, especially in the case of cystic fibrosis, hinder the effective treatment with drug delivery systems due to increased amounts of thick and sticky mucus. In consequence, the mucus production of both cell lines was examined.

Since the highly viscous mucus is one of the major hallmarks in cystic fibrosis, a mucus layer is an important part of an *in vitro* cystic fibrosis model. Thus, alternative mucus sources were probed in the second part of this work.

In the third part of this thesis the model pathogen *P. aeruginosa* PAO1 was characterized for its ability to build biofilms on abiotic and biotic surfaces like epithelial lung cells and the optimal biofilm growth conditions were evaluated.

With the knowledge gained from these first three chapters, the main aim to establish an *in vitro* model of *P. aeruginosa* biofilms on the apical surface of tight human bronchial epithelial cell monolayers, grown at an air-liquid interface, was pursued. Two different approaches to such an *in vitro* tool were assessed.

In a fifth section of this work the resulting model was used to test the safety and efficacy of aerosolized antibiotic nanocarriers produced in another part of the FiDel project. Readouts like the reduction of bacterial burden, as well as maintenance or restoration of epithelial cell viability and barrier function were used to evaluate the efficacy of the drug delivery systems and the applicability of the *in vitro* co-culture model for such a purpose.

3 Characterization and comparison of two human bronchial epithelial cell lines

The author of the thesis made the following contribution to this chapter:

Planned and performed all cell culture experiments, measured TEER and permeability, prepared cells for confocal analysis, histology and scanning electron microscopy and took the images, analyzed and interpreted all obtain experimental data and wrote the chapter.

3.1 Introduction

Local delivery of antibiotics to the lungs seems the best option to treat chronic infections occurring sooner or later in CF patients. To evaluate novel drugs and drug delivery systems for their safety and efficacy, a rising need for suitable *in vitro* models has evolved in recent years. In addition, implementation of the 3R principle (replacement, reduction, and refinement) in labs all over the world makes such models that reduce the use of animals even more valuable. Even though such models are more robust, offer simplicity, high throughput and better predictions, they need to be thoroughly characterized and later on standardized and validated to use them as tool for drug screening in pharmaceutical industry.

Although primary cells are still considered as gold standard for cell growth *in vitro*, their use is restricted due to unreliable supply, time consuming isolation methods, high variability between donors as well as their limited live span [116]. This makes the use of continuous cell lines even more convenient [117, 118]. The human-derived cell lines A549 (alveolar region), Calu-3 and 16HBE14o- (bronchial region) have already been studied extensively. The latter two offer a bronchial epithelial cell-like phenotype and the ability to develop barrier properties [104]. Since the aim of this work was a co-culture model of epithelial cells and bacteria mimicking chronic infections in CF, the use of the CFBE41o- cell line (human bronchial origin, homozygous for ΔF508 mutation) was also a promising option. To simulate a healthy and CF affected host, Calu-3 and CFBE41o- cells, respectively, were therefore considered for this *in vitro* model. The cells should present appropriate barrier properties so as to withstand the infection with bacteria and be used for drug delivery experiments later on. Also, the production of mucus by the cells seems mandatory, since the accumulation of thick and sticky mucus plays a key role in CF disease and the development of chronic infections with *P. aeruginosa*.

Although Calu-3 cells are already well described in the literature and also several studies regarding the CFBE41o- cells have been published, both cell lines were cultivated again under liquid-covered conditions as well as at the air-liquid interface to be compared. They were further characterized regarding their ability to develop barrier properties by way of measuring transepithelial electrical resistance (TEER), staining of the tight junction (TJ) protein occludin and permeability studies using the paracellular

transported marker sodium fluorescein (NaFluo). Also, the secretion of mucus under the different culture conditions was assessed for both cell lines with acridine orange (AO) and peridoc acid-Schiff/Alcian blue staining (PAS/Alcian blue). In addition, scanning electron microscopy (SEM) images were taken to get more insight into cell morphology and mucus production.

3.2 Material and Methods

3.2.1 Cell culture

CFBE41o- cells were received as a kind gift from Dr. Dieter C. Gruenert (University of California, San Francisco, CA, USA) and passages 4.74 to 4.94 were used for experiments. Cells were cultivated in Minimal Essential Medium (MEM, Gibco™ Thermo Fisher Scientific Inc., Waltham, MA, USA) supplemented with 10% fetal calf serum (FCS, Lonza, Basel, Switzerland), 1% non-essential amino acids (NEAA, Gibco™) and 600 mg/l glucose (Sigma-Aldrich, Munich, Germany) at 5% CO_2 atmosphere, 95% relative humidity, and 37°C in T75 cell culture flasks (Corning, Wiesbaden, Germany). Calu-3 cells (clone HTB-55) were obtained from American Type Culture Collection (ATCC; Rockville, MD, USA) and used from passage 31-51 and cultivated in MEM supplemented with 10% FCS, 1% NEAA and 1% sodium pyruvate (Gibco™, Thermo Fisher Scientific Inc., Waltham, MA, USA) under the same conditions as the CFBE41o- cells. Cells were fed every 2-3 days with fresh medium and passaged weekly to a new T75 flask with a density of $2x10^5$ cells (CFBE41o-) or $2x10^6$ cells (Calu-3). For further experiments both cell lines were seeded with a density of $0.5x10^5$ (CFBE41o-) or $1x10^5$ (Calu-3) into 12 well Transwell® (Corning, Wiesbaden, Germany) plates with a pore size of 0.4 µm and 1.12 cm² growth area per well. For liquid-covered conditions (LCC) medium was set to 500 µl apical and 1500 µl basolateral. To achieve air-liquid interface (ALI) conditions, typically 2-3 days after seeding of the cells, medium was removed from both compartments and only 500 µl medium was added to the basolateral compartment.

To evaluate the influence of seeding density and culture time on mucus production, the CFBE41o- cells were additionally also seeded with a density of $0.25 x10^5$/per insert into a 12 well Transwell® plate, lifted to ALI 2-3 days after seeding and cultivated in that way up to 10 days. Medium was changed 3 times per week in all cases.

3.2.2 Transepithelial electrical resistance (TEER)

To determine the confluence of cell monolayers and tightness of their intercellular junctions, the transepithelial electrical resistance (TEER) can be measured [119]. Cells on Transwell® filters were taken out of the incubator and placed on a heating plate to avoid TEER fluctuations due to temperature change. Medium from cells cultivated at ALI conditions was replenished to 1500 µl basolateral and 500 µl apical and cells were

left to equilibrate for 30 min. Electrical resistance of cell layers was measured with chopstick electrodes connected to an epithelial voltohmmeter (EVOM; World Precision Instruments, Sarasota, FL, USA). TEER was calculated by subtracting the background value of an empty Transwell® containing only medium (110 Ω) and multiplying the result with the growth area of the well (1.12 cm²). Cells showing TEER values >300 Ω·cm² were considered to have barrier properties. After TEER measurement ALI conditions were restored.

3.2.3   Transport studies

Transport studies are a useful tool to measure the permeability of cell monolayers for specific marker molecules and to evaluate their suitability for drug transport studies. The hydrophilic marker sodium fluorescein (NaFluo) is primarily transported via the paracellular route and can therefore be used as an indicator of tightness of the TJs that control this pathway. The calculated parameter in such studies is the apparent permeability coefficient (P_{app}), which describes the percentage of a compound transported over a certain area over time [104]. It can give a hint to the potential bioavailability of the compound *in vivo* [119]. In order to determine the P_{app} (cm/s) as a function of the used culture conditions, Calu-3 and CFBE41o- cells were seeded on Transwell® plates as described in chapter 3.2.1. Two to three days after seeding cells were divided into two groups. They were either further cultivated under LCC or lifted to ALI. To monitor cell growth and determine the day when the cells show barrier properties, TEER values were measured every 2-3 days as described above (see chapter 3.2.2). When cells showed considerable barrier properties (usually on day 10 or 5 after seeding for Calu-3 and CFBE41o- cells, respectively) transport studies were performed according to a previous protocol [120] with small modifications. Briefly, before starting the transport experiment TEER values were measured as specified under 3.2.2. Afterwards, cells were washed twice with 37°C warm Krebs-Ringer Buffer (KRB; NaCl 142.03 mM, KCl 2.95 mM, $K_2HPO_4*3H_2O$ 1.49 mM, HEPES 10.07 mM, D-glucose 4.00 mM, $MgCl_2*6H_2O$ 1.18 mM, $CaCl_2*2H_2O$ 4.22 mM; pH 7.4) and then further incubated with 500 µl apical and 1500 µl basolateral pre-warmed buffer for another 60 min. TEER values were measured again. Buffer was then removed and replaced with 520 µl of NaFluo solution (10 µg/ml in KRB) to the apical compartment (donor), as well as 1700 µl of fresh KRB to the basolateral compartment (acceptor) of

the Transwell®. Directly after adding the marker solution, samples were taken from both compartments (20 µl apical and 200 µl basolateral) and transferred to a 96-well plate. Further samples of 200 µl were taken from the basolateral compartment every 30 min for 3 h and sample volume was replaced each time with 200 µl fresh pre-warmed KRB. During the experiment the Transwell® plates were kept in the incubator at 37°C on a horizontal shaker with constant rotation speed (150 rpm). After the last sampling from the acceptor another sample from the apical compartment (20 µl) was taken to determine the final concentration of the donor. TEER was measured again at the end of the experiment to assure that the integrity of the monolayer was not compromised throughout the course of the experiment. All taken samples were measured with a plate reader (TECAN, infinite M200 pro, Männedorf, Switzerland). Excitation and emission wavelength were set to 480 nm and 530 nm, respectively. The transport properties depending on the setup (LCC ft. ALI) are expressed with different apparent permeability coefficients (P_{app}). This parameter was calculated according to the equation:

$$P_{app} = (\Delta Q / \Delta t) * (1/A * C_0)$$

where, Q, t, A and C_0 are the cumulative amount of drug permeated across the cell monolayer, time of the experiment, surface area of the Transwell® and the initial donor concentration, respectively.

3.2.4 Confocal laser scanning microscopy (CLSM)

To visualize differences in TJ pattern due to culture conditions cells were seeded on Transwell® filters as described in 3.2.1 and cultivated under LCC or at ALI conditions. When cells expressed barrier properties, measured through TEER determination (3.2.2) the medium was removed and cells were fixed with formaldehyde (500 µl apical) for 10 min at room temperature (RT). Fixation was removed and cells washed 3 times with Phosphate buffered saline (PBS, 500 µl). To avoid unspecific binding and permeabilize the samples were blocked for 10 min with a PBS solution containing 1% bovine serum albumin (BSA) and Tween. Solution was removed and the primary antibodies against the TJ protein occludin (mouse anti-occludin, Catalog No 33-1500, Invitrogen, Carlsbad, USA) and against the cytokeratin (rabbit anti-cytokeratin, catalog No Z0622, DAKO,

Santa Clara, USA) were diluted 1:500 in PBS and incubated with the cells at 4°C over night. Primary antibodies were removed and cells washed 3 times with PBS (500 µl) and blocked again with 1% BSA solution in PBS for 10 min at 37°C and subsequently washed once with PBS. Secondary antibodies for occludin (goat anti-mouse Alexa Fluor 633, Catalog No A21050, molecular Probes, Eugene, USA) and cytokeratin (swine anti-rabbit-FITC, Catalog No F 0054, DAKO) were diluted 1:500 in PBS and cells were incubated with secondary antibody for 1 h at 37°C. Cells were then washed once and nuclei stained with propidium iodide (PI, 1:2000 in PBS) for 3 min at RT. Samples were washed 2 times and filters cut from Transwell® inserts, placed on an objective slide and enclosed with a cover slide. Images were taken with a Carl Zeiss Laser scanning system LSM 510 (Zeiss, Jena, Germany). Excitation wavelengths were set to 488 nm and 633 nm for cytokeratin (green) and occluding (red) signal, respectively. Using the 100x oil immersion objective (EC Plan-Neofluar 100x/1.3 Oil M27) images were taken with a 1024×1024 resolution and processed with Fiji software (ImageJ 1.48r, Rasband W., National Institute of Health, USA [121, 122]).

3.2.5   Scanning electron microscopy (SEM)

For scanning electron microscopy (SEM) preparation medium was removed from the cells and cells washed once with PBS. Afterwards they were fixed with a formalin/glutaraldehyde solution for 45 min at RT. Samples were then washed with PBS and de-hydrated with a graded series of ethanol (30-100%). After removing ethanol 100%, hexamethyldisilazane (HMDS, Sigma Aldrich) was added for another 10 min to achieve a complete de-hydration. HMDS was then removed and Transwells® placed under fume hood to allow organic solvent residues to evaporate. Filters were then cut from inserts and mounted on aluminium stubs, which were equipped with a carbon disc. Samples were sputtered with gold (Quorum Q150R ES, Quorum Technologies Ltd, Laughton, UK) and images taken with an EVO HD 15 microscope (acceleration voltage 5kV; Software SmartSEM, Zeiss, Jena, Germany) under vacuum conditions.

3.2.6 Mucus detection with periodic acid-Schiff (PAS) and Alcian blue

In order to visualize the amount of mucus produced by the cell lines depending on the used culture conditions (e.g., LCC or ALI) a PAS/Alcian blue staining for neutral and sour mucins was conducted. Medium was removed and cells washed once with PBS. Alcian blue solution was then pipetted on the cells for 5 min, cells washed thoroughly with water before periodic acid was put on the cells for 10 min. After that step samples were washed again with water and subsequently, cells were treated with Schiff's reagent for another 15 min. Hereafter, cells were washed again and immediately imaged with a light microscope (Vert.A1, Zeiss, Jena, Germany) equipped with a camera (AxioCam ERc5s). The objectives wit magnification of 10x and 20x were used. Due to the staining sour mucosubstances will appear in bright light-blue and neutral polysaccharides and mucopolysaccharides in purple.

3.2.7 Mucus detection with acridine orange (AO)

Another staining useful to detect mucus in particular mucoglycoproteins is with the dye acridine orange (AO) [123]. AO is a dye widely used to stain nucleic acids. A green fluorescence can be observed when it intercalates with DNA, where as an interaction with RNA results in a red fluorescence [124]. This spectral shift can also be observed when AO interacts with other sour cell components, e.g., mucins. Mucus containing cells will therefore appear red. Staining was performed as described in Teubl et al. [125]. Briefly, medium from cells was removed; samples washed once with 100 µl HBSS, and stained with a solution of HBSS containing 80 µg/ml AO (Sigma Aldrich) for 10 min at 37°C. Staining solution was removed, cells washed twice with 100 µl HBSS, and cut from their Transwell® supports. Membranes were placed on objective slides, submerged with FluorSave™ (Merck Millipore, Darmstadt, Germany), and covered with a cover slide. Samples were imaged with a Carl Zeiss Laser scanning system LSM 510 (Zeiss, Jena, Germany) right away. Excitation wavelengths were set to 543 nm for red signal (mucus) and 477 nm for green signal (cytoplasm). Images with a 1024×1024 resolution were taken with the 25x water immersion objective (LCl Plan-Neofluar 25x/0.8 Imm Korr DIC M27) and further analyzed with the Fiji software.

3.2.8 Statistical analysis

Data are presented as mean ± standard error of the mean (SEM) from 2-3 independent experiments. Statistical analysis was performed with the GraphPad Prism 5 software. The change in P_{app} depending on the applied culture condition was compared with a t-test; $p < 0.05$ was considered significant.

3.3 Results and Discussion

3.3.1 Calu-3 and CFBE41o- cells exhibit tight barriers when cultivated under liquid-covered conditions (LCC), but only Calu-3 show barrier properties when grown at the air-liquid interface (ALI)

Epithelial barriers are crucial for human survival, because they separate us from our external surroundings [126, 127] and represent the first cellular barrier that inhaled compounds are confronted with [104]. Tight junctions (TJs) together with adherens junctions, gap junctions and desmosomes form this barrier [126]. TJs were first discovered in 1963 by Farquhar and Palade with electron microscopy [128]. These structures bring neighbouring cell membranes in close contact and result in the formation of a permeability barrier for inhaled toxins or pathogens [129, 130], but also control the flux of water, ions and other macromolecules between the cells. In addition, they maintain epithelial cell polarity [126]. The transmembrane domain of the TJ complex contains a minimum of three different proteins: claudin, occluding and junctional adhesion molecules (JAMs) [127], but also the more recently identified proteins tricellulin and the coxsackie and adenovirus receptor as well as many other proteins are associated with the TJ complex [131, 132].

The cytoplasmic plaque (i.e., scaffolding, cytoskeletal and adaptor proteins) connects the transmembrane proteins to the cytoplasm and function as regulator of adhesion and paracellular permeability. Additionally, it is responsible for signal transmission from the junction to the inner cell, and thus regulates cellular processes such as gene expression and migration [133]. Such peripheral proteins are for example zonula occludens ZO-1, -2, -3 and cingulin [134, 135].

Today hundreds of proteins are known for their association with the TJs [132, 136]. TJs not only regulate the paracellular pathway for molecules of all kind and separate different body compartments from one another [137], but they also take an active part in gene transcription, regulation of cell proliferation and cellular differentiation [138].

In order to analyze the barrier properties of epithelial cells three methods can be applied: visualization of TJs with thin section electron microscopy, measurement of TEER, which gives a number to the tightness of the epithelium, and measuring the permeability of tracer molecules transported only via the paracellular route [119].

For the bronchial cell line Calu-3 it could be shown, that when grown under LCC conditions or at the ALI cells develop barrier properties *in vitro* of >300 Ω*cm² [139]. This number of transepithelial electrical resistance should be reached to use such models for drug transport studies [104].

To evaluate the ability of both cell lines considered for the co-culture model to exhibit barrier properties when grown under different culture conditions (LCC or ALI), the cells were seeded on Transwell® plates as described under 3.2.1. TEER values were then measured every 2-3 days. As expected Calu-3 cells showed considerable barrier function 7 days after seeding (Fig. 3.1) when grown under LCC (512 ± 39 Ω*cm²) or at the ALI (324 ± 20 Ω*cm²). TEER values increased further and barrier properties were highest between day 9 and 12 after seeding, 1208 ± 63 Ω*cm² on day 12 for LCC cultures. Barrier properties for cells grown at the ALI although lower than the LCC cultures still reached with 742 ± 17 Ω*cm² considerable TEER values 12 days after seeding. Therefore, for further experiments (e.g., drug transport studies or infection with *P. aeruginosa)* cells were used between days 9-12 after seeding. After longer culture times TEER values decreased again, as shown in Figure 3.1 with the unfilled symbols (to give a trend preliminary data from 1 experiment was used). Differences in TEER values depending on the culture conditions were already described in a number of studies [139-141] but absolute values differ from lab to lab and have to be determined for the cells at hand.

Figure 3.1: Barrier properties of Calu-3. Cells were cultivated under LCC (red) or at the ALI (blue) conditions. The TEER values were measured every 2-3 days for up to 14 days. Data shown are mean ± SEM (n≥6) from at least two independent experiments. Unfilled symbols are from one experiment and give a trend.

The CFBE41o- cells reached their peak in TEER when grown under LCC already on day 7 after seeding with $1475 \pm 53\ \Omega*cm^2$ (Fig. 3.2.) Afterwards values decreased again but still remained well above $600\ \Omega*cm^2$. In contrast the cells cultivated at the ALI expressed highest barrier properties between day 5 and 6 with $271 \pm 13\ \Omega*cm^2$ on day 5. Later on TEER values fluctuated around $200\ \Omega*cm^2$. Similar to the findings of Ehrhardt et al. [108] the ALI cultures did not reach considerable barrier properties to make them suitable for further experiments (e.g., infection with pathogens).

Of note, the lower TEER values of both Calu-3 and CFBE41o- cells when grown at ALI might to some part be related to stress. In order to measure TEER, cells had to be incubated with culture medium, and after the measurement restored to ALI conditions (see 3.2.2). The mechanical stress related to the medium change (e.g., shear, hydrostatic pressure change) might also be a reason for the lower TEER values observed in cells cultivated at ALI.
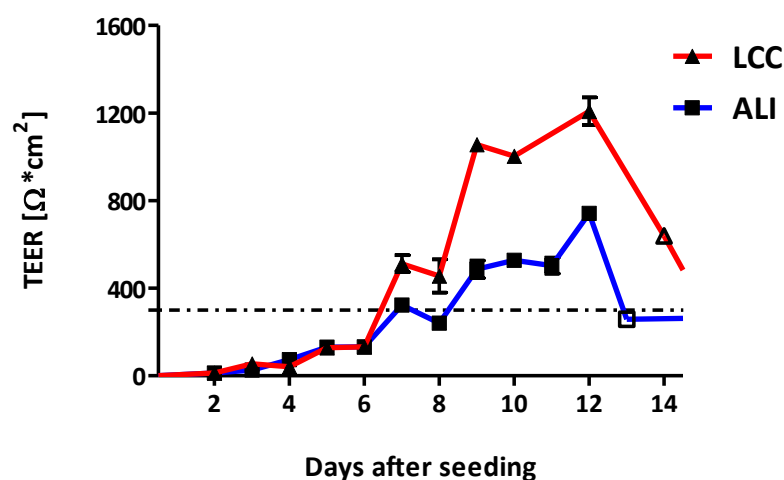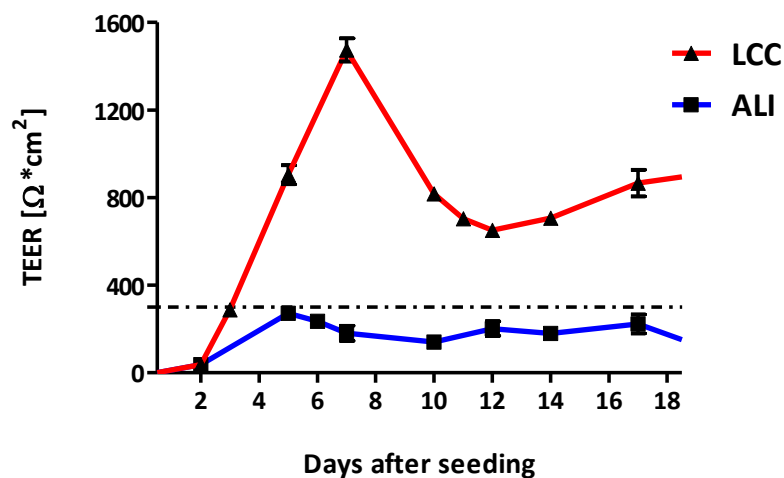

Figure 3.2: Barrier properties of CFBE41o- cells. Cells were cultivated under LCC (red) or at ALI (blue) conditions. The TEER values were measured every 2-3 days for up to 19 days. Data shown are mean ± SEM (n≥8) from at least three independent experiments.

3.3.2 CFBE41o- express a tight pattern of occluding only when cultivated under liquid-covered conditions (LCC)

To find an explanation for the lower TEER values in the ALI cultures a staining of TJ proteins was conducted. Since occludin is a key player in transepithelial electrical barrier function [126] and is nowadays considered as regulator of TJ assembly and function *in vitro* [130, 132], this protein was stained and the expression of the same under different culture conditions (LCC ft. ALI) was compared (Fig. 3.3). The left image in Figure 3.3 shows a tight pattern of the occluding protein surrounding the under LCC cultivated cells (A). In contrast the ALI cultured cells (B) exhibit a rather diffuse pattern, indicating an inhomogeneous distribution of the TJ protein. This could explain the lower measured TEER values in the ALI cultures of the CFBE41o- cells. Similar findings were also made by Ehrhardt et al. [108]. In addition, they also stained other TJ associated proteins (e.g., ZO-1 and claudin-1) and found that also for these proteins the expression profile in the ALI cultures is irregular, whereas the stained TJ proteins in LCC cells show a regular appearance and can explain the higher TEER values measured in these cultures.
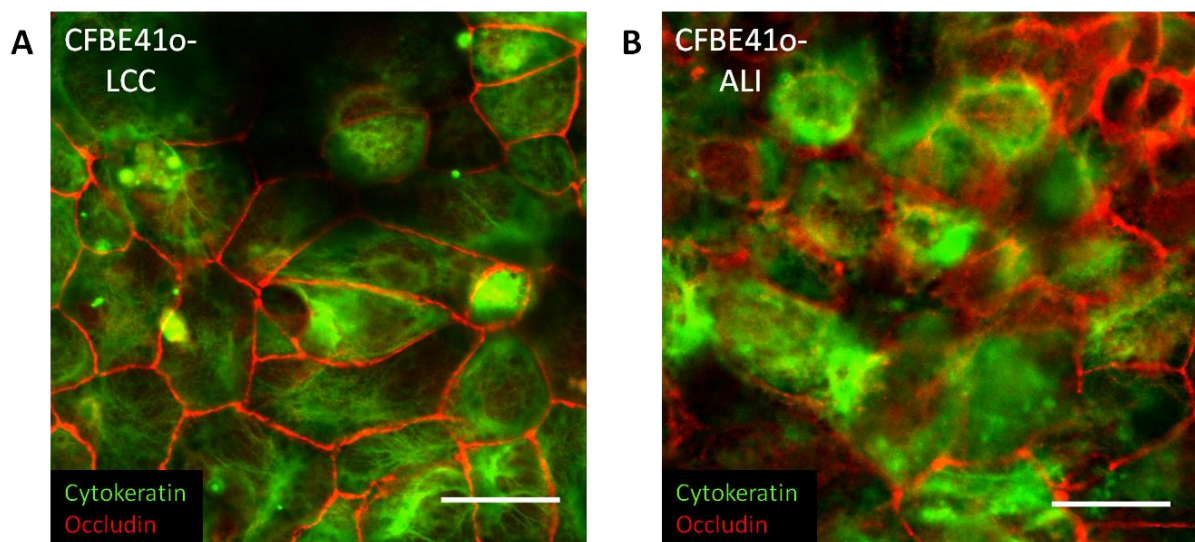
Figure 3.3 Tight junction staining in CFBE41o- cells. CLSM images of CFBE41o- cells cultivated under LCC (**A**) or at the ALI (**B**) for 18 days before fixation. TJ protein occludin (red) and the cytoskeleton (green) were stained. Scale bar: 20 μm

3.3.3 Culture condition influences transcellular permeablilty in CFBE41o- cells but not in Calu-3 cells

In order to also shed some light on the difference in drug transport depending on the applied culture conditions, permeability studies with the paracellular transported model drug NaFluo, which can easily be detected by fluorescence spectroscopy, were conducted.

Since the paracellular route is guarded by the TJs and the here used NaFluo is primarily transported this way, TEER values and P_{app} values, both markers for the tightness of the epithelial barrier, should correlate. An inverse correlation between TEER and P_{app} of paracellular transported markers was reported in several studies [141-143]. However, no further decrease of P_{app} values was observed for Calu-3 cells that had already reached TEER values of 450 $\Omega*cm^2$ [141], indicating that even higher TEER values did not influence the permeability of paracellular transported drugs any further. This also holds true for the Calu-3 cells used in these studies. Even though TEER values in cells cultivated under LCC were higher than in cells cultivated at the ALI (see Figure 3.1) P_{app} values did not differ significantly from one another (Figure 3.4).
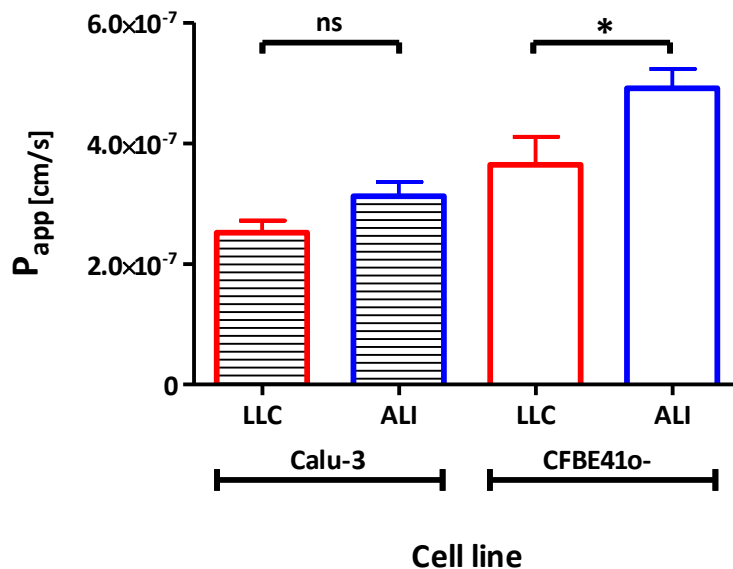
Figure 3.4 Permeability studies with Na-Fluorescein on Calu-3 and CFBE41o- cells. Cells were cultivated under LCC (**red**) or at the ALI (**blue**) for 10 (Calu-3) or 5 days (CFBE41o-) before transport study was conducted. Data shown are mean ± SEM (n ≥ 12) from two (Calu-3) or three (CFBE41o-) independent experiments. * p < 0.05

In contrast, the CFBE41o- cells, which did not reach considerable barrier properties with ALI conditions (Figure 3.2), also showed a significant difference in P_{app} values (Figure 3.4). This illustrates that low TEER values result in an increased permeability of the cell monolayer and therefore an increase in P_{app} values. This emphasizes the fact that the CFBE41o- cells cultivated at the ALI are not suitable for additional experiments (e.g., use as cell line for infected CF model) without improvement of the ALI cultures that could alter TEER values and therefore the cellular barrier properties.

Another aspect that comes to mind is that the measured P_{app} values of the Calu-3 cells are in general a little lower than for the CFBE41o- cells. This is no surprise for the cells that were cultivated at the ALI. CFBE41o- cells did not reach considerable barrier properties under these conditions. But cells that were grown under LCC showed higher TEER values on their peak than the Calu-3 cells. Even though P_{app} values differ from cell line to cell line and can still differ slightly from laboratory to laboratory even if the same cell line was used, they are usually in the same range [139-141, 143-146]. Thus, the observed differences in P_{app} values between CFBE41o- and Calu-3 cells could also be a hint to another barrier that plays a major role in the lung: mucus.

3.3.4 Calu-3 cells produce mucus when cultivated at the air-liquid interface whereas CFBE41o- cells lack mucus production

Mucus serves primarily as a cytoprotective layer for most surfaces in the body. Especially epithelial cells are often covered with this viscous endogenous hydrogel composed of gel-forming mucins [147, 148]. To replenish the gel-layer these mucin glycoproteins are continuously synthesized and secreted by mucous cells in the gastrointestinal tract, the genitourinary tract, the ocular surface, the middle ear, as well as in the pulmonary airways. In the lungs the mucus gel is continuously propelled toward the trachea by ciliary beating, thus clearing inhaled pathogens and particles from the airways in a relatively short period of time [21, 149-151]. These protective barrier properties of mucus have to be taken into account, namely when thinking about therapeutic drug carriers such as nanoparticles (NPs) intended for pulmonary drug delivery, since they might impose a significant challenge for them [149, 152].

Since mucus would protect the cells from a presumable infection, but simultaneously presents a drug delivery barrier for the applied NPs, it was mandatory to investigate if the cell lines used in this work are able to produce mucus.

Typically, acridine orange (AO) is used to stain cells and mucoglycoproteins for fluorescence spectroscopy. Using the pH sensitivity of AO and taking into account that mucus has acidic properties, this staining results in a green fluorescence for neutral cell compartments (cytoplasma) and a shift to red emission for the sour mucoglycoproteins [125]. In histology the PAS reagent is commonly used to stain glycoproteins, glycogen, polysaccharides and mucins [153] such as neutral mucopolysaccarides, while the dye Alcian blue is used to detect sour mucosubstances. In combination this allows to distinguish between neutral and sour mucins in one sample. In addition, scanning electron microscopy can be applied to image the cell surface, which allows to detect mucin fibers on top of the cells if present. All three techniques were used in this study.

For Calu-3 cells it was shown that they express typical gens for mucus-secreting cells (e.g., MUC1, MUC2, MUC4, MUC5) [154, 155]. Mucus secretion is also depended on the used culture condition and can be enhanced when cells are cultivated at ALI [139]. The majority of studies even report that Calu-3 cells only produce mucus when exposed to air [139, 140, 146, 156]. However, some studies also report the production of mucus under LCC conditions [157, 158].

Calu- 3 cells used in this study revealed an increased mucus production when grown at ALI conditions. When sour mucins were stained with AO just small amounts of mucus could be detected in the LCC culture (Figure 3.5 A), whereas the cells cultivated at ALI showed more sour mucins on the cell surface (Figure 3.5 B), evident by higher amounts of red emission.
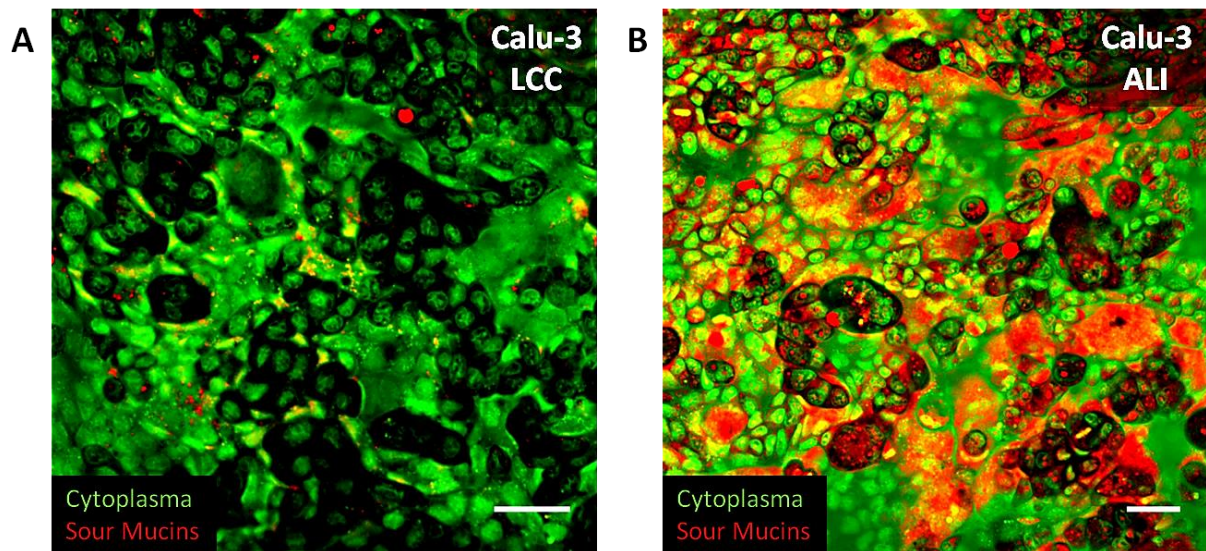
Figure 3.5 Acridine orange staining of Calu-3 cells. CLSM images of Calu-3 cultures. Cells were cultivated under LCC (**A**) or at the ALI (**B**) for 18 days before staining. The cytoplasm shows a green emission, while the sour mucins exhibit a red emission. Scale bar: 50 μm

Similar results were obtained when mucus was stained with PAS/Alcian blue. Here as well, cells cultivated at ALI conditions (Figure 3.6 B) showed high amounts of sour mucins (blue colour), as well as high evidence of neutral mucins (pink colour). On the other hand, on top of the cells that were covered with liquid during cultivation just neutral mucins could be detected (Figure 3.6 A).

Since mucus has a cytoprotective role and ALI conditions expose the cells to more stress, the increased mucus production can be a cellular response to the cultivation at these conditions. On the other hand, mucus production might be similar under submerged conditions. However, the produced mucins might dissolve in the overlaying liquid and are removed with medium change. Grainger et al. made similar observations regarding mucus production and also concluded the culture medium exchange as possible removal of secreted mucus [139]. Since it could be shown that Calu-3 cells,

grown in tissue culture flasks (LCC conditions) express MUC5/5AC mRNA and secrete this mucin in the surrounding medium [155], this seems a likely explanation.
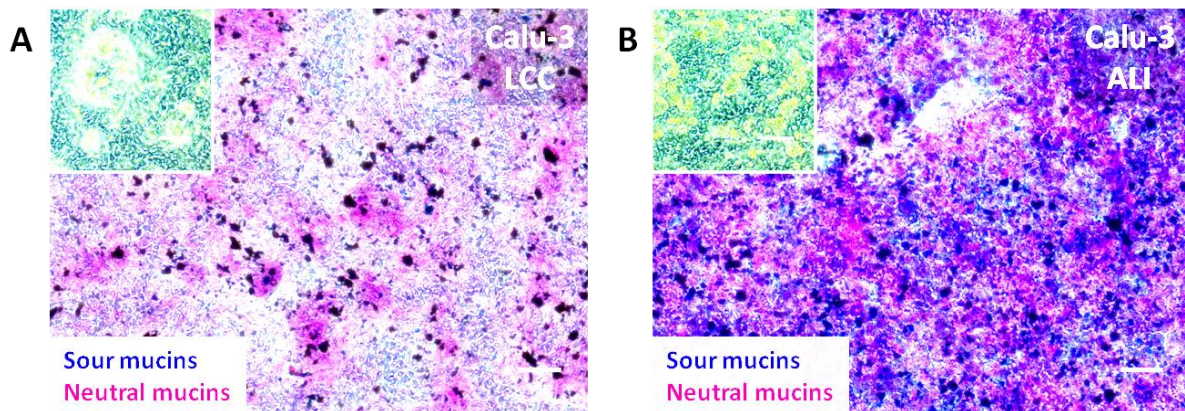
Figure 3.6 PAS/Alcian blue staining of Calu-3 cells. Light microscopy images of Calu-3 cells cultivated under LCC (**A**) or at the ALI (**B**) were taken after staining with periodic acid-Schiff (PAS) for neutral mucins and Alcian blue for sour mucins. More mucins are present when cells are cultivated at ALI. Small inserts in top left corner show unstained control of cells. Scale bar: 200 µm

In the SEM images of the Calu-3 cells the structure of the monolayer becomes evident. Cell boundaries are visible (Figure 3.7). Cracks in the cell layer are due to sample preparation. Long mucin fibers (strand like structures) can be seen on the surface spanning over several cells. But as already seen with AO and PAS/Alcian blue staining, mucus is more evident in ALI cultivated cells (e.g., more mucin fibers in Figure 3.7 B). Of note are the apical cell protrusions covering almost all cells in both images (Figure 3.7 A, B). However, it remains to be investigated, if these structures are indeed cilia, typical for primary airway cell cultures. Reports from several studies with Calu-3 cells hold opposing views regarding this cell organelle. Some groups describe these structures as cilia [142, 156-158], while others report them as microvilli [139, 143, 144, 154, 159] indicating that this is still a matter worth investigating.
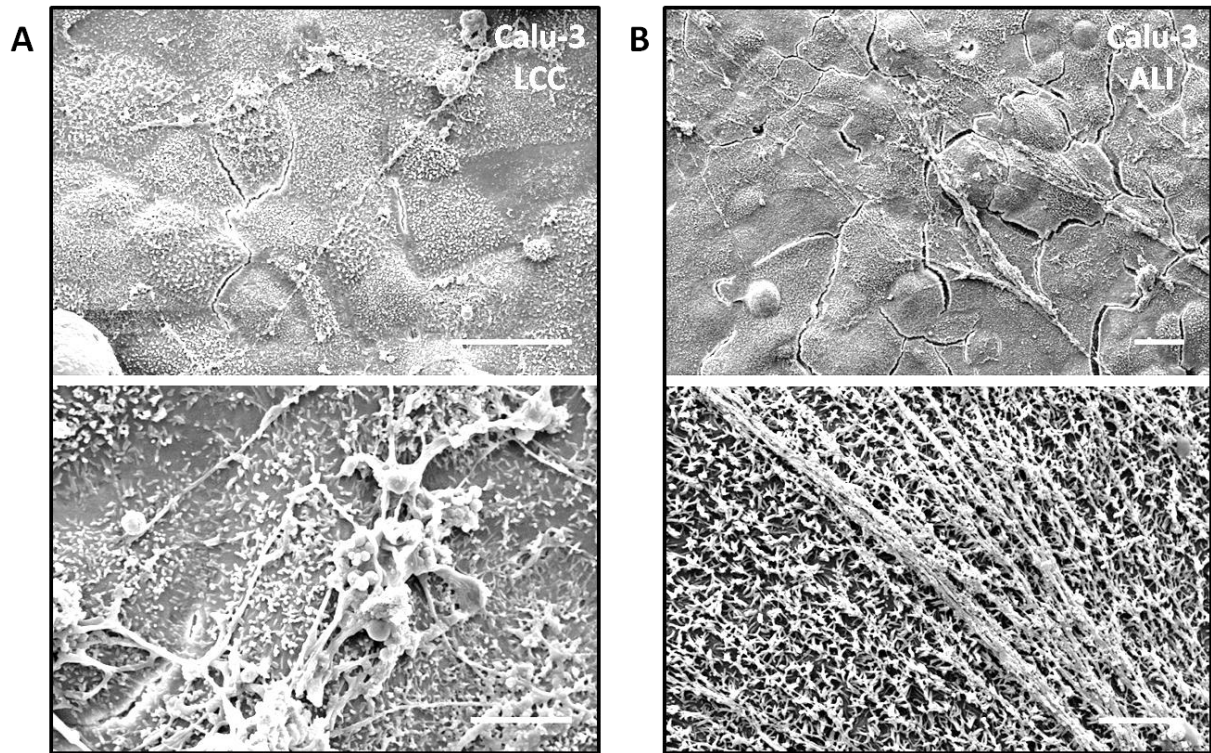
Figure 3.7 Morphology of Calu-3 cells. SEM images of Calu-3 cells cultivated under LCC (**A**) or at the ALI (**B**) were taken. Under both conditions mucin fibers are evident on top of the cells. Microvilli on the cell surface are present under both culture conditions. Scale bar: 20 µm top pictures and 5 µM bottom pictures.

CFBE41o- cells, though not as widely used as Calu-3 cells, are also already very well described in the literature. However, reports on mucus productions are scarce and were therefore conducted with the above-mentioned techniques.

Similar to the Calu-3 cells the AO staining showed more sour mucins (red emission) when cells were cultivated at ALI (Figure 3.8 B). LCC cultured cells just showed sporadic red emission (Figure 3.8 B), indicating a reduced mucus production or removal due to media exchange much like the Calu-3 cells. However, PAS/Alcian blue staining of the CFBE41o- cells cultivated submerged show small amounts of neutral mucins (Figure 3.10 A, pink stained secretions on top of the cells), whilst the air exposed cells show no evidence of mucus production at all (Figure 3.9 B). This stands in contrast to the Calu-3 cell line, where ALI condition massively increased the mucus production. On the other hand, this is in agreement with the findings of Moreau-Marquis et al. and Price et al. who also found that CFBE41o- cells do not produce mucus [160, 161].
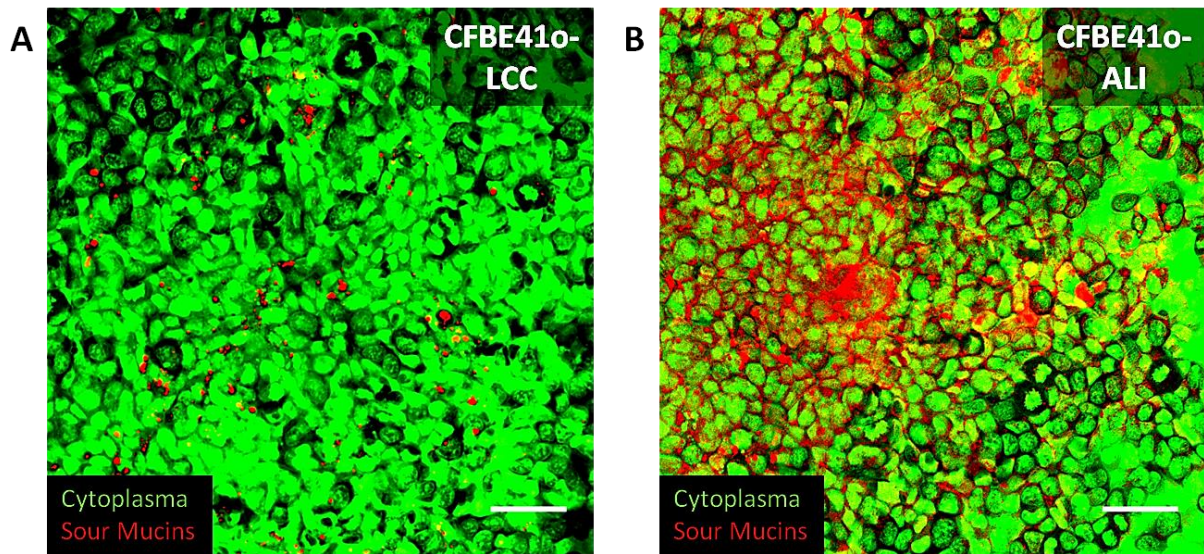
Figure 3.8 Acridine orange staining of CFBE41o- cells. CLSM images of CFBE41o- cultures. Cells were cultivated under LCC (**A**) or at the ALI (**B**) for 18 days before staining. The cytoplasma shows a green emission, while the sour mucins exhibit a red emission. Scale bar: 50 µm

To exclude that the lack in mucus production results from a shorter cultivation time at ALI conditions (5 days for CFBE41o- cells in contrast to 10 days for Calu-3), cells were cultivated for up to 10 days at ALI conditions and PAS/Alcian blue staining was repeated. But results remained the same (data not shown). No secretion of mucus could be detected in CFBE41o- cells, irrespective of culture condition and culture time.
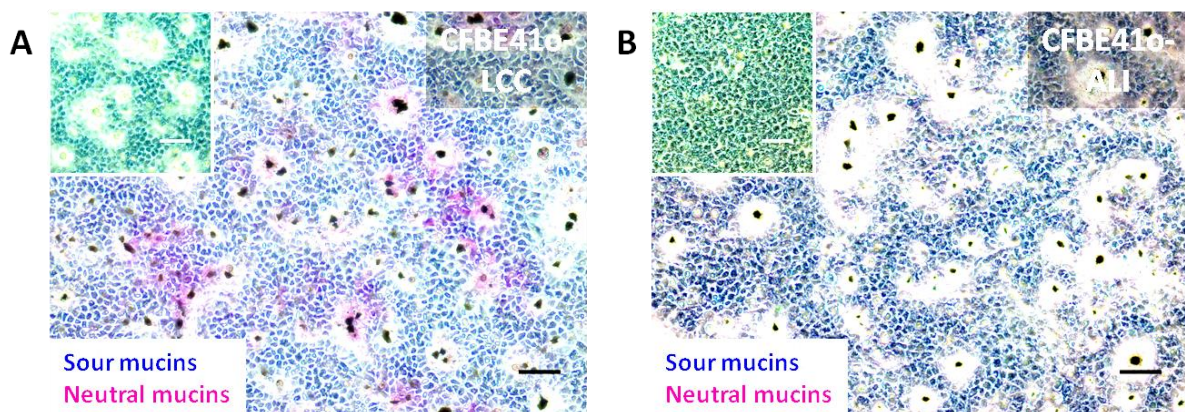
Figure 3.9 PAS/Alcian blue staining of CFBE41o- cells. Light microscopy images of CFBE41o- cells cultivated under LCC (**A**) or at the ALI (**B**) were taken after staining with periodic acid-Schiff (PAS) for neutral mucins and Alcian blue for sour mucins. Only a couple of neutral mucins are detected in the LCC culture, while no mucins are evident in ALI sample. Small inserts in top left corner show unstained control of cells. Scale bar: 200 µm

To further confirm the lacking mucus production in this cell line, but also get some additional insight on the morphology of those cells SEM images were taken. Cell monolayers of cells with clearly visible boundaries can be seen in Figure 3.10 (top row). In the enlargement of Figure 3.10 A the LCC grown cells exhibit apical cell protrusions similar to the Calu-3 cells under the same conditions. Even more prominent are the microvilli-like structures in the bottom image of Figure 3.10 B. The ALI cultured cells exhibit these structures in different length on individual cells. The long filaments in this enlargement of CFBE41o- cells might even resemble cilia. Nonetheless, no mucin fibers could be detected on either of the samples. This contributes to the fact that the CFBE41o- cells indeed lack mucus secretion. Since these cells are of bronchial origin obtained from a CF patient and should therefore be able to secret mucins, they might have lost this ability during the immortalization process with the simian virus (SV40) [107].
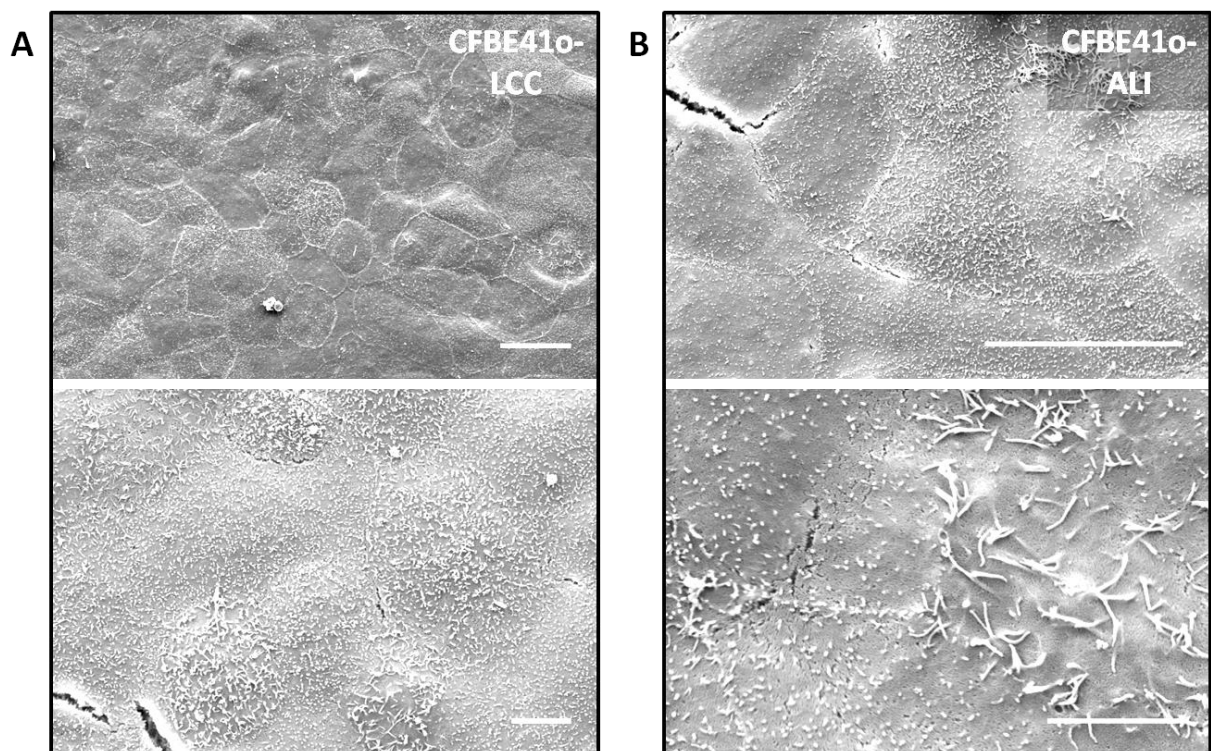
Figure 3.10 Morphology of CFBE41o- cells. Scanning electron microscopy images of CFBE41o- cells cultivated under LCC (**A**) or at the ALI (**B**) were taken. No evidence of mucin fibers could be detected. Microvilli in different length on the cell surface are present under both culture conditions. Scale bar: 20 µm top pictures and 5 µM bottom pictures.

3.4 Conclusion

SEM images of Calu-3 and CFBE41o- cells confirm that both cell lines form monolayers when seeded onto Transwell® filters. While Calu-3 cells exhibit high TEER values when grown under both LCC and at ALI conditions, CFBE41o- cells only show considerable barrier properties when grown under submerged conditions. CLSM images showed a diffuse pattern of the tight junction protein occludin in ALI cultures of CFBE41o- cells. This could explain the difference in TEER values observed under different culture conditions in this cell line.

The permeability of a paracellular transported model drug NaFluo was significantly different in CFBE41o- cells depending on the applied culture condition. Even though TEER values in Calu- 3 cells differed in height depending on the growth conditions, no significant effect on the P_{app} was observed in this cell line.

With AO, PAS/ Alcian blue staining and SEM images it could be shown that Calu-3 cells produce mucus under both LCC and ALI conditions but secretion of mucus is drastically increased when cells were grown exposed to air.

While the AO staining gave the impression that also CFBE41o- cells exhibit an increased mucus production when grown at ALI, SEM images and the PAS/alcian blue staining actually showed that these cells lack mucus production irrespective of the used culture condition.

To conclude from the presented results only the Calu-3 cell line has potential to be used at ALI in further studies, for example for drug deposition with the Pharmaceutical Aerosol Deposition Device On Cell Cultures (PADDOC) [110, 162] or infection with *P. aeruginosa*. In order to also use the cystic fibrosis cell line at ALI conditions in such experiments their barrier properties and TEER values need to be improved. One possibility could be to supply those cells with an external mucus layer to increase those parameters and adapt permeability to that of LCC grown cells.

4 Alternatives to mucus produced by the cell line

The author of the thesis made the following contribution to this chapter:

Planned and performed all cell culture experiments, measured TEER and viability, prepared, analyzed and interpreted all obtained experimental data and wrote the chapter.

Pig tracheas were provided by the slaughter house Zweibrücken. Porcine mucus was obtained from pig tracheas together with Dr. Xabi Murgia. Further processing of porcine mucus and entire human mucus preparation was performed by Dr. Xabi Murgia.

4.1 Introduction

Mucus has numerous functions, but especially in the lungs it serves as barrier to prevent inhaled pathogens and pollutants but also therapeutic NPs from entering the underlying cells [163]. But mucus also hydrates the airways and has antioxidant, antimicrobial and antiprotease activities [164]. In CF thick and sticky pulmonary mucus presents a major hallmark of the disease, leading to airway obstruction, inflammation and infection, which in turn are the cause for morbidity and mortality in patients suffering from CF [57, 58].

Given, that mucus plays a major role as a barrier that needs to be considered when thinking about drug delivery to mucus producing organs (e.g., gastrointestinal tract, lung, eye), the development of mucus models has gained more and more attention. They can be useful tools to mimic this barrier and study drug diffusion.

In view of the fact that the CFBE41o- cells used in this study are unable to produce mucus, but are otherwise well suited for the *in vitro* co-culture model, since they are derived from a CF patient and are homozygous for the most common mutation in CF, the supplementation of the cells with an external mucus layer to achieve a more *in vivo* like model was therefore the obvious solution. Besides, this opened up the opportunity to use different mucus sources for the *in vitro* model.

Numerous models of mucus are described in the literature ranging from simple *ex vivo* to complex *in vivo* models. Application of plain mucins, artificial mucus compositions, to native mucus from horse, pig, cow or human have been described. It is even possible to use pathologic mucus to better mimic certain diseases such as CF [165].

The fact that pigs have a similar anatomy in respect to lung size, physiology, metabolism, and pathology to humans and in addition have a longer lifespan compared to rodents, makes the pig a valuable species for models of human lung diseases [166-168] and to acquire mucus from.

To model the mucus barrier in the lung a lot of published studies use a commercially available porcine gastric mucin [163, 169], relate to freshly isolated gastric mucins [170], create their own artificial mucus [147, 171], or use native mucus isolated from animals [172] or humans [147, 173]. In a lot of cases the source organ differed from the mimicked model organ (e.g., artificial mucus with porcine gastric mucin for CF mucus) [171].

Even though the exact source of mucus might not be of importance to study interaction and penetration of drug delivery systems such as NPs, airway mucus (i.e., pulmonary porcine mucus and endotracheal human mucus) was used for these studies. It could be shown that the major two human airway mucin glycoproteins, the mucins MUC5AC and MUC5B, are present in pig lung as well [166]. Rheological properties of the airway porcine mucus used are typical for cross-linked gels and similar to human tracheal mucus [149]. To go even further one could use the mucus of genetically engineered pigs with cystic fibrosis, as it was shown that they develop typical hallmark features of CF like airway inflammation, mucus accumulation, and infection [174].

Even though porcine mucus is very similar to the human mucus, the human one should be favored as external mucus supply for the CFBE41o- cells. Nonetheless, the supply of human mucus is even more difficult than that of porcine airway mucus. With access to CF mucus one could even further improve the here described *in vitro* model. But to proof the hypothesis, that the low TEER values and questionable barrier properties of the CFBE41o- cells could be improved, we related to the above mentioned porcine airway mucus and human mucus (obtained via endotracheal tube method) from healthy donors.

4.2   Material and methods

4.2.1   Pulmonary porcine mucus

Pulmonary porcine mucus was collected from pig tracheas as described in Murgia et al. [149]. Briefly, tracheas of slaughtered pigs were cut below larynx and before carina resulting in a 10 cm long section of the windpipe. Tracheas were stored on ice prior to mucus extraction. Tracheas were cut in half in a longitudinal direction (i.e., along the trachealis muscle) and mucus was carefully extracted with a spatula (100-300 µl of mucus sample per trachea). Samples were stored at -20°C and freeze dried afterwards, which led to a destruction of bacteria usually found in mucus. Furthermore, it allowed determining the mucin contents of the freeze-dried samples, thus, ensuring the use of equal amounts of mucus in all experiments.

4.2.2   MTT assay

To investigate if the CFBE41o- cells tolerate the porcine mucus at all, CFBE41o- cells were seeded in a 96 well plate with a density of 20,000 cells/well and grown until approximately 70% confluent (usually 2-3 days after seeding). Medium was then removed and cells incubated with 200 µl per well of mucus resuspended in KRB (in different concentrations e.g., 1 mg, 5 mg and 10 mg per ml). The viability of the cells was checked with an MTT assay 24 h after mucus application. The positive control (100% viability) being only KRB, whereas the negative control (0% viability) consisted of 1% Triton X in KRB. After the 24 h incubation time, supernatants where removed, cells washed once with 200 µl KRB/well and then further incubated with 110 µl MTT solution (500 µg/ml MTT) for another 4 h. After that time 100 µl DMSO was added in each well to dissolve the developed formazan crystals. Absorption at 550 nm was measured with a plate reader (TECAN, infinite M200 pro, Männedorf, Switzerland).

4.2.3   TEER measurements

To evaluate the effect of mucus on the barrier properties, TEER values were measured every other day after mucus application on cells seeded on Transwells® as described under 3.2.3. To ensure that mucus would not be removed when ALI conditions were restored after measurement, excess medium was removed with a manual pipette.

4.2.4   Human mucus

With the PAS/Alcian blue staining described under 3.2.6 it was confirmed that CFBE41o-cells do not produce mucus [160, 161]. But since mucus is a major component in a CF *in vitro* model the use of a mucus source is mandatory. Undiluted human mucus was obtained by the endotracheal tube method [173, 175-177]. This protocol was approved by the Ethics Commission of The Chamber of Medicine Doctors of the Saarland under the file number 19/15. The obtained mucus was stored at -20°C and gradually thawed and left to reach RT when needed. Single drops (weight approximately 30-40 mg each) of the thawed mucus were transferred to a Teflon$^{®}$ template with circular cavities. Mucus filled templates were then placed in an autoclavable sealing bag and stored at -80°C for 4 h. Subsequently, they were freeze-dried overnight (Alpha 2-4 LSC, Christ, Germany). After completing the freeze-drying course, the resulting mucus disks (with an estimated solid content of 1.7 ± 0.1 mg and 95% water content) were sealed in the autoclaving bag and stored until use at RT in a dry atmosphere.

These mucus disks were then carefully removed from their template with tweezers and placed on top of CFBE41o- monolayers 5 days after seeding. Mucus disks were rehydrated with 50 µl of cell culture medium. The Transwell$^{®}$ plates with CFBE41o- cells and additional human mucus were then placed on a shaker platform inside an incubator (at 5% CO_2 atmosphere and 37°C) and rotated at 150 rpm until the following day. This allowed an even distribution of the mucus over the cell monolayer.

4.2.5   Statistical analysis

Data are presented as mean ± standard error of the mean (SEM) from 2-3 independent experiments. Statistical analysis was performed with the GraphPad Prism 5 software. The differences in viability and TEER were compared with a Two-way ANOVA and a Bonferroni post test; * $p < 0.05$ and *** $p < 0.001$ were considered significant.

4.3   Results and Discussion

4.3.1   Porcine mucus is well tolerated by CFBE41o- cells

Since the CFBE41o- cells lack mucus and even a longer cultivation at ALI conditions led to no secretion of mucins, the application of an external mucus layer seemed appropriate. Thanks to a well-established collaboration with a regional slaughter house (in Zweibrücken, Germany) pulmonary porcine mucus was the first option for external mucus because of its unrestricted supply and similarity to human mucus [166]. The obtained mucus was freeze-dried and resupsended as needed.

In order to ascertain that the freeze-dried pulmonary porcine mucus had no cytotoxic effects on the CFBE41o- cells, different amounts of mucus were applied onto the cells and the viability was checked with an MTT assay 24 h later (Figure 4.1).
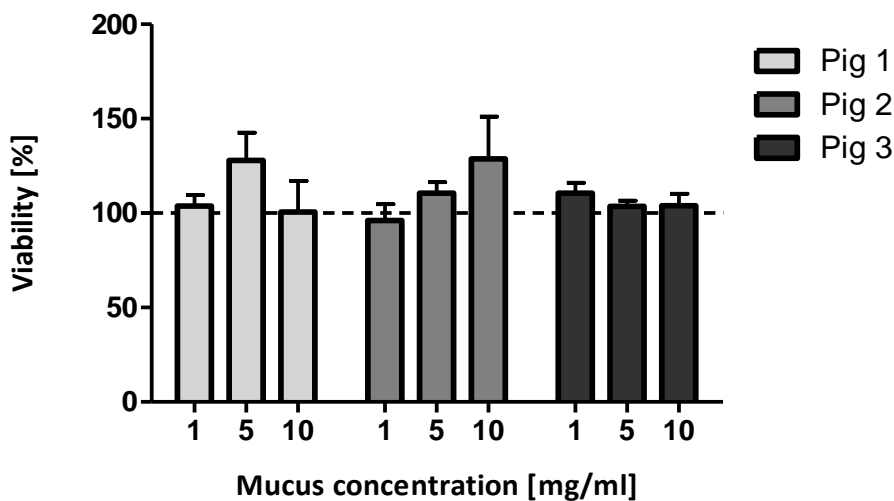
Figure 4.1: Viability of CFBE41o- cells after porcine mucus application. Porcine mucus from 3 different pigs was applied on the CFBE41o- cells. 24 h later an MTT assay was performed to measure the cell viability. Data shown are mean ± SEM (n=9) from three independent experiments.

The applied mucus had no cytotoxic effect on the cells after 24 h. Similar results were reported by Teubl et al. [125]. They could show that applied porcine mucus (from stomach) had no impact on the mitochondrial activity of TR 146 cells, an oral epithelial cell line. Although variability between different donors (Pig 1-3) could be observed, it did not reach significance. Since MTT measures the mitochondrial activity of the cells an increase of viability over 100% (compared to the positive control; cell culture medium) in the samples from pig 1 and 2 for the concentration 5 mg/ml and 10 mg/ml,

respectively, could indicate that the cells activity is amplified, which can happen when cells are under stress. A longer incubation with mucus would clarify, if an actual cytotoxic effect is to be expected at a later stage from the applied mucus. But from the findings of Teubl et al. who had similar increased viability over 100% after 4 and 24 h but no cytotoxic effect after 48 h [125], we can presume that this is probably not the case.

Even though long-term cytotoxicity remains to be investigated, the second highest mucus concentration (5 mg/ml) was chosen for further studies. This concentration might better resemble the clinical picture of CF, where the accumulation of thick mucus contributes massively to the development of chronic infections in CF, bearing in mind that mucus offers good growth conditions for bacteria.

4.3.2 Porcine mucus only increases TEER values of air-liquid interface cultivated CFBE41o- cells

In general, cells in ALI show reduced barrier properties compared to the submerged culture (see chapter 3.3.2). When mucus (5 mg/ml) was applied to the ALI cultivated cells on day 5 after seeding, TEER values increased up to day seven and reached $318 \pm 87 \, \Omega\text{*cm}^2$, the difference in TEER between cells w/o porcine mucus ($104 \pm 13 \, \Omega\text{*cm}^2$) being highly significant on that day (Figure 4.2).

Figure 4.2: Barrier properties of ALI cultured CFBE41o- cells after mucus application. Porcine mucus was applied on the CFBE41o- cells after TEER measurement on day 5 after seeding (green arrow). TEER was measured for up to 14 days after seeding. Data shown are mean ± SEM (n≥5) from at least two independent experiments. *** p <0.001

After that, barrier properties decreased again and on day 10 after seeding even dropped below values of cells that did not receive extra mucus (Figure 4.2). These cells however never reached considerable TEER values as described previously (Figure 3.2).

Of note is that mucus alone did not show barrier properties ($42 \pm 11 \, \Omega\text{*cm}^2$, data not shown). This was assessed by measuring TEER values in cell free Transwells® that were supplemented with mucus in the same concentration as the mucus treated cells (5 mg/ml; data not shown). Thus, simple physical factors (e.g., clogging of the Transwell® pores by mucus) were not the reason for the increased TEER values observed on day seven after seeding.

Why the increase of the cells barrier properties just lasted for a short amount of time remains to be investigated. One possible explanation is the removal of the applied

mucus with culture medium after TEER measurement. Even though this step was done very cautious, it cannot be avoided that some of the mucus dissolves in the medium and is thereby removed. If this is indeed the case or the increase of TEER values after mucus application is just temporary could be proved by a repeated application of porcine mucus and continuous TEER measurements. On the other hand, also a delayed cytotoxic effect of the porcine mucus might be a possible route cause for the decreasing TEER values after day 7. Since viability of the cells was just measured 24 h after mucus application (see chapter 4.3.1), also a later toxic potential of the porcine mucus might be a possible explanation.

When mucus was applied to the submerged culture (Figure 4.3), TEER values decreased in comparison to the LCC cultured cells without porcine mucus (1631 ± 140 Ω*cm² for LCC versus 777 ± 140 Ω*cm² for LCC+mucus) In contrast to the ALI cultivated cells, the applied mucus seems to have a negative effect on the barrier properties of the CFBE41o- cells in this case. This observation even reached significance on day 7, 12 and 14 after seeding. Similar adverse effects, where the exogenous porcine mucus even disrupts epithelial monolayer, were already reported. The group of Bough et al. observed a dramatic decrease of TEER values after porcine intestinal mucus was applied to Caco-2 cells [178].
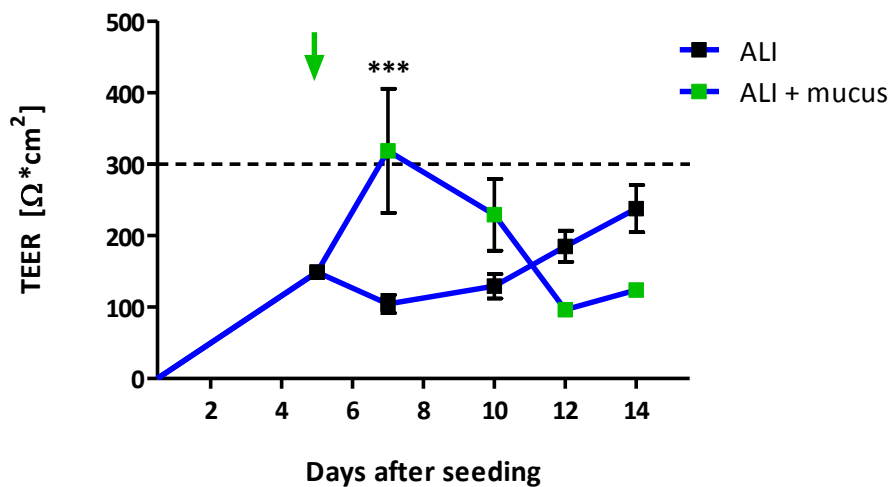

Figure 4.3: Barrier properties of LCC cultured CFBE41o- cells after mucus application. Porcine mucus was applied on the CFBE41o- cells after TEER measurement on day 5 after seeding (green arrow). TEER was measured for up to 14 days after seeding. Data shown are mean ± SEM (n≥5) from at least two independent experiments. *** p <0.001; * p <0.05

Considering that porcine mucus is slightly different from human mucus after all and even decreases the TEER values of the LCC cultured cells, it appears that the addition of an external mucus layer only makes sense for ALI cultivated cells. Here it can be concluded that with the application on day 5 after seeding highest barrier properties can be expected on day 7 after seeding. The infection with bacteria as next step in the direction of a co-culture model should therefore be performed on that day, because high barrier properties likely increase the cellular resistance to the infection and favour the survival of the epithelial cells.

4.3.3 Human mucus increases TEER values of air-liquid interface cultivated CFBE41o-cells by 7-fold

The addition of porcine airway mucus did not achieve the desired results of raising the TEER values of the CFBE41o- cells considerably (just about 300 Ω*cm² for one day, see Figure 4.2) but nevertheless an increasing effect could be observed on the ALI cultivated cells. However, this effect did not last. Besides, LLC cultivated cells even showed decreasing TEER values. This was in agreement with previous studies, which showed similar adverse effects (e.g., disruption of barrier properties and cytotoxicity) when porcine mucus was applied on epithelial cells [125, 178].

Nevertheless, we hypothesized that due to same mutual human origin CFBE41o- cells and human airway mucus might accomplish better results. Therefore, further experiments with human mucus were conducted.

First evaluations concerning cytotoxicity and rheological behavior of human airway mucus were already performed by Murgia et al. [177]. They found, similar to the porcine mucus, a slightly increased viability after 24 h compared to the control cells. This might even suggest a positive effect of mucus on the CFBE41o- cells. They confirmed the compatibility of the exogenous human mucus with the epithelial cells even further through a live dead staining, finding a high cell viability in mucus incubated cells. When they applied the mucus to LCC cultured CFBE41o- cells, TEER was slightly increased, although values did not reach significance [177].Reassured by those observation the freeze-dried human mucus was thus applied on the ALI cultivated CFBE41o- cells on day 5 after seeding and indeed, human mucus raised the TEER values of the ALI cultivated CFBE41o- cells notably in contrast to porcine mucus (Figure 4.4). Barrier properties increased by 7-fold (230 ± 20 Ω*cm² without mucus versus 1573 ± 126 Ω*cm² for cells with mucus). Human mucus alone (cell-free Transwell® with mucus) only reached 21 ± 8 Ω*cm². Thus, the applied mucus does not create a physical barrier (e.g., by clogging of the Transwell® pores). Therefore, a synergistic effect, and not an additive one, must be causing the higher TEER values observed after mucus application.
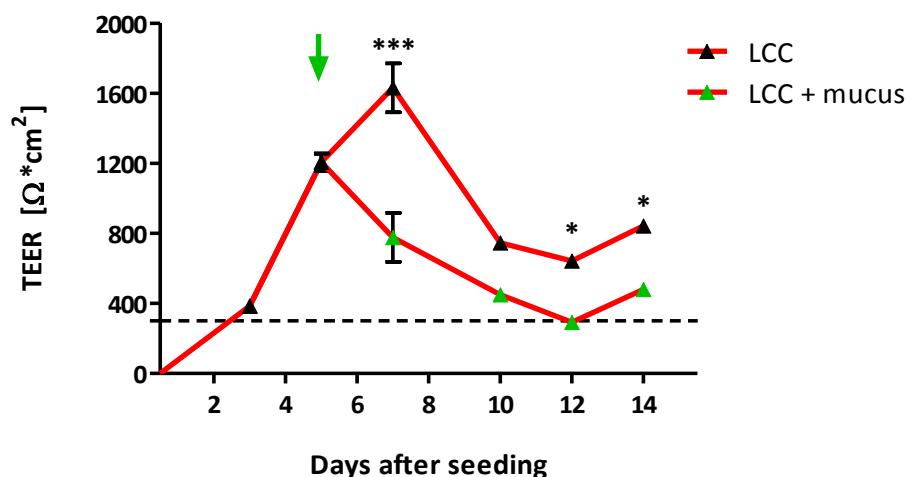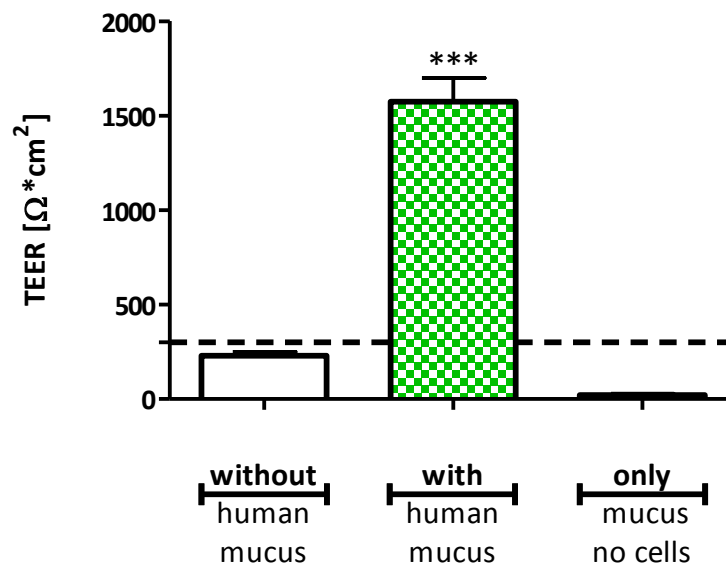
Figure 4.4: Barrier properties of ALI cultured CFBE41o- cells after human mucus application. Human mucus was applied on the CFBE41o- cells on day 5 after seeding (green checkered). TEER was measured on day 7 after seeding. Data shown are mean ± SEM (n≥18) from at least 3 independent experiments (only mucus; n=4 from two independent experiments). *** p <0.001.

Of note is also, that no bacterial contamination was detected when freeze-dried human mucus was used. Since mucus contains bacteria even in healthy state, the freeze-drying process probably reduced the bacterial load of the exogenous human material [177]. That the freeze-drying procedure had no effect on the rheological properties of mucus was confirmed in the study by Murgia et al. They showed that the freeze-dried and re-suspended mucus had a comparable rheological behavior to the undiluted native mucus and behaved as a semi-permeable layer, indicating that this mucus offers the additional mucus barrier the CFBE41o- cells are still lacking [177].

4.4 Conclusion

CFBE41o- cells do not produce mucus, a key cytoprotective element found in the lung. But apart from that, they offer valuable features such as the expression of TJ proteins and proteins relevant for pulmonary drug transport and in addition a shorter cultivation time compared to Calu-3. For those reasons the aim was to improve this cell line with exogenous mucus to use it for the co-culture model. Two external mucus sources were evaluated: porcine airway mucus and human airway mucus.

Both mucus sources proved to be non-cytotoxic to the cells as seen by the high viability of the CFBE41o- cells after 24 h incubation with either form of mucus.

Meanwhile, the effect on the barrier properties of the epithelial cells was quite diverse. Porcine mucus decreased TEER values of LCC cultivated cells significant, but on the other hand could slightly improve barrier properties of ALI cultivated cells for a short time period.

In contrast, human mucus increased TEER values of ALI cultivated CFBE41o- cells significantly over 300 $\Omega*cm^2$ regarded as the threshold value to present a tight barrier. This positive effect on the CFBE41o- cells can probably be explained by the common human origin of both cell line and mucus and was therefore favoured over the porcine mucus. The disc-like form of the human mucus achieved through freeze-drying on a template makes it easy to apply to the cell culture. In addition, the microbiological burden was reduced in the course of the freeze-drying process avoiding bacterial contamination by the exogenous human material.

Further studies on rheology of the freeze-dried human mucus and uptake studies with NP of different size by Murgia et al. [177] proofed that this human airway mucus is indeed a perfect option to supplement the non-mucus producing CFBE41o- cells with a mucus layer. Thus, by introducing human mucus, a protective element to the epithelial cell monolayer, and at the same time another important biological barrier could be added to the *in vitro* model.

5 Cultivating *Pseudomonas aeruginosa* and optimizing biofilm formation

The author of the thesis made the following contribution to this chapter:

Planned and performed all bacterial experiments, measured OD$_{600}$, stained and quantified crystal violet assays, analyzed and interpreted all obtain experimental data and wrote the chapter.

5.1 Introduction

Pseudomonas aeruginosa is the most common pathogen in adult CF patients [41]. By late adolescence the majority of patients suffering from this genetic disease is infected with it [25, 26]. This Gram-negative bacterium uses its flagella and type IV pili to swim in media and move on solid surfaces by means of reversible flagella rotation and twitching motility, respectively [179]. In addition, the flagella of *P. aeruginosa* play an important role in biofilm formation. It has been shown that *P. aeruginosas* flagella contribute to the initial colonization by means of mucin-adhesion, and thus to the start of biofilm formation [180].

P. aeruginosa's ability to build biofilms and the resulting resistance against common antibiotic therapy, qualifies this pathogen as model organism in our CF co-culture model, and thus test the efficacy of novel drug delivery systems against chronic infections in CF caused by this pathogen.

Since the development and presence of a biofilm is cause for the failure of current treatment therapies, mimicking the same in our model was crucial. Given that biofilm development needs time and is dependent on a lot of parameters [181], the aim was to find the optimal growth conditions for *P. aeruginosa* to develop a biofilm *in vitro*. In view of the fact that bacteria can respond to nutrient conditions very rapidly, the contents of the growth medium are essential for their regulation of biofilm formation [182-184]. As culture medium usually a minimal medium like M63 [185], supplemented with different carbon and energy sources, is to be favored. Such a medium facilitates biofilm formation in *P. aeruginosa* [186]. Studies from O'Toole et al. showed that LB medium or M63 supplemented with either glucose, glycerol, citrate, lactate, glutamate, succinate, gluconate or casamino acids would promote biofilm formation [186] and first microcolony formation can already be detected after 3 h [160]. Also the combination of a carbon source (mostly glucose) and casamino acids is widely used. Furthermore, Caiazza et al. found that the addition of arginine to the minimal medium M63 as sole carbon and energy source results in enhanced biofilm formation [187]. Therefore, the aim was to try those different supplements to the M63 alone or in combination, in order to find the best conditions for the strain used in these studies: *P. aeruginosa* PAO1.

The *P. aeruginosa* strain PAO1 was originally isolated from a burn wound in 1955 [188]. It is a widely used laboratory strain and also the first *Pseudomonas* species with a complete sequenced genome [189]. Around 770 articles have been published in the last 5 years alone, as listed on the NCBI PubMed database [190], using this specific *P. aeruginosa* strain. About 15% of these studies are related to CF research. Several studies compared clinical CF isolates to the model strain PAO1. Penesyan et al. found, that even though PAO1 and the clinical isolates had a high similarity in their proteome, they significantly differed in their metabolism and physiology [191]. However, Jørgensen et al. found just small changes in respiratory reduction when comparing PAO1 to early lung isolated strains of CF patients [192]. In addition, one has to consider the high diversity found in clinical isolates from CF patients. The four isolates compared in the studies of Penesyan et al. differed among other things in colony morphology, type of flagella, swimming motility and their ability to form a biofilm. One of the strains analyzed was not able to build a biofilm. Also their ability to bind to mucins, and the production of certain virulence factors (e.g., phenazine, pyoverdine) was very diverse [191]. These substantial phenotypic differences between the clinical isolates make it extremely difficult to select just one strain for an *in vitro* model.

So despite the observed differences to clinical isolates, PAO1 shows a lot of traits that are important for lung colonization as it is found in CF patients (e.g., flagella expression and medium binding to mucins, biofilm formation, production of virulence factors) [191]. Thus, PAO1 was used as model strain in this work. However, in future the use of clinical isolates, that do not lack biofilm formation, might be an option.

The initiation of biofilm development can occur on biotic (e.g., human cells) and abiotic (e.g., plastic cell culture dishes) surfaces likewise. Therefore, a useful tool to indirectly monitor the biofilm development is staining with crystal violet (CV) [183]. This purple dye stains the bacteria and biofilm, but not the plastic of the culture dishes. The amount of biofilm formation can be quantified by solubilizing the biofilm associated dye and determining its absorbance at 600 nm [186].

5.2 Material and Methods

5.2.1 Overnight cultures

To obtain overnight cultures in which the bacteria, *P. aeruginosa* strain PAO1 and a fluorescent labelled PAO1 strain (ATCC® 10145GFP™), are in exponential growth phase, one colony was picked with a sterile pipette tip from an agar plate containing the desired bacteria and the colony was transferred in 10 ml sterile LB broth (Sigma-Aldrich, Munich, Germany) supplemented with necessary antibiotics for the GFP labelled strain (300 µg/ml ampicillin; Carl Roth, Karlsruhe, Germany). Inoculated broth was incubated for 16-18 hours at 37°C and 180 rpm.

5.2.2 OD$_{600}$ measurements

Overnight cultures were centrifuged at 1250 g and supernatant was discarded. The bacterial pellet was then resuspended in 10 ml sterile PBS. Optical density at 600 nm (OD$_{600}$) of the bacterial solution was measured with a plate reader (TECAN, infinite M200 pro, Männedorf, Switzerland). Concentration of the bacterial solution was adjusted to achieve an OD$_{600}$ ~ 0.1.

5.2.3 Medium optimization for biofilm formation

With the aim to find the optimal medium composition to grow *P. aeruginosa* PAO1 biofilms, different supplements to the minimal growth medium M63 (1 l of medium contained: 13.6 g of KH_2PO_4, 2 g of $(NH_4)_2SO_4$, 0.5 mg $FeSO_4$, 1 mM $MgSO_4·7H_2O$) [193, 194] were evaluated. Single use or combinations of a carbon source (e.g., 0.2% of glucose or glycerol), casamino acids (Sigma Aldrich, 0.5%) and/or arginine (Sigma Aldrich, 0.4%) were examined. Thus, overnight cultures of *P. aeruginosa* PAO1 were prepared as described under 5.2.1 and diluted 1:50 (OD$_{600}$ of ~ 0.1) in the different media compositions adapted from the protocol of O'Toole [100]. To allow biofilm formation, 100 µl of each inoculated medium was transferred in a 96-well plate (4 replicates each) and incubated for 24 h at 37°C under static conditions. After the incubation time, the supernatants were removed and the resulting biofilms stained with crystal violet.

5.2.4 Biofilm staining with crystal violet

To stain the resulting biofilm and quantify its mass, a crystal violet (CV) staining was conducted as described by O'Toole [100, 186]. Briefly, supernatant of each well was discarded and the plate rinsed two times with water to remove unattached and planktonic bacteria. Hereafter, 125 μl of a 0.1% CV solution was added in each well and incubated for 12 min. After that time the CV solution was removed and plate rinsed 3 times with water and then left to dry. Staining was dissolved by adding 125 μl of ethanol 96% for another 12 min under gentle shaking. From each well 100 μl were transferred to a new plate and absorption at 600 nm was measured with a plate reader. Higher absorption values are an indicator for a larger biofilm mass that was stained.

5.2.5 Statistical analysis

Data are presented as mean ± standard error of the mean (SEM) from 4 independent experiments (n=16) for the medium addition to M63 and 4 independent experiments (n=12) for the combination of supplements. Statistical analysis was performed with the GraphPad Prism 5 software. The differences in absorption were compared with a One-way ANOVA and a Bonferroni post test; $* p < 0.05$ and $*** p < 0.001$ were considered significant.

5.3 Results and Discussion

5.3.1 Arginine as supplement in minimal bacterial growth medium M63 shows best results in enhancing *P. aeruginosa* biofilm formation

In order to enhance *P. aeruginosa* PAO1 biofilm formation, different supplements were added to the minimal medium M63. The resulting biofilms attached to the assay plate were stained with CV, solubilised and quantified. The minimal medium M63 alone almost did not allow for any biofilm formation (A_{600} = 0.0436 ± 0.0052; Figure 5.1, white bar). Also the addition of the energy source glucose (medium grey bar in Figure 5.1) had no effect on biofilm formation. This stands in contrast to the findings of O'Toole et al. [183] who reported that glucose alone promotes biofilm formation. Although one has to keep in mind that their experiments were performed with *Pseudomonas fluorescens*, which might behave slightly different then *P. aeruginosa*.

On the other hand, the addition of arginine to the medium enhanced the resulting biofilm mass significantly by 17-fold (A_{600} = 0.7290 ± 0.0339, Figure 5.1, light grey bar). Furthermore, also glycerol and casamino acids showed significant increase in biofilm formation (dark grey and black bar in Figure 5.1, respectively), but not to the extent of arginine. Similar results for *P. aeruginosa* were also reported by Caiazza et al. [187]. They found that bacteria grown in arginine enriched M63 medium or LB showed a robust biofilm formation, while glucose as supplement only resulted in a weak biofilm.
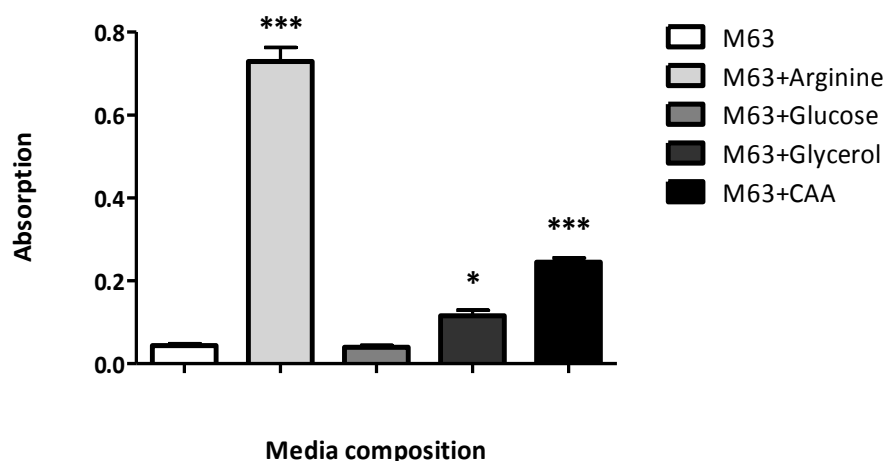

Figure 5.1: Biofilm development of *P. aeruginosa* in enriched M63 media. Bacteria were inoculated for 24 h with M63 enriched with different supplements. Biofilms were stained with CV and quantified. Data shown are mean ± SEM (n=16) from four independent experiments. *** $p < 0.001$; * $p < 0.05$.

However, intermediate levels of biofilm formation were observed, when glucose and CAA were both added to the medium. Also several other studies use a combination of glucose and CAA as M63 supplements to study biofilm formation. Thus, the mixture of arginine, glucose or glycerol with CAA was tested in order to find out if biofilm formation could be further enhanced (Figure 5.2).

As hypothesised, the addition of CAA to glucose or glycerol enriched M63 medium enhanced *P. aeruginosa* biofilm formation significantly by 7-fold and 3-fold, respectively (medium and dark grey bars in Figure 5.2). But this is probably just an additive effect of both components together. Surprisingly, for the arginine minimal medium this effect was not observed. Even though measured absorption was slightly higher when a combination of arginine and CAA was used as culture medium, values did not reach significance (light grey bar in Figure 5.2). But since both components are amino acids, a mixture of both might not trigger further biofilm formation in *P. aeruginosa*. Even though the combination of supplements could achieve a higher biofilm mass in two cases, arginine as sole addition to the minimal medium M63 offered the best results for the here used strain PAO1. Consequently, this media composition was used for all further studies with *P. aeruginosa* PAO1, where biofilm formation was desired.
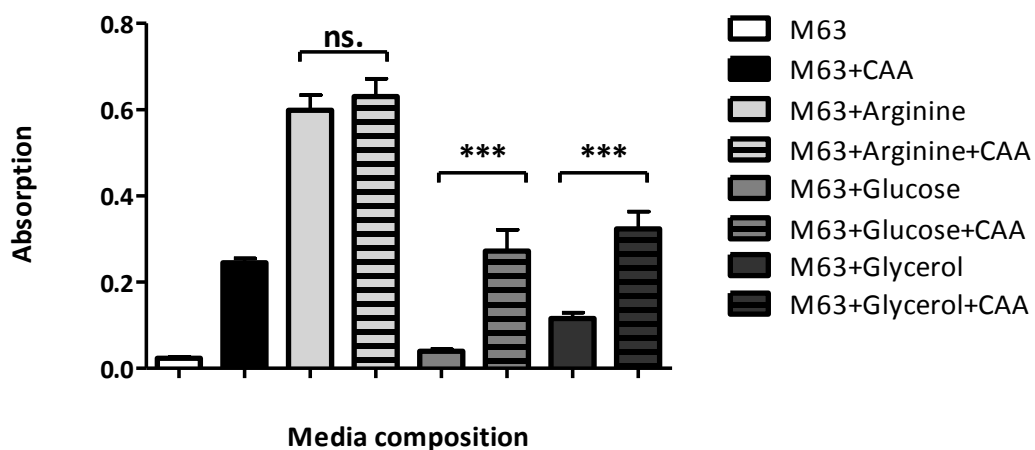
Figure 5.2: Biofilm development of *P. aeruginosa* in M63 media enriched with combination of supplements. Bacteria were inoculated for 24 h with M63 enriched with different supplements. Biofilms were stained with CV and quantified. Data shown are mean ± SEM (n=12) from three independent experiments. *** p <0.001; ns = not significant.

Of note, Anderson et al. found that this media composition not only enhances *P. aeruginosa* biofilm formation, but also delays the killing of the epithelial cells, thus, allowing biofilm formation on an intact monolayer of CFBE41o- cells [112]. However, in their co-culture model consisting of CFBE41o- cells, grown under submerged conditions, and *P. aeruginosa* PA14, monolayer integrity was preserved for up to 9 h. If the same conditions in the model of ALI cultivated CFBE41o- cells and *P. aeruginosa* PAO1 would allow for sufficient biofilm formation in order to test the efficacy of the novel drug delivery system (DDS) was to be investigated.

5.4 Conclusion

In order to find the best media composition for *P. aeruginosa* PAO1 to form a biofilm, different supplements and combinations of them were evaluated. Even though combinations of a carbon and energy source (e.g., glucose or glycerol) with casamino acids showed enhanced biofilm formation in contrast to the sole energy source, the addition of arginine as only supplement to the minimal medium M63 offered the best results in promoting the biofilm formation. In addition, it was shown that arginine also preserves the monolayer integrity of epithelial cells [112], thus, offering two benefits in one. No further improvement was achieved when arginine and CAA were combined hence, making arginine as sole supplement to the M63 medium the best option for these studies. Since first biofilm formation can be observed only after 3 h further analysis is necessary in order to see, if these condition are favourable enough to allow a biofilm formation on a viable epithelial cell monolayer, and permit a subsequent application of drug loaded NPs for their evaluation.

6 Co-culture of human bronchial epithelial cells and *P. aeruginosa* PAO1

Parts of this chapter will be submitted for publication:

Jenny Juntke, Xabier Murgia, Nazende Günday Türeli, Akif Emre Türeli, Cristiane Carvalho-Wodarz, Marc Schneider, Nicole Schneider-Daum, Claus-Michael Lehr "Novel co-culture model of human airway cells and *P. aeruginosa* biofilms"

The author of the thesis made the following contribution to this chapter:

Planned and performed all cell culture experiments, cultivated bacteria and measured OD_{600} and CFU and set up the co-culture, prepared co-cultures for confocal analysis and scanning electron microscopy and took the images. The author of this thesis analyzed and interpreted all obtained experimental data and wrote the chapter.

Mucus disk preparation and confocal laser scanning microscopy images were conducted by Dr. Xabi Murgia.

6.1 Introduction

Co-cultures of human epithelial cells and bacteria to mimic the infection with pathogens in cystic fibrosis patients have already been described. Especially the infection with *P. aeruginosa* and the formation of an antibiotic resistant biofilm on top of epithelial cells are of great interest, since this situation will overtake in almost all CF patients rather sooner than later. Due to the lack of adequate treatment these infections become chronic and further enhance the endobronchial inflammation and tissue destruction in the lung, leading to decrease in pulmonary function and inevitable early death in CF patients [16, 195].

In order to test new treatment options against these chronic infections predominantly caused by *P. aeruginosa,* suitable *in vitro* models mimicking this situation need to be developed. *P. aeruginosa*s ability to build biofilms has been studied quite extensively on abiotic surfaces (e.g., glass or plastic), in static, or even flow cell conditions [112]. Additionally, growth conditions and ways of staining resulting biofilms of this pathogen have been published [100, 186]. However, studying the infection and biofilm development on a more relevant substrate (e.g., human cells), would help to better understand the airway infections as they occur in CF patients [112].

The first tissue-culture based model to study biofilm formation on human epithelial cells derived from a CF patient was reported by Anderson et al. [112]. They infected LCC cultivated CFBE41o- cells with *P. aeruginosa* PA14 with a multiplicity of infection (MOI, ratio of bacteria to originally seeded epithelial cells) of 30:1 and found that 4 to 6 h after the infection most of the epithelial cells had died presumably because of bacterial killing. This time window however did not allow for efficient biofilm formation. In an effort to find more suitable conditions, that would allow biofilm formation while keeping the epithelial cells alive, they discovered that the addition of arginine to the tissue culture medium preserved the integrity of the cell monolayer for up to 9 h, thus, allowing for more time for the biofilm formation. Furthermore, it could be shown that arginine also enhances *P. aeruginosa*s ability to build a biofilm grown on an abiotic surface [187].

However, even though co-cultivation was possible, one major aspect, the cultivation at the air-liquid interface, as it would be found *in vivo,* was not addressed. The same group further improved the model and cultivated the epithelial cells on permeable

filters at ALI conditions. Nevertheless, Moreau et al. did not keep the ALI conditions after the infection with *P. aeruginosa* PAO1 (MOI 20:1), but rather continued with LCC growth of the co-culture [27, 111, 160]. Interestingly, they found that biofilms grown on biotic surface develop much faster and to greater extent than abiotic grown biofilms. To achieve biofilms equal to those found when cultivated on top of human cells after 6 h, *P. aeruginosa* needs to be grown on an abiotic surface (e.g., plastic) for at least 24 h. In addition, also the resistance to antibiotics increased dramatically when biofilms were grown on cells [160, 196].

These facts support the hypothesis that a co-culture model is most relevant to evaluate novel anti-infectives and treatment options. The aim was therefore to further improve the above-mentioned models by keeping the ALI conditions during the whole experiment and also increase the possible time of the co-culture before the cells succumb to the infection. This would not only mimic the actual *in vivo* situation better, but would also allow the evaluation of aerosolized anti-infective treatments for safety and efficacy on that model.

6.2   Material and Methods

6.2.1   Direct infection approach

Since first biofilm development can already be observed a couple hours after an infection [160] with *P. aeruginosa*, the direct infection with the pathogen was used to achieve a co-culture of human bronchial epithelial cells and *P. aeruginosa* biofilms. Thus, an overnight culture of PAO1 (see section 5.2.1) was prepared and diluted to an OD_{600}~0.1. With reference to literature data and results from preliminary experiments a MOI of 20:1 was used to infect the human cells as soon as they built a tight monolayer and showed barrier properties (typically 7 after seeding for CFBE41o- and 12 days after seeding for Calu-3 cells, respectively). Since different amounts of the human cells were seeded in the beginning (see section 3.2.1) 15 µl for CFBE41o- and 30 µl for Calu-3 cells of the washed and diluted overnight culture had to be used to achieve a MOI of 20:1. To allow a better distribution of the bacteria on top of the cell monolayers these amounts of the overnight culture were diluted with M63 to achieve a total volume of 100 µl per well. Cells were infected with this solution and incubated for 1 h. After that time unattached bacteria and excessive medium were carefully removed and the basolateral medium changed to medium that was additionally supplemented with 0.4% arginine since this promotes biofilm formation and helps the cells survive the infection [112, 187, 197].

6.2.1.1   Determination of colony forming units (CFU)

The supernatants of each well were removed 24 h after the infection, transferred into Eppendorf® tubes and serially diluted (1:10) with PBS. A volume of 100 µl per samples was then plated on agar plates to determine the planktonic colony forming unit (CFU) fraction of the co-culture. Inoculated plates were incubated overnight at 37°C. Resulting colonies were counted the next day and the CFU calculated accordingly.

6.2.2   Light microscopy images of epithelial cells and co-culture

The co-culture was imaged 4, 8 and 24 h after the infection with *P. aeruginosa* PAO1 with a light microscope (Axiovert 25; Zeiss, Jena, Germany) and an attached digital camera (Canon EOS 600D, Canon, Tokio, Japan).

6.2.3 Scanning electron microscopy

For SEM images the supernatants from each well were removed carefully and the cells washed once with 100 µl apical and 1 ml PBS basolateral. Samples were then fixed with 3% glutaraldehyd for 2 h at RT and subsequently washed with PBS. Afterwards the co-culture was de-hydrated with a graded series of ethanol (each step for 10 min from 30-100%). The filters were then cut from their Transwell® support and mounted on aluminium stubs, which were equipped with a carbon disc, and next sputtered with gold (Quorum Q150R ES, Quorum Technologies Ltd, Laughton, UK). SEM images were taken under vacuum conditions with an EVO HD 15 microscope (acceleration voltage 5kV; Software SmartSEM, Zeiss, Jena, Germany).

6.2.4 Confocal laser scanning microscopy

For confocal images epithelial cells and *P. aeruginosa* PAO1 were pre-labelled with Vybrant® CFDA SE Cell Tracer Kit (Invitrogen) and CellTrace™ Far Red (Thermo Fisher Scientific), respectively, according to the manufacturer's protocol before coming in contact with each other. Briefly, the medium from epithelial cells was removed and cells were incubated with 500 µl PBS with Vybrant® CFDA Cell Tracer (5 µM working solution). After 15 min at 37°C the staining was removed and 500 µl of medium added apically to inactivate excessive dye. For the bacteria the overnight culture was washed and diluted to OD_{600}~0.1 as described under 5.2.2. The required amount of bacteria was pelleted and diluted in PBS containing CellTrace™ Far Red (10 µM working solution) for 20 min at 37°C. After that time 5x the staining volume of medium was added to inactivate unnecessary dye and bacteria were incubated for another 5 min. The bacteria were then pelleted again and resuspended in M63 to be used for the infection. After the appropriate infection period, the co-culture was fixed with 800 µl of 3% PFA from the basolateral side for 30 min at RT. Subsequently, nuclei were stained with DAPI (200 ng/ml, Life Technologies, Darmstadt, Germany) for 30 min at RT. The co-culture was washed once with 300 µl of PBS and filters cut from Transwell® support and placed on a glass slide, mounted with 1 drop of DAKO and covered with a cover slip. Samples were then examined with Zeiss LSM 710 confocal laser scanning microscope (Zeiss, Jena, Germany). Images were taken with a 1024×1024 resolution using the 25x water

immersion objective (Fluotar VISIR 25x/0.95 water) and processed with ZEN 2012 SP1 (black edition) software (Zeiss).

6.2.5 Preformed biofilm approach

For biofilm growth an overnight culture of PAO1 in exponential growth phase was washed and diluted to an OD_{600} 0.1 (CFU/ml ~ $5x10^7$) and 15 µL of this dilution were used to inoculate minimal medium M63 (M63, supplemented with 0.4% arginine) to a final volume of 200 µl in 24-well plates. Cultures were then incubated under static conditions at 37°C for another 24 hours to allow biofilm formation. This was confirmed in preliminary experiments with crystal violet staining (see section 5.3.1). To evaluate the MOI for the infection with the preformed biofilm, the CFU of such a 24 h old biofilm was measured by plating serial dilutions of the biofilm on agar plates as described under 6.2.1.1.

Tight monolayers of Calu-3 cells and CFBE41o- cells cultivated at ALI conditions were then infected with such preformed biofilms. Therefore, biofilms were scratched with a pipette tip from 24 well plates and one biofilm per well was transferred to the apical side of the epithelial cells. The so transferred biofilms were allowed to attach to the human cells for 1 h. Subsequently, unattached bacteria were removed from the apical side by carefully aspirating the supernatant with a pipette. Additionally, the basolateral medium was changed to cell culture medium that was additionally supplemented with 0.4% arginine. The integrity of the epithelial cells was checked 4 and 24 h after the infection with a light microscope (ZEISS, Vert.A1).

6.2.5.1 GFP labeled strain PAO1-GFP

Another possibility to visualize the bacteria is the use of a fluorescent labelled strain like ATCC® 10145GFP™. This strain carries a plasmid on which the green fluorescent protein GFPmut3 is encoded. This protein exhibits a green fluorescence under UV light (Excitation: 501 nm; Emission: 511 nm) and offers the possibility to visualize the bacteria without further staining. The same plasmid also carries an ampicillin resistance gene. To avoid the loss of the plasmid, and therefore the green fluorescence during culturing, it is mandatory to maintain a concentration of 300 µg/mL ampicillin at all times in the culture medium. Through this measure the bacteria will keep the plasmid as selective advantage when replicating, and thus the possibility to visualize them with

UV light. The growth rate of PAO1-GFP is a little lower than that of the regular PAO1 strain (data not shown). This is probably due to the fact that the PAO1-GFP bacteria face a higher selective pressure (i.e., culture medium with ampicillin), and also need time to double the plasmid containing the fluorescent protein when replicating. However, the growth rate does not necessarily influence the ability to form a biofilm [198]. In addition, biofilm formation is dependent on the nutrient conditions [183, 184]. Since these were kept the same for both PAO1 and PAO1-GFP, the produced biofilm after 24 h was considered equivalent in these studies.

6.2.6   Confocal laser scanning microscopy

The GFP labelled strain *P. aeruginosa* PAO1-GFP was used when confocal images had to be taken during the experiment. For cultivation and biofilm formation see 5.2.2. and 5.2.2.1. The co-culture was stained apically with propidium iodide (PI) (40 µg/ml PI in PBS) for 15 min and washed once with PBS prior to the fixation with 800 µl 3% paraformaledhyd from the basolateral side at RT for 30 min. Afterwards cell nuclei and extracellualar DNA were stained with 300 µl DAPI (200 ng/ml, Life Technologies, Darmstadt, Germany) for 30 min from the apical side at RT. In view of the fact that PI can only enter a cell and intercalate with its nucleic DNA when the membrane is already damaged, this staining allows to differentiate between dead cells (red nuclei from PI) and living cells (blue nuclei from DAPI). After DAPI staining the co-culture was washed once with 300 µl PBS and the filters were cut from the Transwell® inserts. They were transferred on glass slides mounted with one drop of DAKO and covered with a coverslip. Samples were examined with a Leica TCS SP8 microscope with AOBS beam splitter and Leica HyD detector (Mannheim, Germany). Images were taken with a 1024×1024 resolution using the 25x water immersion objective (Fluotar VISIR 25x/0.95 water) and processed with LAS X software (Leica).

6.3   Results and Discussion

6.3.1   A direct infection and live biofilm formation on the epithelial cells does not lead to a stable model

Similar to Moreau-Marquis et al. [160] the ALI cultivated epithelial cells were infected with an overnight culture of *P. aeruginosa* PAO1 (MOI 1:20), but opposed from their protocol ALI conditions were kept during the whole experiment. Images of the co-culture were taken after 4, 8 and 24 h with a light microscope or after fixation with a scanning electron or confocal scanning laser microscope.

Calu-3 cells seem to tolerate the infection very well for the first 4 h, as depicted in Figure 6.1 A. The cells form a tight monolayer with clearly visible cell boundaries and no signs of cell death. However, 8 h after the infection (Figure 6.1 B) Calu-3 cells appear to have a slightly rounder shape and first dead cells are visible on the apical side. Although cells still form an intact monolayer, these are already signs that the cells are starting to die due to the infection. Even more evident is the situation 24 h after the infection (Figure 6.1 C). No epithelial cells can be detected anymore, indicating that the monolayer was disrupted and more or less all Calu-3 cells died due to the overgrowth with the pathogen. Given that the uninfected control cells (Figue 6.1 D) still form a confluent monolayer 24 h after the infection experiment was started, it's evident that the cell death must indeed be caused by the infection with *P. aeruginosa*.

If the amount of mucus present on the cells at the time of the infection has an influence was not investigated in this thesis. But considering the role mucus plays for the CFBE41o- cells (see chapter 4.3.3), it might indeed improve the survival of the cells after the infection. In Figure 3.6 B a homogenous mucus layer was found on the cells grown at ALI conditions. In addition to these findings also several other studies show a confluent mucus layer on top of the Calu-3 cells after 10-14 days at ALI conditions [139, 144, 156, 199], while one group reported that mucus production might also depend on the used passage of the cells and a confluent mucus layer may take up to 21 days to be build up [145]. Although further experiments showed that the Calu-3 cells are more vulnerable to the *P. aeruginosa* infection and are therefore not the first choice as cell line for the *in vitro* model, the influence of the mucus amount present at the time of the infection might still be of interest and should be further investigated. Especially in view of the fact that mucus plays a major role in the CF pathogenesis and has influence

on how the pathogen can interact with the underlying epithelium [200], a longer cultivation time leading to a thicker mucus layer might prolong the survival of the infected Calu-3 cells.

Figure 6.1 Morphology of Calu-3 cells infected with *P. aeruginosa* PAO1. Light microscopy images of the co-culture cultivated at ALI conditions were taken 4, 8 and 24 h after the infection with PAO1 (MOI 20:1). At the first two time points (A and B) an intact monolayer is still evident. No Calu-3 cells can be recognized in the image taken 24 h (C) after the infection. Picture D shows the uninfected control after 24 h. Scale bar: 200 µm major image and 100 µm enlargement top right corner.

Similar results were obtained when the CFBE41o- cells supplemented with human mucus were infected with a MOI 20:1 of *P. aeruginosa* PAO1.

Four hours after the infection (Figure 6.2 A) cells still form a confluent monolayer with no indication of cell stress. Yet, another 4 h later CFBE41o- cells start to show a rounder shape (Figure 6.2 B), a sign for starting necrosis or apoptosis. First dead cells (see enlargement in 6.2 B) can be seen on top of the still intact monolayer. Another 16 h later, 24 h after the infection, no epithelial cells (indicated by clear cell boundaries as in

images 6.2 A and B) can be identified anymore. Just a mixture of biofilm and planktonic bacteria all over the well is visible. Here again the uninfected control of the human cells (Figure 6.2 D) indicates that the infection is cause for the evident cell death. Similar results obtained by Anderson et al. [112] and Moreau-Marquis et al. [111] show that the CFBE cells were not able to withstand the infection with *P. aeruginosa* for more than 8 h due to the rapid bacterial overgrowth. In addition, their used co-culture model was not kept at ALI conditions after the infection with *P. aeruginosa,* which is mandatory for aerosol application.
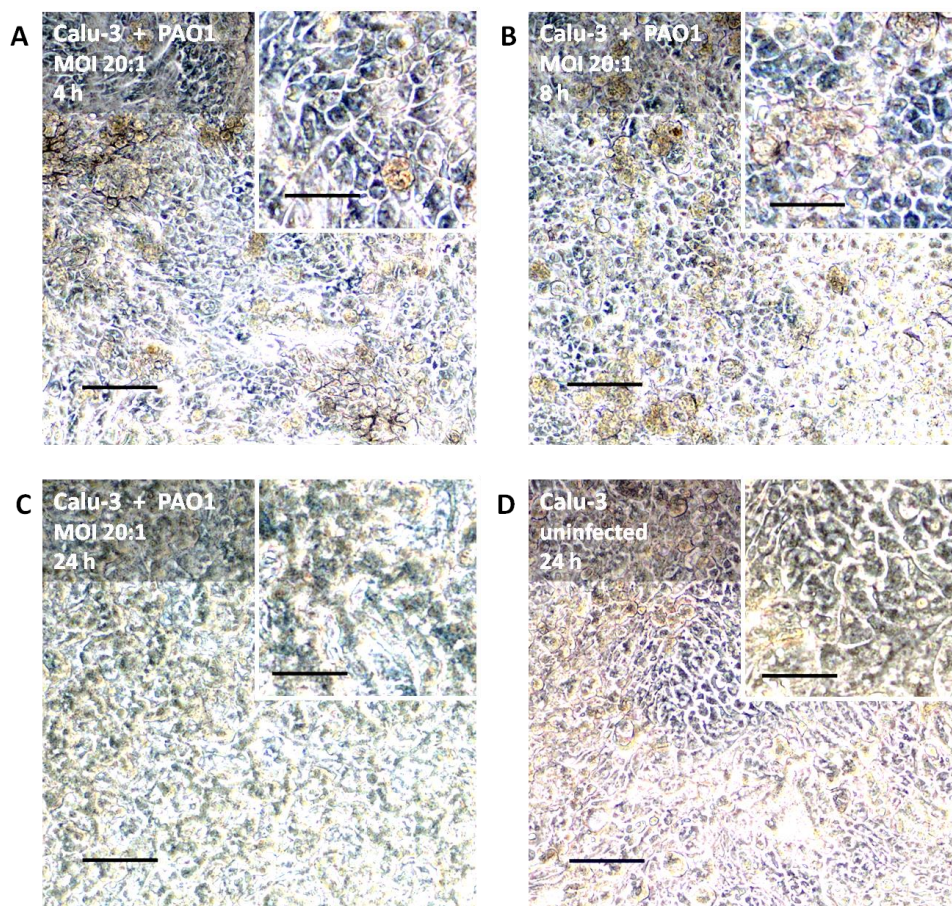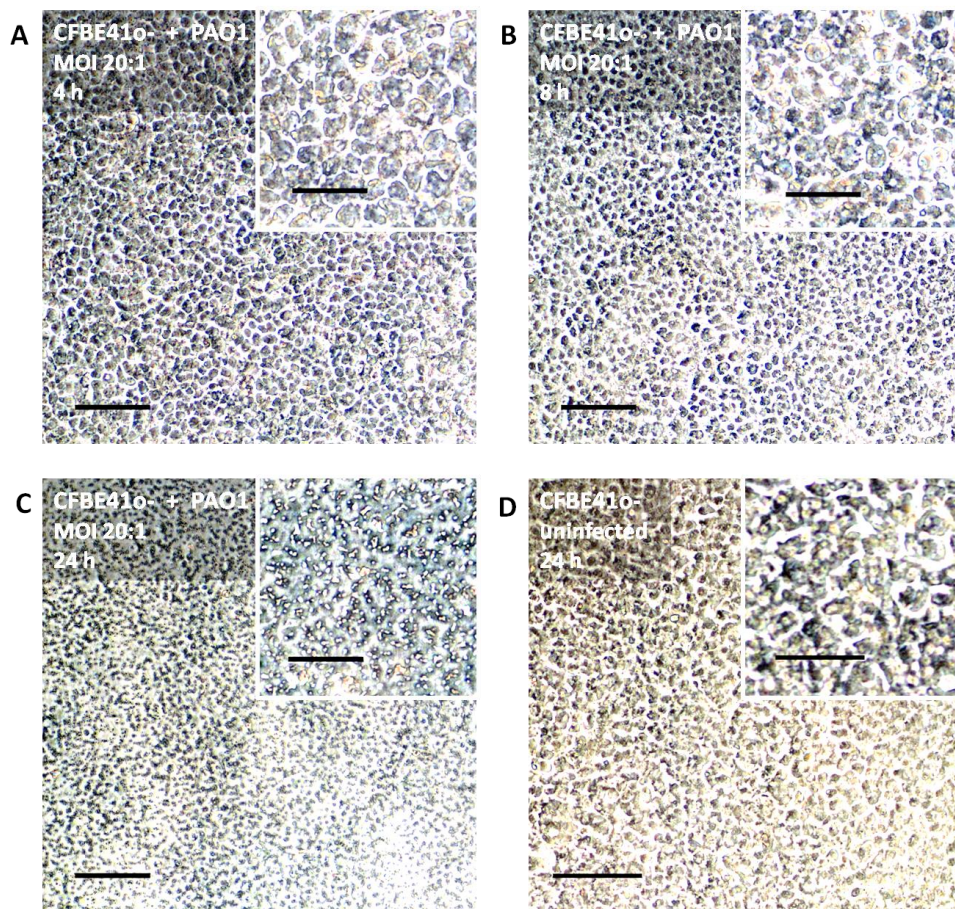

Figure 6.2 Morphology of CFBE41o- cells infected with *P. aeruginosa* PAO1. Light microscopy images of the co-culture cultivated at ALI conditions were taken 4, 8 and 24 h after the infection with PAO1 (MOI 20:1). At the first two time points (A and B) an intact monolayer is still evident. No clear cell boundaries of the CFBE41o- cells can be recognized in the image taken 24 h (C) after the infection. Picture D shows the uninfected control after 24 h. Scale bar: 200 µm major image and 100 µM enlargement top right corner.

One possible option to enhance the survival of the model could be to incorporate repeated washing steps into the experimental protocol. This would allow to reduce the number of planktonic bacteria, which are the leading cause of acute toxicity and cell death of the human bronchial epithelial cells due to their rapid growth. Also, a major threat in acute *P. aeruginosa* infections, the activation of the type 3 secretion system could be kept under control by such a measure [111, 112, 201, 202].

To get better insight into the status of the *in vitro* model after 24 h, the remains of the co-culture were fixed and SEM images were taken. As shown in Figure 6.3, a layer of biofilm grown bacteria is covering the Transwell® insert. No sign of the former epithelial cell monolayer can be detected and in the enlargements (Figure 6.3 right side) even the pores of the Transwell® filter are visible, a clear sign that human cells underneath the bacteria are destroyed. Notably, the bacteria seem to be embedded in some kind of matrix. This self-produced matrix is typical for biofilms and is responsible for the adhesion of the biofilm to surfaces and forms the scaffold for their 3-D architecture. It consists of the so-called EPS (extracellular polymeric substances). These include polysaccharides, proteins, lipids and nucleic acids. The eDNA (extracellular deoxyribonucleic acid) is a major component of the EPS, especially in *P. aeruginosa* biofilms. Here it is responsible for stabilization of the biofilm and functions as intercellular connector [32, 203]. Some of the eDNA from lysed epithelial cells might be a part of the matrix seen in Figure 6.3.
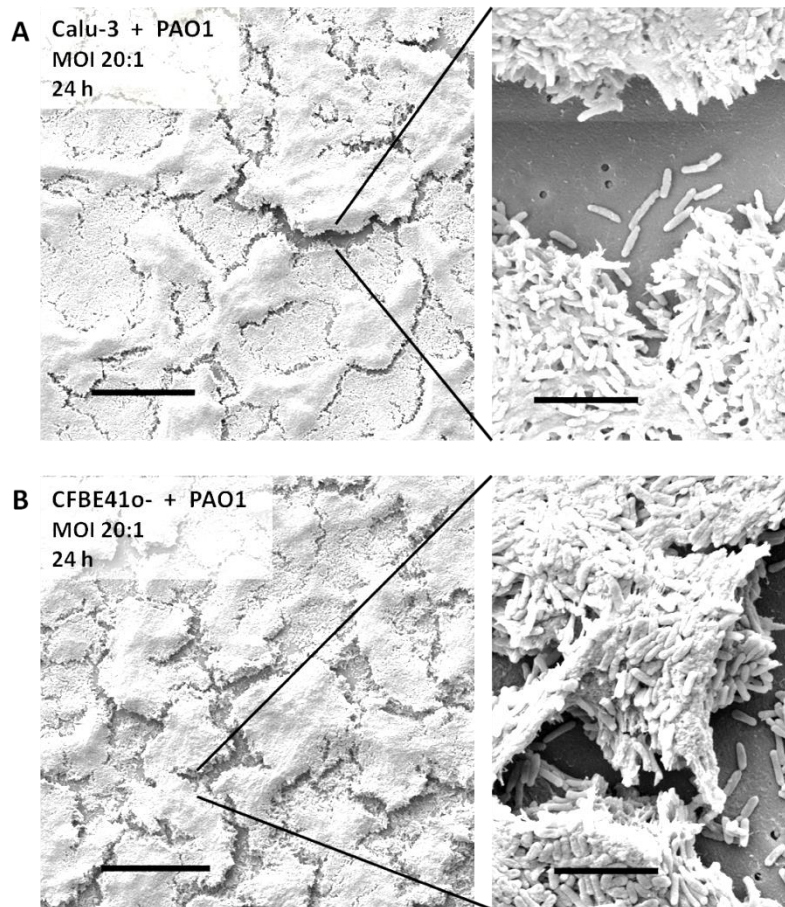
Figure 6.3 Morphology of Calu-3 and CFBE41o- cells infected with *P. aeruginosa* PAO1. SEM images of the co-culture of Calu-3 (A) or CFBE41o- (B) and PAO1 cultivated at ALI conditions were taken 24 h after the infection (MOI 20:1). At this stage only a biofilm of PAO1 covering the whole well but no viable epithelial cells are visible. Pores of the Transwell® filter membrane can be seen in the enlargements in the darker gray areas. This holds true for both Calu-3 (Figure 6.3 A) and CFBE41o- cells (Figure 6.3 B) in co-culture with PAO1. Scale bar: 50 µm left images and 5 µm enlargements on the right.

Even though cells did not survive the infection beyond 24 h and first signs of a starting cell death can be detected as early as 8 h after the infection, a biofilm development on a still intact monolayer can be seen already after 4 h.

The confocal images in Figure 6.4 show the CFBE41o- and Calu-3 cells in co-culture with *P. aeruginosa* PAO1 4 h and 8 h after the infection, respectively. At the earlier time point only small colonies of PAO1 (red color) can be seen on the intact monolayer of the CFBE41o- cells (Figure 6.4 A), as indicated by tight pattern of blue stained nuclei and green cytoplasma. Bacterial colonies increase during the course of the infection and 8 h after the infection approximately 25% of the Calu-3 cells are covered with

biofilm. Even though nuclei still form a tight pattern, their shape and also the blurry green color are signs for the starting cell death of the human lung epithelial cells.
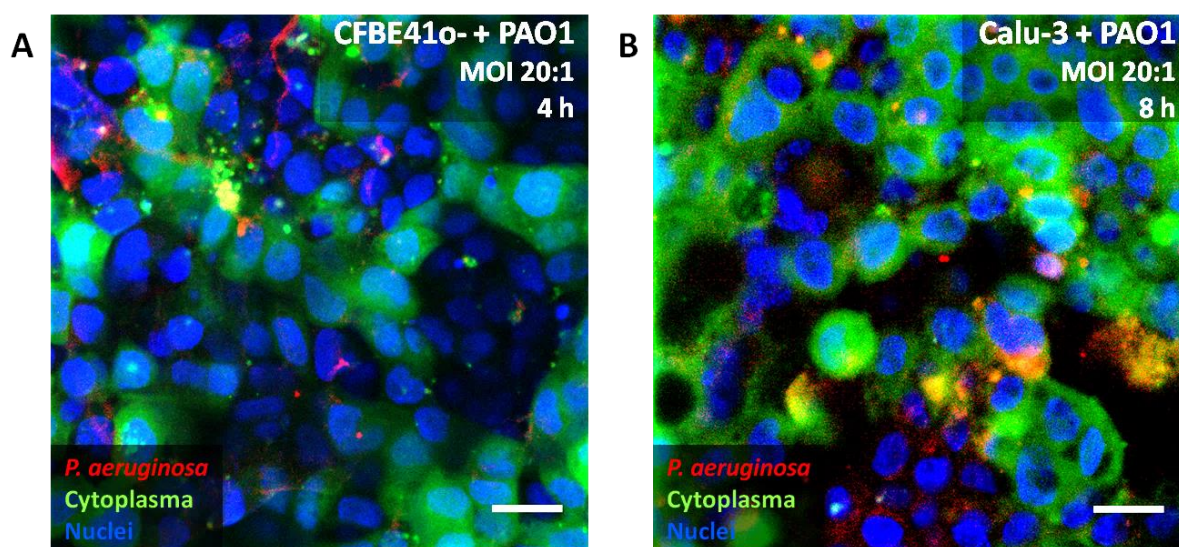
Figure 6.4 CLSM images of CFBE41o- or Calu-3 cells infected with *P. aeruginosa* PAO1. CLSM images of the co-culture of CFBE41o- (A) or Calu-3 (B) and PAO1 cultivated at ALI conditions were taken 4 h or 8 h after the infection (MOI 20:1), respectively. Human cells were stained with CFDA SE (green) and PAO1 with CellTrace™ Far Red (red). Nuclei were stained with DAPI. After 4 h small biofilm aggregations are visible on top of the CFBE41o- cells. Eight hours after the infection almost 25% of the Calu-3 cells are covered with attached bacteria. Scale bar: 20 µm.

Taken all the obtained results into account it is obvious, that a direct infection approach with biofilm development on the cells does not lead to a stable model where a rather mature biofilm co-exists with viable epithelial cells. To some extend a viable co-culture with some biofilm development could be achieved after 4 h. Furthermore, Moreau-Marquis et al. could show that biofilm formation on CFBE41o- cells is 1500-fold increased compared to abiotic biofilm growth after 6 h [160]. However, this does not reflect the situation *in vivo* with much older and more mature biofilms. Therefore, in order to achieve a stable model with both a mature biofilm and viable epithelial cells another approach had to be taken.

6.3.2 Application of a preformed biofilm of *P. aeruginosa* to achieve a co-culture model ready for testing of novel drug delivery systems

The direct infection with PAO1 and live biofilm development on the cells did not lead to a stable model suitable for further drug testing (see chapter 6.3.1). In order to get a more mature biofilm in co-culture with the human bronchial epithelial cells, the biofilm was preformed externally for 24 h and then transferred to the apical side of the cell monolayer. After the initial attachment phase of the transferred biofilm, planktonic bacteria were removed manual with a pipette and the co-culture was further kept at ALI conditions. This set up now allowed the application of aerosolized drugs for their safety and efficacy evaluation.

The CLSM images in Figure 6.5 show the co-culture of Calu-3 (A) or CFBE41o- (B) with biofilms of *P. aeruginosa* PAO1-GFP on top one hour after the infection. Both cell lines depict a tight monolayer with just a few dead cells visible on top. Notably, the CFBE41o-co-culture (Figure 6.5 B) appears to have more dead cells on top then the Calu-3 co-culture (Figure 6.5 A). However, this might be an artefact of the depicted section of the well (14% of the whole growth area), since in truth the Calu-3 cells are more susceptible to the infection. This will be discussed in detail in following chapter.

The green labelled bacteria form small clusters on top of the human cells, but do not cover them completely. Bearing in mind that the biofilm is transferred manually with a pipette to the apical surface of the epithelial cells and consequently has to endure some physical forces, can partially explain the small biofilm fractions found in Figure 6.5. Nevertheless, biofilms have astonishing self-healing properties as shown by Lieleg et al. [204]. Despite the fact that bigger biofilm agglomerates might have been destroyed by means of pipetting the biofilm from the culturing well of the pre-formed biofilm (see section 6.2.5) to the apical epithelial cell surface, the remaining smaller biofilm fragments will recover their former viscoelastic behaviour and the ruptured interactions between biofilm polymers and the bacteria will be re-established within minutes [204]. On the other hand, these smaller biofilm fractions as seen in the CLSM images (Figure 6.5) might even mirror the *in vivo* situation better. Here, the biofilm can be found only in some sections of the lung tissue rather than covering the whole surface comprehensively [205].
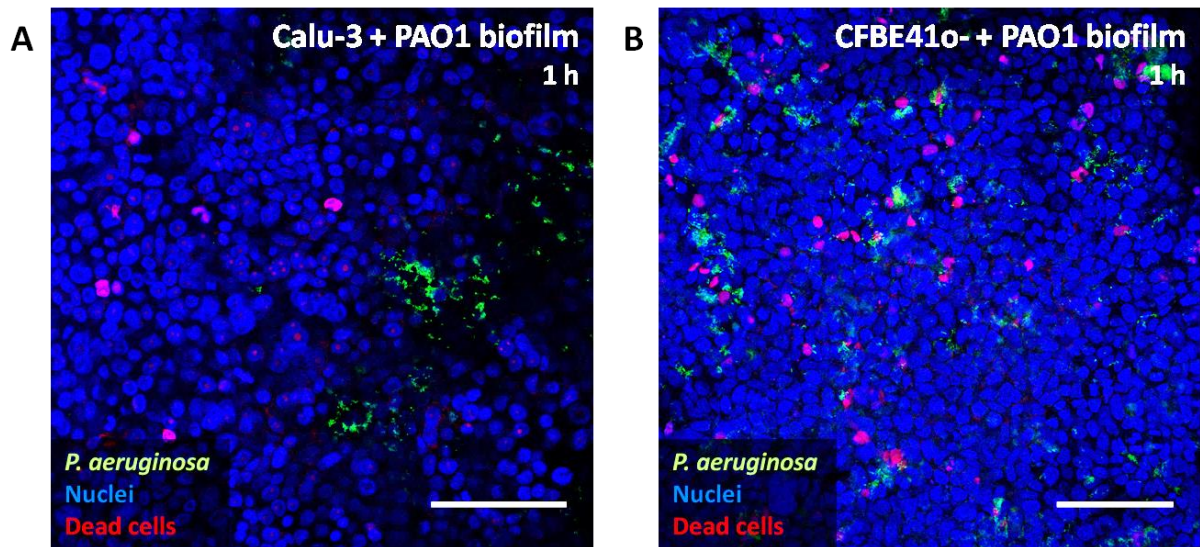
Figure 6.5 CLSM images of Calu-3 or CFBE41o- cells infected with *P. aeruginosa* PAO1 biofilms. CLSM images of the co-culture of Calu-3 (A) or CFBE41o- (B) and PAO1 biofilms cultivated at ALI conditions were taken 1 h after the infection. Nuclei were stained with DAPI (blue) and dead human cells were counterstained with PI (red). The fluorescent labeled strain PAO1-GFP (green) was used. One hour after the infection with the preformed biofilm a tight monolayer of epithelial cells with few dead cells on top is visible. The bacteria in the biofilm can be found in small clusters on top of the human cells. Scale bar: 100 μm.

Although the biofilm was cultivated for 24 h before being transferred to the epithelial cells and can therefore be considered as rather mature, it differs from biofilms grown on biotic surfaces. However, according to the literature [160, 196] at least 24 h of maturation on abiotic surfaces (e.g., plastic of culture dishes) are necessary to provide an equal mature biofilm as it would appear when grown for 6 h on a biotic surface (e.g., epithelial cells).

Another option for further improvement of the model would be to use even older biofilms (e.g., 48 h or 72 h old). Furthermore, there is the possibility to pre-grow the biofilm on human epithelial cells prior to transferring it to the actual model. This will inevitably lead to the death of those host cells but will also offer a more physiological substrate and could enhance the maturation of the biofilm.

To further evaluate the role of mucus in the CFBE41o- co-culture model and to get images of the biofilm fragments with higher magnification, SEM pictures of the co-culture were prepared 1 h after the infection (Figure 6.6). A tight monolayer of the epithelial cells with their typical small microvilli-like structures can be observed. A fragment of the previously applied mucus is indicated by the black arrow (Figure 6.5 left). Biofilm agglomerates (white arrows) of different sizes and also some single bacteria are visible on top of the human cells. The enlargement on the right shows that most of the bacteria are embedded in some kind of matrix or are connected by fibers. The presence of such biofilm fragments shows that with the transfer of the pre-grown biofilm a successful relocation of an already existing biofilm is possible. Seeing that this co-culture was fixed and imaged already 1 h after the infection, proofs that not only planktonic bacteria are transferred during the set-up, since the time into the infection would be rather to short two allow a biofilm formation of that extent. Similar to the CLSM image (Figure 6.5 B) the bacteria are not covering the whole cell surface but rather form agglomerates in certain areas.
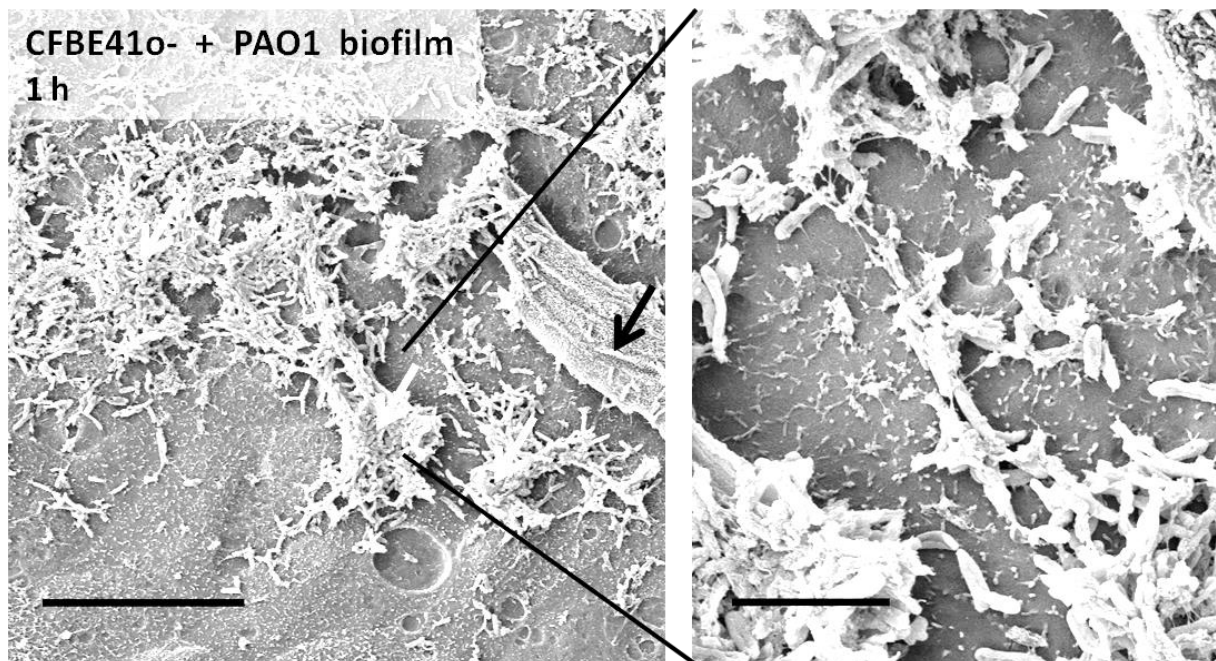
Figure 6.6 SEM images of CFBE41o- cells infected with *P. aeruginosa* PAO1 biofilms. Scanning electron microscopy images taken 1 h after the infection show an intact CFBE41o- monolayer in co-culture with PAO1 biofilms. On top of the monolayer some mucus fragments (black arrow), planktonic bacteria and biofilm agglomerates (white arrows) can be seen. The single bacteria can be considered as planktonic. The enlargement on the right shows microvilli like structures of the CFBE41o- cells and biofilm agglomerates. Scale bar: 100 µm left images and 5 µm enlargement on the right.

Further co-cultivation of the CFBE41o- cells with the preformed biofilm led to monolayer disruption and cell death as early as 4 h after the infection (data not shown). But considering that the bacterial load on the epithelial cells during the infection with the preformed biofilm is considerably higher as in the case of the direct infection (MOI 1800:1 preformed biofilm approach versus 20:1 direct infection), the earlier death of the host cells in this method can be explained.

Nevertheless, also in the case of the application of a preformed biofilm regular washing steps after certain time periods (e.g., 1 h) would additionally enhance the survival of the model by removing the planktonic bacteria as already discussed under 6.3.1 for the direct infection approach.

So even though several options for further improvement of the model seem feasible and are currently evaluated, the experimental set-up described here now allowed safety and efficacy testing of aerosolized antibiotic-loaded NPs against *P. aeruginosa* biofilms *in vitro* by maintaining air-liquid interface conditions during the entire course of the experiment.

6.4 Conclusion

To obtain an *in vitro* model mimicking the chronically infected lung of CF patients, the presence of a biofilm on top of the epithelial cells seemed mandatory. To further use this model for safety and efficacy testing of aerosolized drug delivery systems, ALI conditions were maintained during the whole experimental procedure. On the basis of previously published studies a direct infection of the epithelial cells with *P. aeruginosa* PAO1 was evaluated. Although first biofilm development could be detected just after 4 h and was even further increased 8 h after the infection, this approach did not lead to a stable model, since first signs of a starting cell death of the human cells were evident at the 8 h time point as well. Twenty-four hours after the infection only a biofilm of *P. aeruginosa* remained on the Transwell® filters.

To achieve a model with viable epithelial cells and a more mature biofilm a different approach had to be taken. With the application of a 24 h preformed biofilm on top of monolayers of bronchial epithelial cells an experimental protocol could be established that allows the testing of aerosolized antibiotic NP formulations against *P. aeruginosa*. Even though the epithelial cells showed signs of a starting cell death already after 4 h, a longer co-cultivation was not necessary since the two major components of the *in vitro* model, a tight epithelial monolayer with mucus, and a mature *P. aeruginosa* biofilm, were already present. Therefore, the preformed biofilm approach offers an appropriate time window to test aerosolized formulations against *P. aeruginosa*.

7 Treatment of the co-culture with ciprofloxacin loaded PLGA nanoparticles

Parts of this chapter were published or will be submitted for publication:

Nazende Günday Türeli, Afra Torge, Jenny Juntke, Bianca C. Schwarz, Nicole Schneider-Daum, Akif Emre Türeli, Claus-Michael Lehr, Marc Schneider
"Ciprofloxacin-loaded PLGA nanoparticles against cystic fibrosis *P. aeruginosa* lung infections"; published

Jenny Juntke, Xabier Murgia, Nazende Günday Türelib, Akif Emre Türeli, Cristiane Carvalho-Wodarz, Marc Schneider, Nicole Schneider-Dauma, Claus-Michael Lehr
"Novel co-culture model of human airway cells and *P. aeruginosa* biofilms"; in preparation

The author of the thesis made the following contribution to this chapter:

Planned and performed all cell culture experiments, measured cytotoxicity of nanoparticle formulations, TEER and viability after bacterial infection, cultivated bacteria and measured OD_{600} and CFU; prepared co-cultures for confocal analysis and scanning electron microscopy and took the SEM images. The author of this thesis analyzed and interpreted all obtained experimental data and wrote the chapter.

Mucus disk preparation and confocal laser scanning microscopy images were conducted by Dr. Xabi Murgia.

Nanoparticle preparation and lyophilization were handled by Dr. Nazende Günday Türeli.

7.1 Introduction

The chronic infection with *P. aeruginosa* already at a young age and the associated lung inflammation and tissue destruction are the major cause for morbidity and mortality in CF patients [57, 58]. To prevent early bacterial infections reaching a chronic state, an antibiotic eradication therapy (AET) is administered as soon as possible after diagnosis of *P. aeruginosa* infection. However, there is no recommended therapy regime for *P. aeruginosa* infections at the moment [24, 60]. In almost all of the published AET studies the use of inhalation therapy is a key element. It typically consists of inhaled colistin or tobramycin with or without the additional administration of an oral antibiotic like ciprofloxacin [60, 206-208]. Also, the use of intravenous antibiotics was evaluated in some AET protocols [209, 210]. Although dose, duration of therapy, number of cycles and combinations of drugs vary in those studies, no AET protocol has shown clear superiority [24, 61]. Besides, the reported success rates in eradicating *P. aeruginosa* from AET studies vary between 61-100%. So even though mean eradication rates of 81.2% can be achieved with some form of AET, there are obviously patients for whom this therapy is unsuccessful [24].

Once a chronic *P. aeruginosa* infection is established, a complete eradication of the pathogen is nearly impossible [61]. In order to at least maintain the lung health of the affected CF patients, administration of chronic suppressive antibiotics and enhancers of the mucociliary clearance have proven useful. The therapy here consists of inhaled tobramycin, aztreonam lysine, colistin, ifacaftor, dornase alpha, mannitol, corticosteroids, and/or hypertonic saline often in combination with oral antibiotics, corticosteroids and ibuprofen [9, 211]. Although the local drug concentration can be increased when administering these drugs via inhalation [59], therapies fail to completely eradicate *P. aeruginosa*. This is associated with the pathogen's ability to build antibiotic resistant biofilms. Such bacterial communities where the pathogens live in a self-produced matrix of exopolysaccharides, DNA and proteins are much more resistant to antibiotic treatment than their planktonic counterparts [28, 32]. One major problem in treating such bacterial infection is the biological barrier represented by the thick mucus/ biofilm mesh, which often leads to failing penetration, low diffusion rates of the antibiotic into the biofilm, and inactivation of the antibiotic agent by biofilm components. Furthermore, nutrient depletion in parts of the biofilm might result in

bacteria entering dormant state, in which they are less susceptible to antibiotics [28, 34-36, 147].

A novel approach to improve the treatment of chronic *P. aeruginosa* infections with antibiotics is their delivery by NPs [36, 71]. In contrast to the bare molecule, these carrier systems should be able to interact with the CF mucus and bacterial biofilm and be able to release their antibiotic cargo in a controlled manner immediately at the site of action. To enable those NPs to penetrate the thick mucus and biofilm mesh typical for cystic fibrosis, they need to have a suitable particle size, usually <200 nm [212-214]. Also their surface charge (Zetapotential) is of importance, since mucoadhesion is most prominent in positively charged NPs [214-216]. Such mucoadhesive particles (MAPs) adhere to the top layers of the mucus and are therefore not able to reach deeper zones of the mucus/biofilm mesh, as desired for particles destined to treat chronic *P. aeruginosa* infections where the bacteria hide in a thick mucus/biofilm mesh. In addition, such MAPs might not spread homogeneously within the mucus/biofilm, which could lead to an unbalanced delivery of the inhaled particles and possibly a decreased drug efficacy [217].

However, through sophisticated engineering of the NPs surface, their ability to penetrate the mucus/biofilm mesh or interact with its components might be further improved [36, 171]. Especially PEGylation of the NPs surface has gained attention, since it can enhance the mobility of those particles in mucus by shielding their surface charge, minimize adhesive interaction between the particle and mucin fibres, and making them more hydrophilic [213, 217-220]. Also for NPs stabilized with a block copolymer like Pluronic® (non-proprietary name poloxamer; (poly(ethylene glycol)-poly(propylene oxide)-poly(ethylene glycol) PEG-PPO-PEG), an enhanced mobility in mucus was described [199, 212, 221]. But since these block copolymers contain high numbers of PEG chains, the similar behaviour compared to PEGylated NPs comes as no surprise. Of note, effectiveness of such PEG and Pluronic® coatings is closely related to the molecular weight (MW). Nanoparticles densely coated with a low MW PEG show good mucus penetration, whereas high MW PEG can lead to mucoadhesion [222]. Furthermore, also the MW of the PPO segment of Pluronic® is of importance. It was found that Pluronic® types with a PPO MW ≥3kDA were able to actively shield the NPs charge and therefore also decrease their mucoadhesion [221].

Engineering NPs of a desired size and charge and additional favourable surface properties is not trivial. Traditional NP precipitation methods lack control over the growth process, resulting in varying NP parameters such as size and polydispersity index (PdI) [212]. However, considering that particle size and distribution are important quality characteristics not only for pulmonary NPs, a precise preparation technique was needed.

With help of the MicroJet Reactor (MJR) technology (Figure 7.1) it is possible to produce NPs under controlled condition. This is a technology of two impinging jets (solvent and non-solvent), which collide in a gas-filled chamber at an angle of 180°. By controlling flow rates, temperature and the gas flow (nitrogen) from the top opening, the particle size can be adjusted. Produced NPs can be collected from the fourth opening on the bottom [223]. These particles are made of the biocompatible and biodegradable Poly(lactic-co-glycolic) acid (PLGA) [224, 225] stabilized and coated with Pluronic® F68 (synonym: poloxamer 188). The antibiotic cargo is the fluoroquinolone ciprofloxacin, which is commonly used for treatment of chronic *P. aeruginosa* infections in CF patients. The drug-loaded NPs were then tested for safety and efficacy on the human bronchial epithelial cells alone and on the preformed biofilm co-culture model.
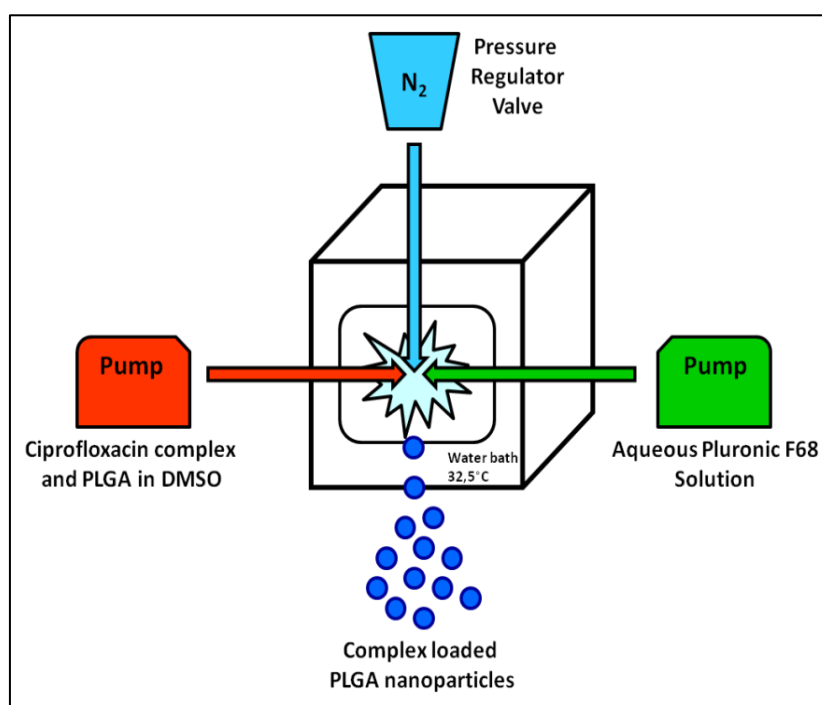

Figure 7.1 Schematic of Micro Jet Reactor (MJR). The MJR set up consist of two pumps for solvent and non-solvent. Their streams collide in the middle of a gas filled chamber controlled by N_2 flow. Resulting NPs can be collected from the bottom opening. The whole system is immersed in a 32.5°C water bath in order to control the process temperature.

7.2 Material and methods

7.2.1 Nanoparticle preparation and characterization

NPs were prepared and characterized by Dr. Nazende Günday-Türeli from MJR Pharmjet. Briefly, they were produced with an optimized nanoprecipitation method [212, 226] for which the MJR (MicroJet Reactor) technology was used. For the NPs used in these studies the solvent system contained 2% ciprofloxacin-SDS complex (equivalent to 1% ciprofloxacin) dissolved in a 0.5% PLGA in DMSO solution, whereas the non-solvent system consisted of a 0.25% Pluronic® F68 in water solution. Both solutions were delivered to the MJR in a 1:10 flow rate with Smartline S100 pumps (Knauer, Munich, Germany). The angle of the two impinging streams was 180°. Nitrogen can be used to control the mixing time in the chamber and therefore can control the particle size. However, this was not the case for the here produced particles. Therefore, the top opening was sealed. Both MJR and the solvent delivering capillaries were submerged in a water bath with the purpose of ensuring a system temperature of 32.5°C. Subsequently the resulting NPs were collected from the bottom opening and purified with Visking dialysis membrane with a molecular weight cut-off (MWCO) of 10 kDa (VWR, Darmstadt, Germany).

7.2.2 Cytotoxicity studies

In order to evaluate the cytotoxic potential of the NPs and their single components (e.g., sodium dodecyl sulfate (SDS), ciprofloxacin as free drug, SDS-ciprofloxacin complex, complex-loaded NPs and unloaded (blank) NPs) increasing concentrations (from 50 - 500 µM) of these were applied on human bronchial epithelial cells. For that reason, Calu-3 and CFBE41o- cells were seeded with a density of 125,000 cells/cm² and 62,500 cells/cm², respectively. Three days after seeding the cells into tissue culture plates, they were incubated with the above mentioned loaded NPs or their single components dissolved in KRB supplemented with 10% FCS. As negative control (0% viability) cells were treated with 1% Triton-X 100 dissolved in KRB and as positive control (100% viability) cells where only incubated with assay medium (KRB+10% FCS). The supernatant (SN) of the 500 µM loaded NPs was obtained by centrifugation of 2 ml NPs suspension in a Centrisart® I (MWCO 300 kDa; Sigma Aldrich) at 2000 g for 15 min. SN was then applied as second positive control to evaluate potential toxic effects of

solubile factors resulting from the NP preparation. Cell viability was assed 4, 8 and 24 hours after incubation with the test compounds with an ToxiLight™ bioassay kit according to the manufacturer's protocol with one minor modification. Just 10 µl of the cell supernatants were used for analysis. Viability values were calculated by subtracting the resulting cytotoxicity values from 100%.

7.2.3   Nebulization of nanosuspension and Panotile eardrops

To achieve a more reasonable application of the nanosuspension on the ALI co-culture than as pure solution, nebulization with an Aerogen® Solo chamber attached to the Aeroneb® lab micropump control unit (Aerogen Ltd., Galway, Ireland) was used to distribute the suspension on the samples. This device works with a vibrating palladium mesh to create an aerosol. A volume of 200 µl of NP suspension (350 µM lyophilized complex-loaded PLGA NPs dissolved in KRB supplemented with 10% FCS) or blank KRB with 10% FCS (as negative control) was added to the Aerogen® Solo chamber and continuously nebulized into the corresponding wells 1 h or 4 h after the infection with the preformed bacterial biofilm. In order to guide the created aerosol directly into the well, a nebulisation chamber developed in-house was attached to the Aerogen® Solo chamber.

As comparison Panotile® CIPRO eardrops (1 ml contains: 2.32 mg ciprofloxacin hydrochloride equal to 2 mg/ml ciprofloxacin; additional ingredients: glycerol, polysorbat 20, sodium acetate, acetic acid 99%, methyl cellulose, hydrochloric acid and sodium hydroxide and water for injection) were chosen and applied in the same manner as the NPs.

7.2.3.1 Recovery rate of nebulized nanocarriers

To estimate the amount that landed on the co-culture after nebulization, 200 µl of the nanosuspension (350 µM) was nebulized into empty wells of a 12 well plate. After settling of the aerosol cloud the content of each well was recovered by pipetting the resulting liquid into Eppendorf® tubes. Samples were diluted 1:100 with KRB and the concentration was measured with an UHPLC method (Dionex Ultimate® 3000 UHPLC with an Accucore™ column (RP 18, 150 mm x 2.1 mm, 2.6 µm, Thermo Fisher Scientific Co., Waltham, MA, USA)). A solvent mixture of 0.02 M Na_2HPO_4 (adjusted to a pH

of 2.7) and acetonitrile in a ratio of 77:23 was used. Temperature in the column oven was set to 25°C. Flow rate during quantification was 0.2 ml/min with a resulting retention time of ciprofloxacin at 4.2 min.

7.2.4 Transepithelial electrical resistance (TEER)

To measure the barrier properties of the epithelial cells at the end of the experiment (e.g., 24 h after the infection) the medium from both compartments was removed, replenished with HBSS (Gibco™) (500/1500 µl) and incubated for 30 min at 5% CO_2 atmosphere and 37°C. Afterwards TEER was measured.

7.2.5 Viability of human cells during and after the infection

7.2.5.1 Viability assay – MTT

Subsequently after measuring the TEER values (see section 7.2.4), the ALI conditions were restored and an MTT assay was performed to assess the viability of the cells. The negative control (0% viability) was treated with 1% Triton X-100 (Sigma-Aldrich) in HBSS for 30 min at 37°C. After that time the co-culture was washed (300 µl HBSS apical and 500 µl basolateral) and all wells incubated with 300 µl MTT solution (500 µg/ml) apical, and 500 µl HBSS basolateral for 4 h at 37°C and 5% CO_2 atmosphere. Following that, 250 µl of apical MTT solution was discarded and replenished with 200 µl DMSO (Sigma-Aldrich) to solubilise the resulting formazan crystals. Thirty minutes later the absorption at 550 nm was measured with a plate reader (TECAN, infinite M200 pro, Männedorf, Switzerland).

7.2.5.2 PI staining and confocal scanning microscopy

The co-culture was stained apically with propidium iodide (PI) (40 µg/ml PI in PBS) for 15 min and washed once with PBS prior to the fixation with 800 µl 3% paraformaledhyd from the basolateral side at RT for 30 min. Afterwards, cell nuclei and extracellular DNA were stained with 300 µl DAPI (200 ng/ml, Life Technologies, Darmstadt, Germany) for 30 min from the apical side at RT. In view of the fact that PI can only enter a cell and intercalate with its nucleic DNA when the membrane is already damaged, this staining allows to differentiate between dead cells (red nuclei from PI) and living cells (blue nuclei from DAPI). After DAPI staining the co-culture was washed once with 300 µl PBS

and the filters were cut from the Transwell® inserts. They were transferred on glass slides mounted with one drop of DAKO and covered with a coverslip. Samples were examined with a Leica TCS SP8 microscope with AOBS beam splitter and Leica HyD detector (Mannheim, Germany). Images were taken with a 1024×1024 resolution using the 25x water immersion objective (Fluotar VISIR 25x/0.95 water) and processed with LAS X software (Leica).

7.2.6 SEM

For SEM images the preparation of the co-culture samples with NP treatment was performed 24 h after the infection. The supernatants from each well were removed carefully and the cells washed once with 100 µl apical and 1 ml PBS basolateral. Further sample preparation was conducted as described under 6.2.3.

7.2.7 CFU determination of planktonic and biofilm bacteria

7.2.7.1 Determination of planktonic CFU

The supernatants of each well were removed 24 h after the infection, transferred into Eppendorf® tubes and serially diluted (1:10) with PBS. A sample volume of 100 µl was then plated on agar plates to determine the planktonic CFU fraction of the co-culture. Inoculated plates were incubated overnight at 37°C. Resulting colonies were counted the next day and the CFU calculated accordingly.

7.2.7.2 Determination of biofilm CFU

To also assess the biofilm CFU of the co-culture after treatment with NPs the medium from TEER measurement (see 6.2.4) was removed carefully. Subsequently, 500 µl of PBS with 0.1% Triton X-100 (Sigma Aldrich) were added apically. The Transwell® plate was placed in a bacterial shaker at 37°C and 150 rpm for 20 min. The co-culture lysates were then scraped from the wells, transferred into Eppendorf® tubes, vortexed thoroughly for at least 3 min, serially diluted and plated on agar plates. CFU was determined the next day as described under 7.2.7.1.

7.2.8 Statistical analysis

Data are presented as mean ± standard error of the mean (SEM) from 3 independent experiments (n≥9) for safety evaluation of the NPs. Viability of the co-cultured cells after treatment was determined in 5 independent experiments (n≥5). For the efficacy testing of the NPs on the co-culture (CFU) ≥3 separate experiments with n≥8 were conducted. Statistical analysis was performed with the GraphPad Prism 5 software. The differences in viability were compared with a Two-way ANOVA and a Bonferroni post test; * $p < 0.05$, *$p < 0.01$ and *** $p < 0.001$ were considered significant.

7.3 Results and Discussion

7.3.1 Ciprofloxacin-complex loaded PLGA nanoparticles are well tolerated by human cells

The NPs used in these studies were prepared with an optimized nanoprecipitation method using the MicroJet Reactor (MJR). With this MJR technology nanoparticles can be produced under controlled conditions [226]. The resulting nanoparticles were of spherical shape and had a size of 190 ± 29 nm with a PDI of 0.089 [212]. They are composed of PLGA and Pluronic® F68, and were loaded with a complex of ciprofloxacin and SDS.

The polyester PLGA is a biocompatible and biodegradable co-polymer of poly lactic acid (PLA) and poly glycolic acid (PGA). These two monomers result again when PLGA undergoes hydrolysis. It was found that a higher content of glycolic acid in the oligomer resulted in a faster degradation rate. Glycolic acid and lactic acid can be easily metabolized via the Krebs cycle. Thus, PLGA is associated with minimal systemic toxicity. It's approved by the Food and Drug Administration (FDA) and the European Medicine Agency (EMA), although not for pulmonary applications yet [224, 225].

Block copolymers like Pluronic®, also known as poloxamers, are so called generally recognized as safe (GRAS) materials and are accepted pharmaceutical excipients in the US and British Pharmacopoeia. These copolymers consist of blocks of ethylene oxide (EO) and propylene oxide (PO) in an EO_x-PO_y-EO_x structure, giving them an amphiphilic character. They are widely used components of drug delivery systems because of their multiple effects [221, 227, 228]. The orange book, FDAs list of approved drug products, lists 57 drug products using poloxamers as excipients in 2018. The Pluronic® F68 (poloxamer 188) is used in almost half of them (28 approved drug products with this poloxamer) [229].

Due to their ability to incorporate into biological membranes and afterwards translocate into the cells, they can affect various cellular functions. For instance, it was shown that Pluronic block copolymers decrease the ATP synthesis, inhibit drug efflux transporters like MRP and Pgp, alter the mitochondrial respiration and enhance the apoptotic signal transduction. Furthermore, they can modify the cells gene expression [230]. These properties make them extremely valuable for drug delivery systems intended for cancer treatment or gene therapy. However, also enhanced bioavailability

and activity of antibacterial drugs against many microorganisms was reported for Pluronic® block copolymers [230]. Even though these polymers (e.g., Pluronic® F68) possess no antimicrobial properties of their own, they can markedly increase the activity of antibacterial drugs such as hexetidine when used in concentrations well below their critical micelle concentration [231].

In the NPs produced for these studies Pluronic® has a stabilizing function. In addition, the PEG chains incorporated in the NP shell through the use of Pluronic® might help to facilitate mucus and biofilm penetration of the NPs by increasing their mobility in these barriers and minimizing interactions with its components [226]. If the stabilizer also increases the activity of the here used drug ciprofloxacin will therefore be of interest in this work.

Even though it could be shown that Pluronic® F68 itself does not induce cell mortality, an increase in cytotoxicity was observed in A549 cells, but not in Calu-3 cells when PLGA NPs stabilized with Pluronic® F68 where applied. This effect might be due to the high amount of NPs internalized into the cells, which is related to the stabilizer Pluronic® F68, since PLGA NPs formulated with different stabilizers (e.g., polyvinyl alcohol or chitosan) were internalized less frequently into the cells [199, 232].

As model drug the broad-spectrum fluoroquinolone, ciprofloxacin was chosen. It is already commercially available especially for treatment of Gram-negative bacterial infections (e.g., *P. aeruginosa*) but it also shows efficacy against Gram-positive pathogens (e.g., *Staphylococcus aureus)* [226]. However, the only commercially available ciprofloxacin formulations for the treatment of pulmonary infections are oral or intravenous drug forms. Pulmonary drug delivery on the other hand would lead to much higher local drug concentration in the airways, while at the same time decreasing the systemic exposure and therefore possible side effects [59]. Even though many studies with ciprofloxacin loaded nanocarriers (e.g., liposomes, nanoparticles or nanoplexes) for pulmonary application have been conducted and show promising results [212, 233-243], no inhalable ciprofloxacin formulation is on the market yet.

Of note, only a dry powder for inhalation (DPI) loaded with ciprofloxacin from Bayer (BAYQ3939) and a formulation containing both ciprofloxacin loaded liposomes and free ciprofloxacin from Aradigm (ARD-3150 Linhaliq™) completed phase III of clinical studies [244]. Nevertheless, even though results from the ciprofloxacin DPI studies (RESPIRE trials conducted by Bayer [243]) were promising, data showed an increase in

ciprofloxacin-resistant *P. aeruginosa* in patients that received the ciprofloxacin DPI compared to those treated with placebo. Also due to other study discrepancies the FDAs advisory panel voted against the approval of the drug [245], which will most likely result in the rejection of the new drug application (NDA). Bayer stopped further development on the DPI for the time being according to their annual report 2017 [246]. Also Linhaliq™, formally known as Pulmaquin® (tested in two phase III trials ORBIT-3 and ORBIT-4 by Aradigm) showed promising results [247] but did not get an approval from the FDA when filing for NDA due to mixed data from the two phase III clinical studies. Aradigm needs to perform a new phase III study before resubmission of NDA [248, 249]. Furthermore, both products were developed and tested for non-CF bronchiectasis and therefore only off-label-use would offer new treatment options for CF patient. Another liposomal ciprofloxacin formulation from Aradigm (ARD-3100 Lipoquin) intended for CF treatment is currently in phase II of clinical studies showing promising results [250].

Nevertheless, taken together this shows the importance of further research on ciprofloxacin-loaded nanocarriers.

Ciprofloxacin suffers from a low solubility and therefore low bioavailability. The drug is poorly soluble in organic solvents and a pH-adjusted aqueous solvent would lead to a faster degradation of the PLGA nanocarrier [251, 252]. Therefore, a drug loading of more than 5% with conventional particle preparation methods cannot be achieved [251]. In order to improve drug loading into the PLGA NPs the counter-ion method was utilized. To proof that with this method a higher drug loading is possible, a complex between ciprofloxacin and the counter-ion sodium dodecyl sulfate (SDS) was formed. The complex formation enhanced the solubility in organic media by 80-fold. In addition, also the antibacterial activity of ciprofloxacin increased in a synergistic way. This is probably due to a steric protection of ciprofloxacins functional group by SDS. Moreover, the drug loading efficiency was improved by complex formation and a drug loading of 14% ciprofloxacin could be achieved. These findings exceed current results for NP loading with this antibiotic considerably [251].

In order to exclude any cytotoxicity triggered by the drug-loaded NPs or their individual components, they were applied on the Calu-3 and CFBE41o- cells in increasing concentrations. This also allowed determining the optimal dose for the following treatment of the co-culture.

Using the ToxiLight™ bioassay kit the viability of Calu-3 and CFBE41o- cells was determined. Both ciprofloxacin complex-loaded and drug free NPs, as well as their single components (i.e., ciprofloxacin, SDS, ciprofloxacin-SDS complex) were applied in increasing concentrations (50-500 µm) to the cells. As additional control also the supernatant of the complex-loaded NPs was evaluated for any cytotoxic potential. Viability of the cells was measured after 4, 8 and 24 h. Results of the lowest and the two highest applied concentrations of all tested compounds are shown in Figure 7.2.

Ciprofloxacin (Cipro, Figure 7.2 A) exhibits no cytotoxic potential neither in Calu-3 or CFBE41o- cells. Due to the mentioned solubility issues only the concentrations 50 and 100 µm were tested.

SDS (Figure 7.2 B) decreased the cell viability in the highest applied concentration (500 µM) already significantly after 8 h. This was the case for both cell lines. However, this was no surprise, since SDS is a surfactant interfering with the cell membrane. Besides, one has to considering that the formed complex was used as proof-of-concept. In future also other, less toxic, excipients can be used as counter-ions. Thus, the here measured SDS toxicity should not be overrated. Besides, the second highest concentration (350 µm) did not show any cytotoxic potential after 24 h.

As alternative counter-ion 1,2-Dipalmitoyl-sn-glycero-3-phosphatidic acid, sodium salt (DPPA) can be utilized. DPPA is biodegradable and easily synthesized precursor of natural lung surfactant [251], and thus a suitable substitute to SDS.

The free Cipro-SDS complex (Figure 7.2 C) was well tolerated by the CFBE41o- cells even in the highest concentration. However, the Calu-3 cells showed a significant reduction of cell viability to 85 ± 4% after 24 h incubation with 500 µM complex solution.

Drug-free NPs (Figure 7.2 D) were well tolerated by the bronchial cells. Nonetheless, a significant viability reduction was seen after 24 h in the CFBE41o- cells. But since this reduction is from 104 ± 1% and 103 ± 1% after 4 h and 8 h, respectively, to 99 ± 1% this result can probably be neglected.

Similar results were obtained for the SN of the drug-loaded NPs (Figure 7.2 E). CFBE41o- cells showed significantly lower viability at the 24 h time point. The values decreased from ~110% to 106 ± 2%. However, considering that the viability is still around 100% this small drop can most likely be disregarded as well.

The drug-loaded NPs in their highest concentration (Figure 7.2 F) decreased the viability from ~100% at 4 h and 8 h to 76 ± 9% and 81 ± 8% after 24 h incubation in the Calu-3

and CFBE41o- cells, respectively. Since the drug-free NPs did not show cytotoxic potential, it was concluded that the observed toxicity of the drug-loaded NPs was directly linked to the Cipro-SDS complex. This drop in viability was highly significant and even though more than 75% of the cells are alive after 24 h the second highest concentration (350 µM) was chosen for further experiments.

It can be concluded that the NPs show a dose dependent toxicity, but are otherwise well tolerated by the epithelial cells. At the same time, they show no toxic effects in the second highest tested concentration (350 µM).

Thus, proofing the safety of the drug-loaded NPs, the aim was now to show the efficacy of the DDS on the established *in vitro* co-culture model.
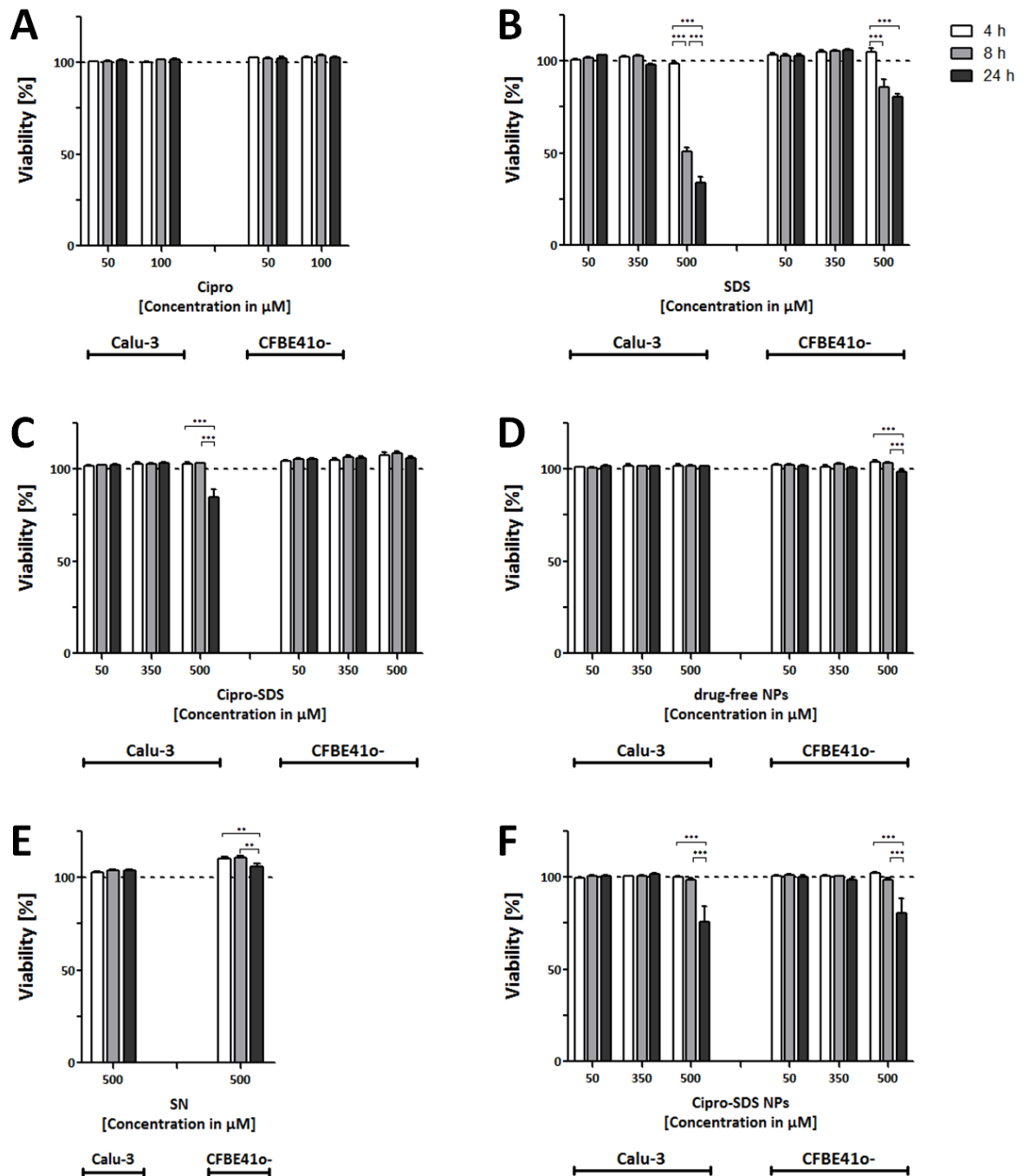
Figure 7.2 Viability of Calu-3 and CFBE41o- cells after NP application. Cell lines were treated with Cipro-SDS loaded NPs (**F**) or their single components i.e., Ciprofloxacin (Cipro, **A**), SDS (**B**), complex of Cipro-SDS (**C**), drug-free NPs (**D**) as well as the supernatant (SN) of the loaded NPs (**E**). Cytotoxictity of compounds was assessed with the ToxiLight™ bioassay kit. Resulting values were subtracted from 100% to obtain cell viability. Data shown are mean ± SEM (n≥9) from three independent experiments. *** p < 0.001; ** p <0.01.

7.3.2 Early treatment with drug-loaded NPs makes epithelial cells survive bacterial infection

After the safety of the NPs was assured, they were evaluate for their potential to eradicate biofilm-grown *P. aeruginosa* on top of human bronchial cells and simultaneously preserve the integrity of the epithelial cell monolayer. For that purpose drug-loaded NPs or KRB buffer as control were deposited as an aerosol onto the co-culture at the ALI at different time points. As read-outs SEM imaging, viability measurements, TEER measurement as well as CLSM images were used.

When the antibiotic-loaded NPs were applied to the co-culture 1 h after the infection CFBE41o- cells still formed a tight monolayer when fixed and imaged 24 h later with SEM (Figure 7.3 B). Mucus and biofilm fragments can be seen on top of the cells, as well as a couple of single bacteria. The Calu-3 cells however, already show holes in the monolayer at the same time point (Figure 7.3 A). Lots of round cell debris can be seen in the top right part of the image. The enlargement shows that remaining cells still show the typical microvilli-like structures on their cell surface. Also biofilm parts with embedded bacteria remain on top of the Calu-3 cells 24 h after the infection and 23 h after the treatment with NPs.

The situation looks much different when the aerosolized NPs are administered 4 h after the infection with *P. aeruginosa* biofilms. Calu-3 cells show an almost completely destructed monolayer (Figure 7.4 A). Piles of dead bronchial cells (spherical shaped debris) dominate the picture. The Transwell® filter with its pores can be seen in the enlargement, which is further evidence that the monolayer is heavily damaged. Single and biofilm-grown bacteria are higher in number compared to picture of the 1 h treatment time point (Figure 7.3 A). A similar situation was found for the CFBE41o- cells (Figure 7.4 B). Even though bigger coherent bronchial cell aggregates remain (left side of the image) a destruction of the cell monolayer is evident here as well. On the right side the underlying Transwell® filter is visible. A mixture of spherical cell debris, mucus and biofilm with embedded bacteria can clearly be detected in the enlargement. Also the total number of remaining bacteria (planktonic and biofilm) is higher than for the earlier treatment time point (Figure 7.3 B).

These images already plainly indicate that in order to efficiently treat the cells and keep up their monolayer integrity, an early treatment is indispensable.
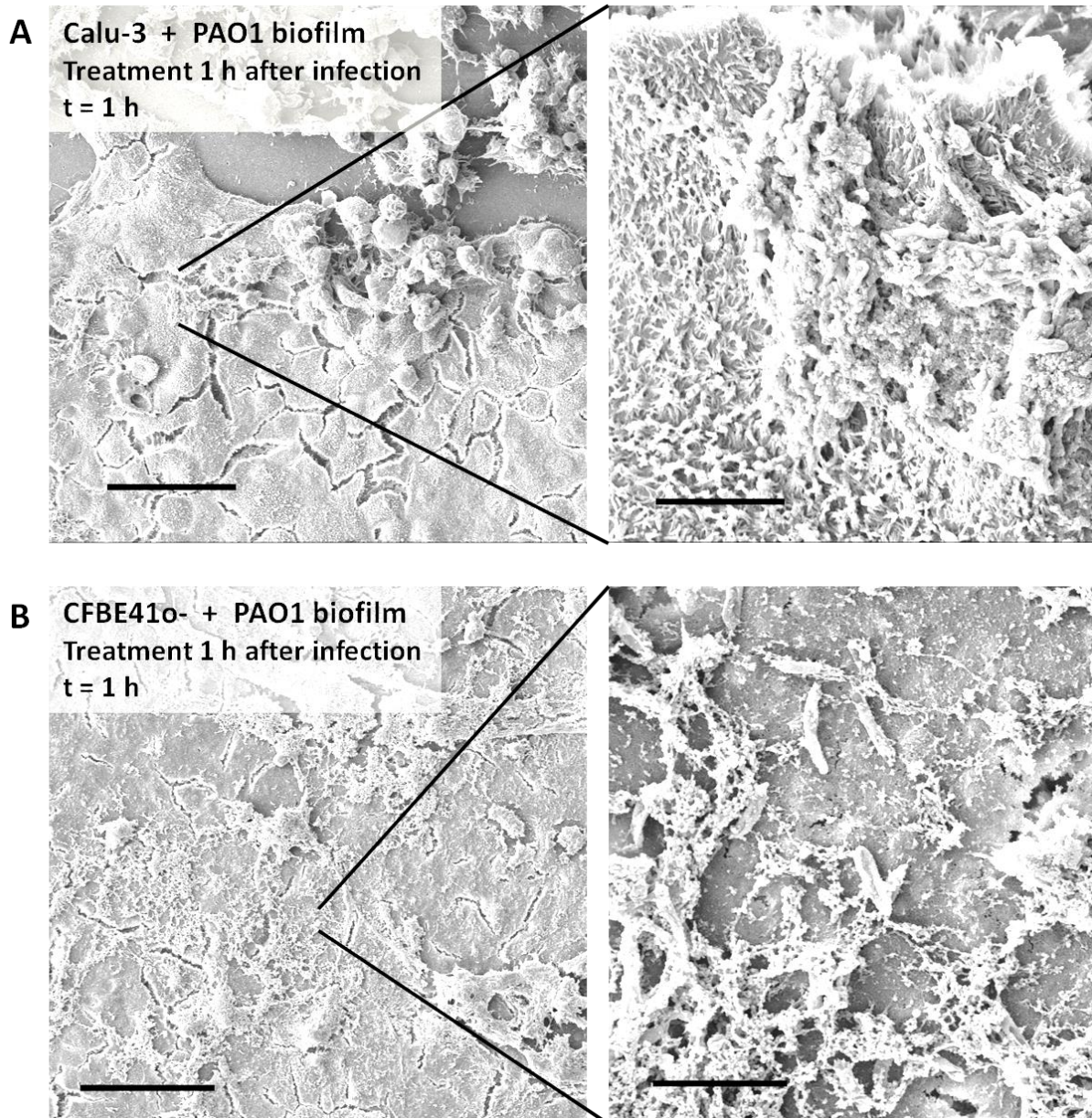
Figure 7.3 SEM images of Calu-3 or CFBE41o- cells infected with *P. aeruginosa* PAO1 biofilms and treated with drug-loaded NPs 1 h after infection. Cells were treated 1 h after the infection with the NPs. Co-culture was fixed 24 h after the infection. Calu-3 cells (**A**) already show holes in the monolayer, whereas CFBE41o- cells (**B**) still form a tight layer. Typical microvilli-like structures of Calu-3 cells are visible in the enlargement. Mucus and biofilm fragments with embedded bacteria are evident in top of both co-cultures. Scale bar: 50 µm left images and 5 µm enlargements on the right.
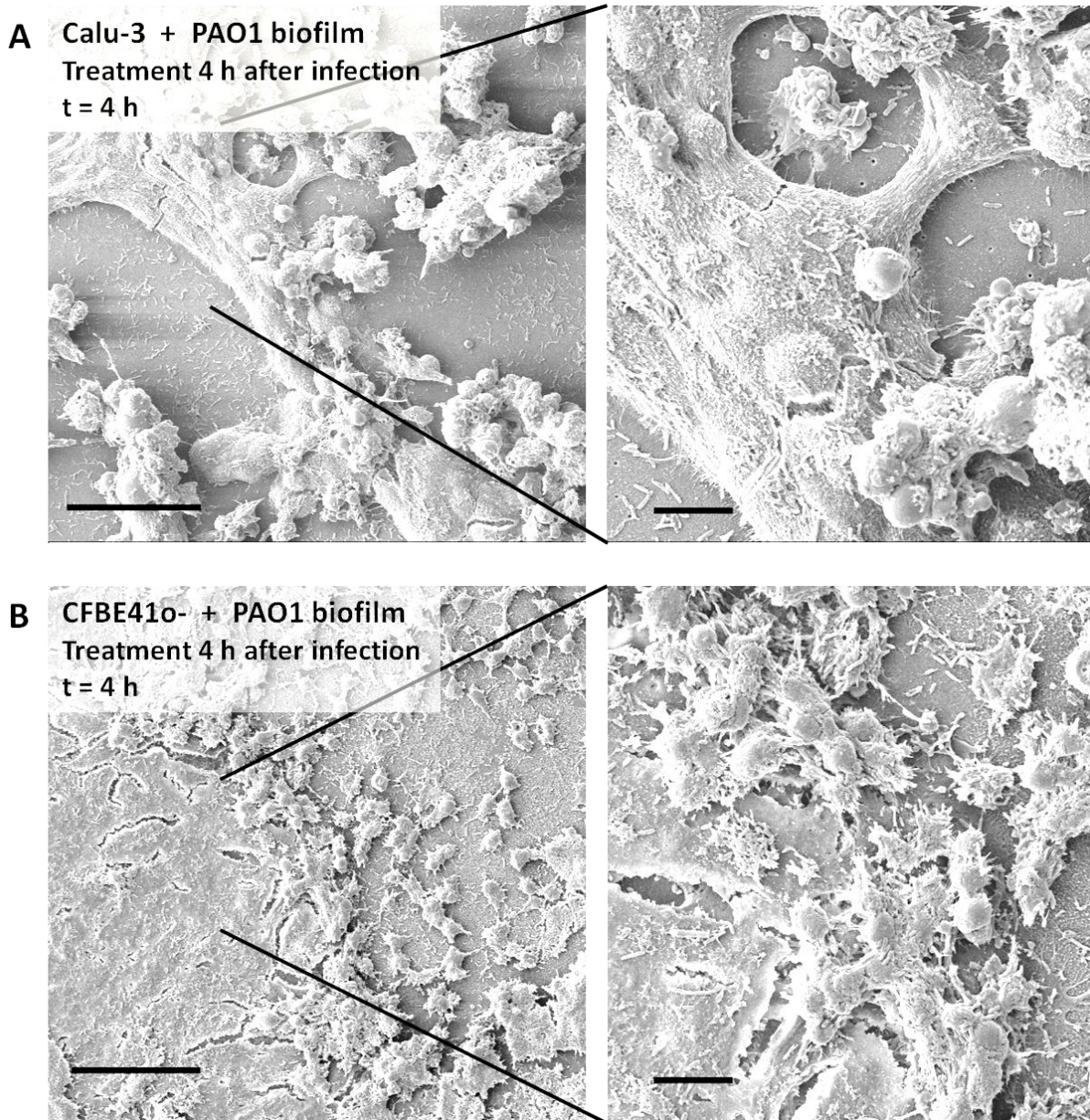
Figure 7.4 SEM images of Calu-3 or CFBE41o- cells infected with *P. aeruginosa* PAO1 biofilms and treated with drug-loaded NPs 4 h after infection. Cells were treated 4 h after the infection with the NPs. Co-culture was fixed 24 h after the infection. Calu-3 cells (**A**) show a completely destructed monolayer with huge holes. Spherical cell remains dominate the picture. The CFBE41o- cells (**B**) show a remaining monolayer with bigger holes in some parts. Dead cells can be seen as well. Mucus and biofilm fragments with embedded bacteria are evident on top of both co-cultures. Planktonic bacteria are numerous in both images. The Transwell® membrane is visible in both cases. Scale bar: 50 μm left images and 5 μm enlargements on the right.

In order to also determine the actual viability of the human bronchial epithelial cells after the different treatment time points, viability assays (MTT) were conducted 24 h after the infection (Figure 7.5). The previously used viability assay (ToxiLight™ bioassay kit) requires cell culture supernatant. Since cells were cultivated at ALI only small amounts of supernatant were expected on the apical side of the co-culture. These amounts of supernatant, resulting from nebulization of the NPs, and cell culture medium transfer from the basolateral compartment to the apical compartment through holes in the cell monolayer, might however not be enough to utilize the ToxiLight™ bioassay kit. Thus, a different assay, not requiring supernatant for the measurement, was needed. Hence, the MTT assay with a more suitable assay protocol (see 7.2.5.1) was used in order to determine the cells viability (i.e., mitochondrial activity) after different treatment time points.

Results confirm the decrease in viability already indicated by SEM images (Figure 7.3 and 7.4). When Calu-3 cells (Figure 7.5 A) received treatment 1 h after the infection their viability after was still at 80 ± 22% 24 h after the infection. When the treatment was delayed for another 3 h only 50 ± 11% of the cells remained viable at the end of the experiment.

With the purpose of examining the effect of mucus on the CFBE41o- cells when infected with *P. aeruginosa* biofilms, viability assays were conducted on cells that received mucus prior to the infection (striped bars Figure 7.5 B) and cells that did not (blank bars). Even with an early treatment (t = 1 h) viability of cells without mucus supplement had already decreased to 65 ± 9%. When antibiotic treatment was administered 4 h after the infection, viability had decreased even further to 51 ± 11%. When the experiment was conducted with cells that had received mucus, the viability of the cells treated 1 h or 4 h after the infection had improved to 94 ± 15% and 80 ± 6%, respectively. These data point out that mucus does not only enhance epithelial barrier properties (Figure 4.4), but also has a protecting role for the CFBE41o- cells against the bacterial infection.
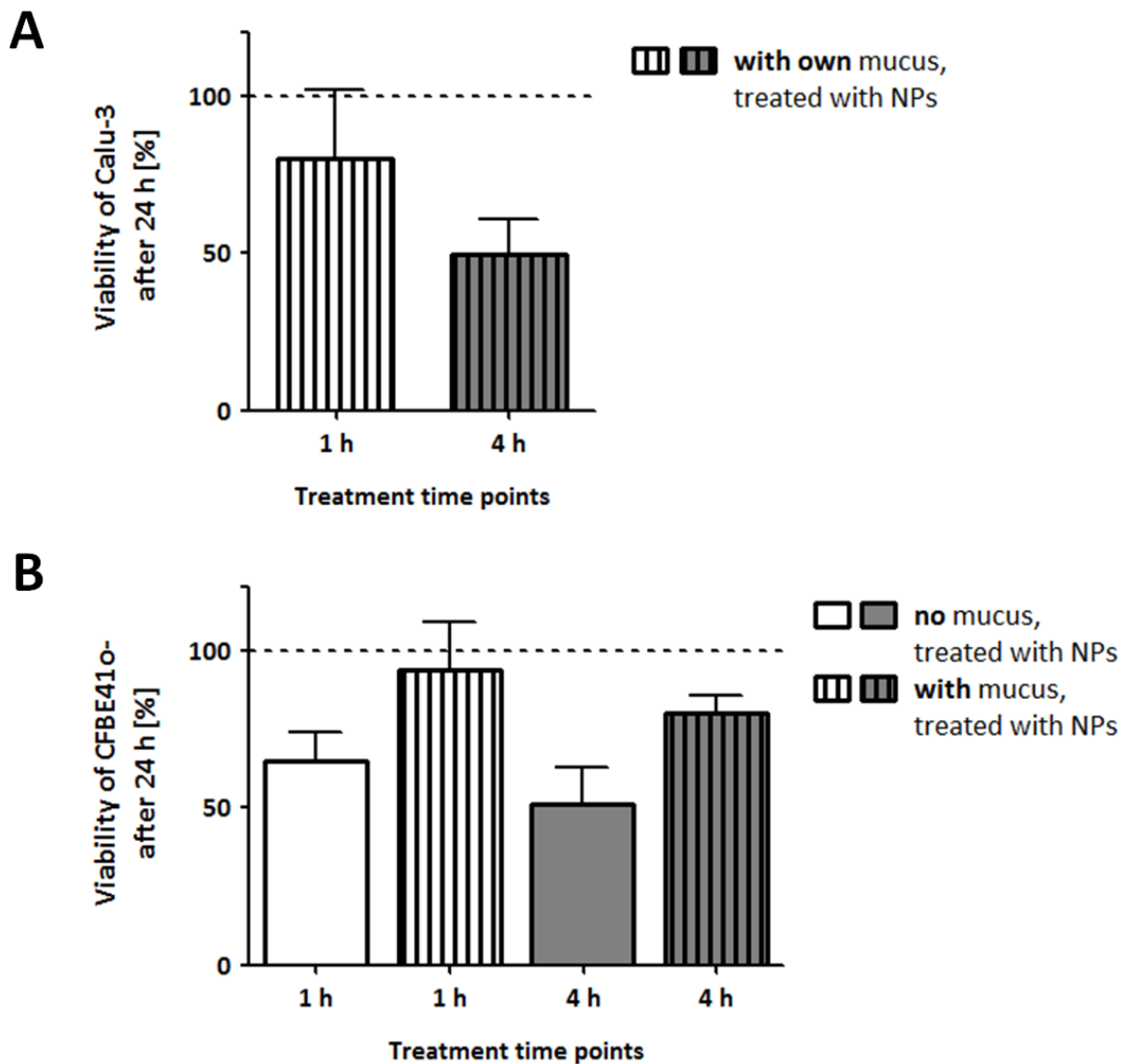
Figure 7.5 Viability of Calu-3 and CFBE41o- cells after infection and treatment with NPs. Viability of Calu-3 (**A**) and CFBE41o- cells (**B**) was measured with an MTT assay. For the Calu-3 cells a decline of cell viability was visible. An early treatment (1 h after infection) with the drug-loaded NPs maintained 80% viability whereas a later treatment (after 4 h) resulted in only 50% viable cells 24 h after the infection. For the CFBE41o- cells an early treatment (after 1 h) with antibiotic NPs helps them to survive the infection. Cells covered by mucus (striped bars) conserved their viability even when NPs was performed at a later time point (after 4 h). Experiments were performed 5 times and results are presented as mean ± SEM.

CLSM images gave additional insight into the status of the co-culture after NP treatment at different time points (Figure 7.6). When treatment was administered 1 h after the infection Calu-3 cells already show signs of starting cell death (red nuclei, Figure 7.6 A) and holes in the cell monolayer. In contrast, CFBE41o- cells still form a complete monolayer and no PI stained (dead) nuclei were visible (Figure 7.6 B). A later treatment (t =4 h) led to an increase of red stained nuclei (Figure 7.6 D) and even some gaps in the cell monolayer. However, the Calu-3 cells (Figure 7.6 C) are in even less good conditions. Just patches of connected epithelial cells are visible and these cells also show signs of necrosis or apoptosis (red). The tight monolayer from the beginning of the experiment is gone. Of note, no living bacteria (green) could be detected in Figure 7.6 A-D. But considering the fact, that after 24 h just a small amount of bacteria (~50 CFU/ml, see chapter 7.3.4, Figure 7.8 C and D) remains in the complete sample and the images just show roughly 14% of it, can explain the lack of the green signal in those images. Total cell monolayer destruction was the case when no antibiotic treatment (just KRB) was applied (Figure 7.6 E, F). No cell nuclei were visible anymore. Given that DAPI and PI both bind to DNA, which is abundant in biofilms, CLSM imaging of the same was feasible and revealed the typical 3-D like structures [181, 196]. The green labelled bacteria seem to dominate the picture of the Calu-3 co-culture while the biofilm of the CFBE41o- cells is composed of equal parts bacteria and DNA visible by the white colour (overlay of red, blue and green signal) of the mushroom like structure. It was reported by Moreau-Marquis et al. that biofilm formation is promoted when *P. aeruginosa* is grown on CF-derived cells. In addition, they could also show that the ΔF508-CFTR mutation enhanced biofilm formation not just in CFBE41o- cells but also in a set of kidney cells with the same mutation [160]. Considering that the Calu-3 cells do not exhibit this mutation could be a possible explanation for the difference in the biofilm after 24 h (Figure 7.6 E, F). Whether the composition of both biofilms is indeed different or this is just an imaging artefact remains to be investigated.

Taken together these CLSM data corroborate the previously presented results regarding cellular viability and monolayer integrity. As already indicated by the SEM images and the MTT assay, the CFBE41o- cells seem to cope much better with the infection provided they were supplemented with mucus. The question remains, if longer cultivation of the Calu-3 cells at ALI conditions prior to the infection and a resulting

higher amount of mucus on the cells would also increase their robustness. Nonetheless, an early treatment (t = 1 h) is to be favored in order to preserve cell viability and monolayer integrity.
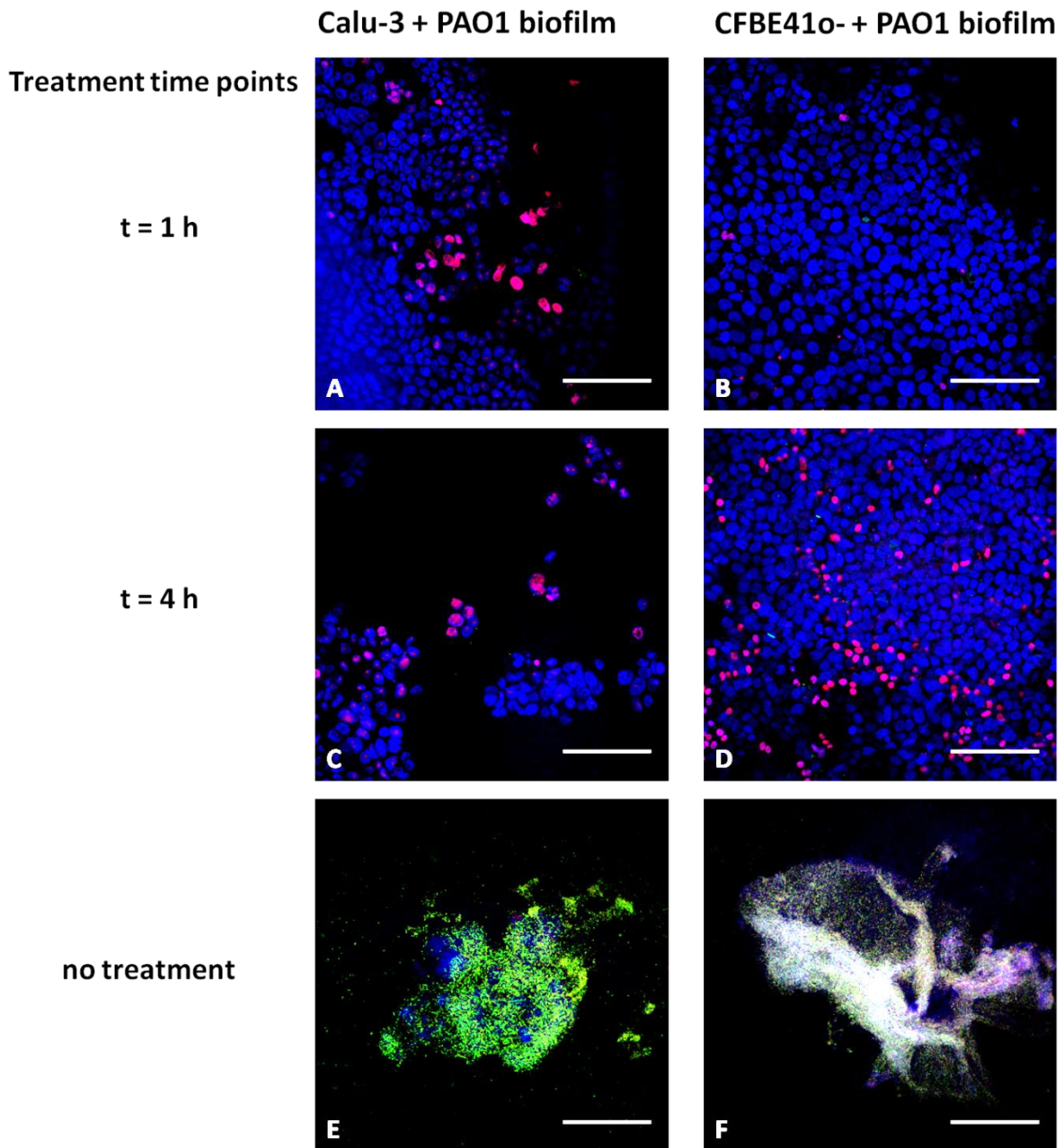
Calu-3 + PAO1 biofilm **CFBE41o- + PAO1 biofilm**

Treatment time points

t = 1 h

t = 4 h

no treatment

Figure 7.6 Representative confocal images of co-cultures after treatment or without treatment. The co-cultures were fixed 24 h after the infection. When drug-loaded NPs were applied after 1 h (**A**, **B**) cells were still forming a confluent monolayer. Treatment after 4 h (**C**, **D**) resulted in increased cell death (red nuclei). CFBE41o- cells visibly cope better with the infection. Calu-3 cells show signs of cell death already at t = 1 h and loose cell aggregates when treatment is given at t = 4 h. No treatment (**E**, **F**) led to complete destruction of the cell monolayer for both cell lines and *P. aeruginosa* was able to build 3-D biofilm structures. DAPI (blue) was used to stain the nuclei of all cells and propidium iodide (red) to label dead cell nuclei; *P. aeruginosa* strain PAO1 carries a plasmid with GFP (green). Scale bar: 100 μm.

7.3.3 Barrier properties of CFBE41o- cells can be maintained when treatment is administered 1 h after infection with *P. aeruginosa* biofilm, whereas Calu-3 loose barrier function even with an early treatment

In view of the fact that mucus helped the CFBE41o- cells to survive the bacterial infection, when treatment was administered early enough, the role of mucus in maintaining epithelial barrier properties after the infection was a matter of particular interest. Thus, TEER measurements were performed 24 h after the infection and treatment with NPs (Figure 7.7).

Calu-3 cells (Figure 7.7 A) lost their barrier properties (TEER = 28 ± 5 Ω*cm²) even when the NPs were deposited on the co-culture at t =1 h. Later treatment decreased this value even further to 13 ± 2 Ω*cm². Although both values are well below the 300 Ω*cm² mark for barrier properties, this difference was significant. Cells that were not infected kept their epithelial barrier function and showed TEER values of 351 ± 47 Ω*cm². Considering that the Calu-3 cells already showed holes in the monolayer even when NP treatment was given early (see Figure 7.3 A and 7.6 A) these results were not surprising. This emphasizes the fact that the Calu-3 cells are probably not the optimal cell line for the co-culture model under the given conditions.

However, the situation looks much different for the CFBE41o- cells (Figure 7.7 B). The cells receiving human mucus prior to the infection exhibited almost twice as high TEER values as the cells without human mucus (361 ± 52 Ω*cm² versus 601 ± 75 Ω*cm²). This was at least true when antibiotic treatment was performed 1 h after the infection. When drug-loaded NPs were applied 4 h after the infection, CFBE41o- were not able to preserve their barrier properties even in presence of mucus (without mucus: 49 ± 5 Ω*cm² versus 115 ± 29 Ω*cm² with mucus).

Untreated co-cultures that just received nebulized KRB scarcely showed any remaining barrier function (data not shown; 12 ± 2 Ω*cm² and 10 ± 2 Ω*cm² for Calu-3 and CFBE41o-, respectively). However, this is in agreement with previous shown results of the completely destructed bronchial epithelium (Figure 6.3 and 7.6 E and F). In contrast, uninfected cells that also received NPs as a control (chequered bars in Figure 7.7) exhibited high TEER values after 24 h (351 ± 47 Ω*cm² for the Calu-3 cells and 2080 ± 273 Ω*cm² for CFBE41o- cells). This indicates that the nebulization process itself had no negative effect on the barrier properties of the cells.
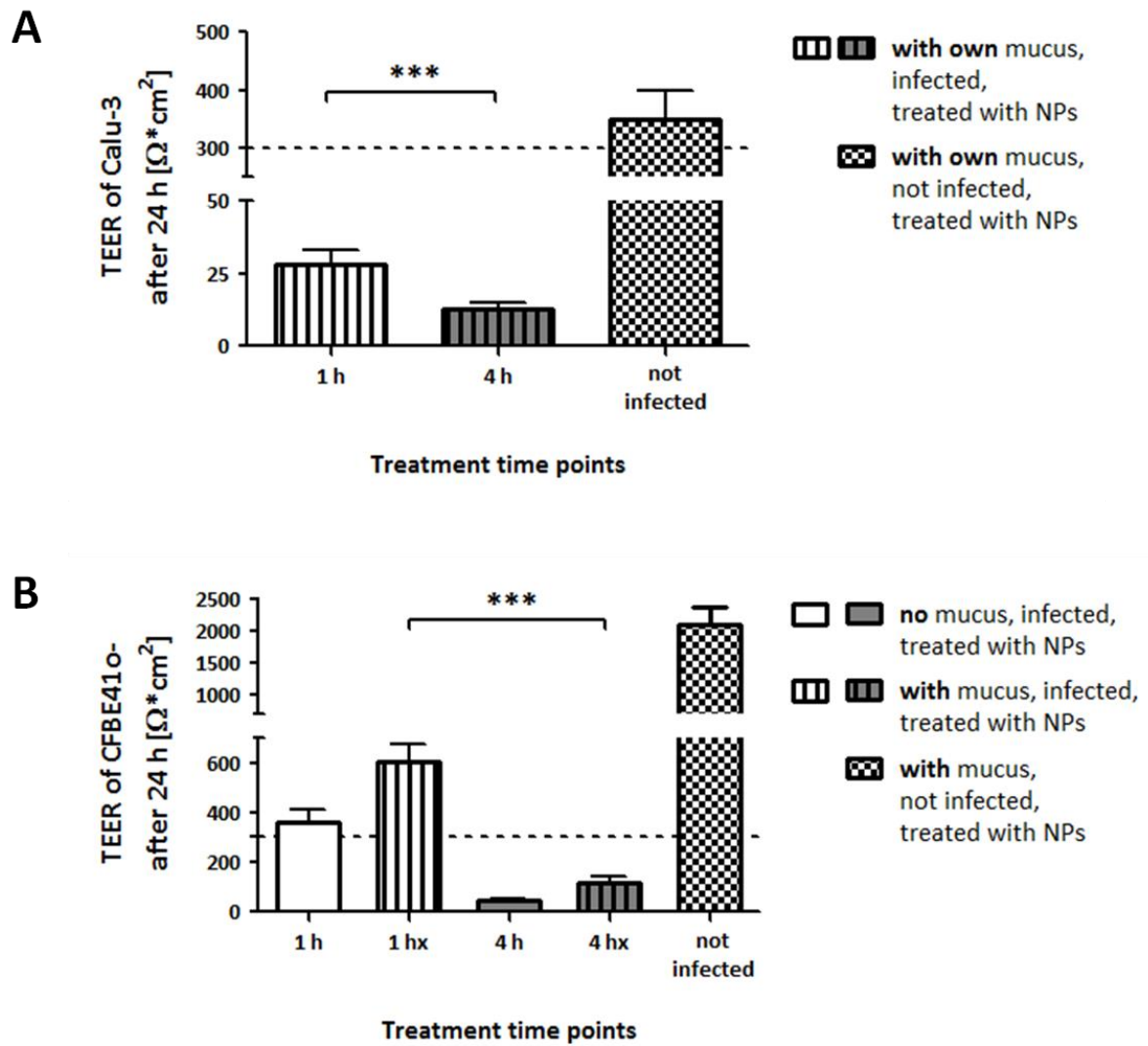
Figure 7.7 TEER of Calu-3 and CFBE41o- cells after infection. For the Calu-3 cells (**A**) even with an early NP treatment (t=1 h) barrier properties were lost. CFBE41o- (**B**) barrier function could be maintained with an early treatment (t =1 h). Later treatment after 4 h resulted in loss of barrier properties as well. Values are presented as mean ± SEM.

7.3.4 CFU of *P. aeruginosa* can be reduced by 6-fold with an early treatment of infected co-culture

After the safety and the effect of the NPs on the co-culture were assessed, also their efficacy in combating the biofilm-grown *P. aeruginosa* was investigated. In order to compare them to a commercially available product, Panotile® CIPRO was chosen as compromise. As mentioned previously no pulmonary applicable dosage form containing ciprofloxacin is on the market yet, not to mention one where the drug is encapsulated in NPs [212]. In addition, the product was aimed to be nebulized. Ciprofloxacin suffers from a low solubility [251]. Thus, the preparation of a ciprofloxacin solution with analogous drug content as the NPs solution was not feasible. One available product with ciprofloxacin already in solution is eardrops. Lacking a better option, the Panotile® CIPRO eardrops were chosen to compare the efficacy of the drug-loaded NPs with a market approved commercial product. After dilution with KRB (supplemented with 10% FCS) to the appropriate concentration (350 µM ciprofloxacin), they were deposited onto the co-culture in the same manner as the NPs. Nebulized KRB buffer served as negative control.

The actual applied dose was assessed by measuring the recovery rate of the nebulized NPs suspension (350 µM) in a preliminary experiment. The recovered suspension had a concentration of 234 ±30 µM, which corresponds to a recovery rate of ~70%. Furthermore, the nebulization process itself had no significant effect on the size of the nanocarriers. Due to the proteins found in the FCS from the dilution buffer (KRB with 10% FCS) the formation of a corona could be observed [253]. The particles size increased from originally 190 ± 29 nm [212] to 374 ± 4 nm. The nebulization slightly reduced the size again to 320 ± 2 nm, the difference not being significant.

The same treatment time points (1 h and 4 h after infection) where chosen to deposit aerosols of NPs, Panotile or KRB onto the co-culture. CFU/ml of planktonic and biofilm fraction of *P. aeruginosa* was determined 24 h after the infection by plating supernatant and lysates from each well on agar plates.

Almost all supernatants from co-cultures that were treated with NPs 1 h after infection showed no bacterial growth (Figure 7.8 A and B). The small amount of remaining bacteria (3 CFU/ml) in the Calu-3 co-culture treated with NPs can probably be neglected. In addition, when treated after 4 h no viable bacteria remained in the

supernatant of the Calu-3 co-culture (Figure 7.8 A). In the CFBE41o- co-culture surviving planktonic bacteria were detected at 40 CFU/ml and 5 CFU/ml for NPs and Panotile®, respectively. But compared to the control wells (i.e., with KRB) where a bacterial growth of $1.1*10^9$ CFU/ml (Calu-3) and $7.7*10^8$ CFU/ml (CFBE41o-) was measured, these numbers show a log 8 reduction of CFU/ml counts. Accordingly, these data suggest that complete eradication of planktonic *P. aeruginosa* is possible, provided that antibiotic treatment is given early enough (1 h post infection).

In order to also determine the efficacy of the drug-loaded NPs and Panotile® against the biofilm fraction, contents of each well were lysed with 0.1% Triton X-100 and plated on agar plates (Figure 7.8 C and D). In contrast to the planktonic bacteria a complete eradication of biofilm-grown bacteria was not possible even when the antibiotics (NPs or Panotile®) were administered already 1 h after infection. This is in agreement with a study by Moreau-Marquis et al., who observed that ciprofloxacin alone or even in combination with other antibiotics was not able to eliminate *P. aeruginosa* biofilms grown on airway cells. They report an increased resistance to clinically used antibiotics already 1.5 h after the initial infection [160]. Nonetheless, a significant reduction by log 6 of CFU/ml counts compared to the non-treated control (KRB only; $7.7*10^7$ CFU/ml and $4.6*10^7$ CFU/ml for Calu-3 and CFBE41o-, respectively) was observed in our study, the difference between t =1 h and t = 4 h being insignificant. However, results showed that NPs have a slightly better efficacy against biofilm-grown bacteria as the Panotile® CIPRO eardrops (24 CFU/ml compared to 264 CFU/ml in Calu-3 co-cultures, t = 4 h; 29 CFU/ml versus 95 CFU/ml, t = 1 h and 52 CFU/ml versus. 183 CFU/ml, t = 4 h in CFBE41o- co-cultures; exception is 1 h treatment time point in Calu-3). Even though these results did not reach significance, they back up the hypothesis, that NPs can interact with mucus and biofilm components, achieve a depot effect and release the drug in a controlled manner. This assumption could be confirmed in the future by integrating additional washing steps in the experimental protocol. Only the NPs, which are able to attach to their deposition site, could release their antibiotic cargo and combat *P. aeruginosa,* whereas the Panotile® CIPRO solution would be washed away. Moreover, NPs could be able to protect the drug from inactivation by biofilm components [36]. This cannot be realized with Panotile® eardrops, where the drug is already dissolved, thus, making an interaction with mucus and biofilm improbable. To

verify this hypothesis additional studies with even older biofilms (48 h or older) and repeated dose applications will give further insight in the potential of such DDSs. Additionally, in future the drug-loaded NPs can also be formulated into microparticles, and thus meeting the necessities in size, shape and aerodynamic properties (see introduction 1.3.3) to be inhaled with a dry powder inhaler, hence, allowing a local treatment at the site of action.
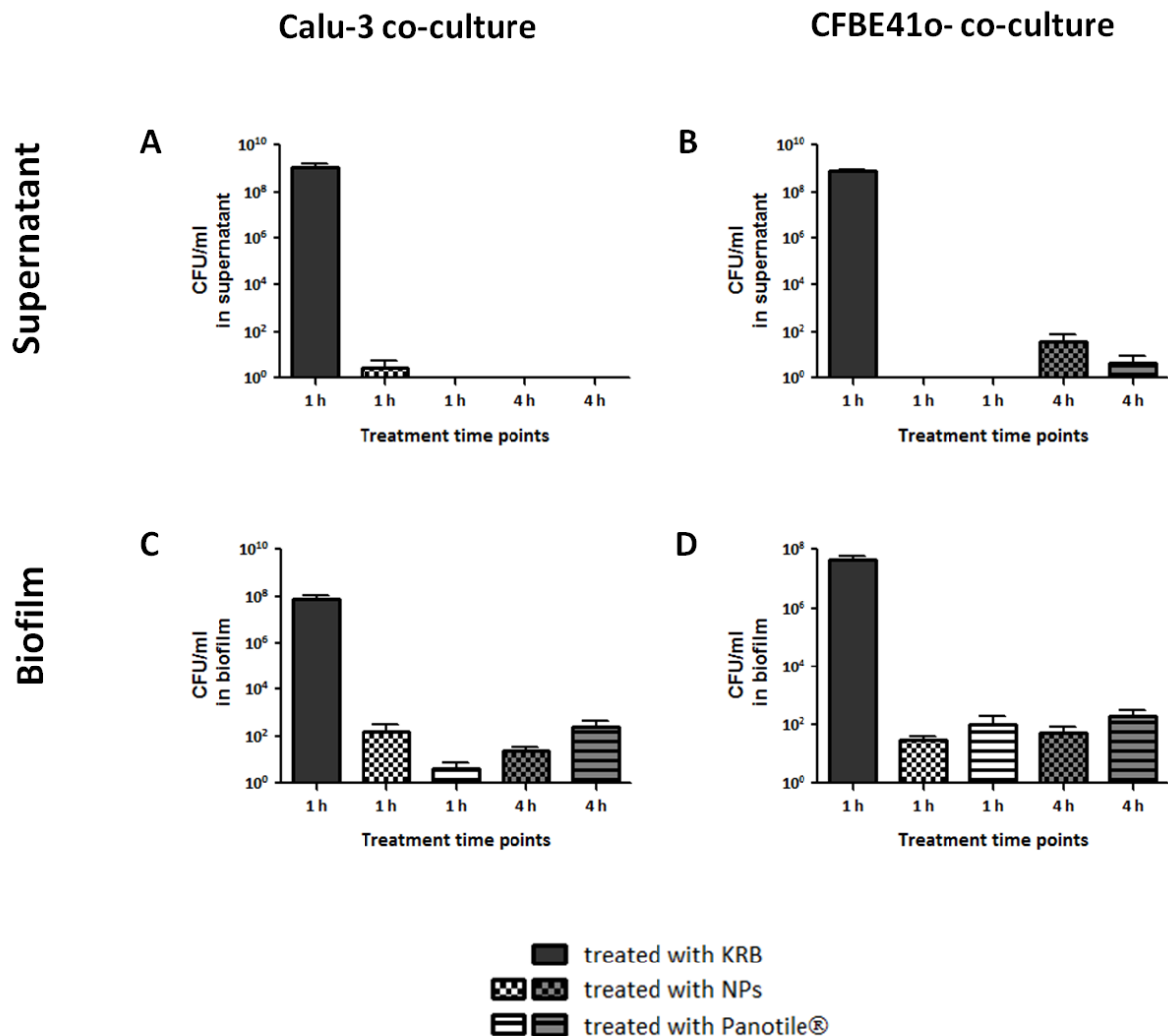

Figure 7.8 Remaining CFU in supernatant and biofilm CFU/ml of PAO1 in supernatant and biofilm of KRB (control), drug-loaded NPs or Panotile® treated co-cultures was determined 24 h after the infection. All planktonic bacteria in supernatant were eradicated when treatment was given 1 h after the infection (exception Calu-3, 3 CFU/ml remain after NPs treatment). Later application of NPs just increased the CFU/ml slightly. CFU count of biofilm fraction exposed that by a later treatment time point the CFU increases. Early treatment (t = 1 h) nearly eradicates all biofilm-grown bacteria. CFU doubles when administration of NPs is conducted at t = 4 h. Control wells (KRB only) exhibited a log 6 higher CFU/ml than wells that were given drug-loaded NPs. Data were log-transformed and are presented as mean ± SEM.

7.4 Conclusion

With the ToxiLight™ bioassay kit the viability of the NPs and their single components were determined. In the second highest applied concentration all compounds were well tolerated by both epithelial cell lines. Thus, this concentration was used for further studies.

In order to find the optimal treatment time point after the infection, a delay of 1 h and 4 h was chosen to apply the antibiotic-loaded NPs. The Calu-3 cells did not endure the circumstances of the infection for long and even with an early treatment (t = 1 h) holes in the monolayer, loss of barrier properties and viability was observed. A later treatment enhanced these negative effects. No treatment led to a complete destruction of the cells and just a bacterial biofilm remained of the co-culture.

On the other hand, CFBE41o- cells were able to maintain their barrier function and viability when treated 1 h after the infection provided they were supplemented with human mucus prior to the infection. However, also in the case of this cell line a longer delay of the treatment led likewise to monolayer disruption, loss of barrier properties and a decreased viability.

In summary the presented data led to the conclusion that the CFBE41o- cells are the superior cell line for the *in vitro* model. Not just because they feature the most common mutation in CF (ΔF508-CFTR), which enhances the biofilm formation, but also because they proof to be more robust when faced with the bacterial burden, thus, offering an appropriate time window to apply and evaluate the novel DDSs.

The ciprofloxacin-loaded NPs showed a good biocompatibility and no cytotoxic potential in the applied concentration (350 µM). They were able to eradicate all planktonic bacteria when administered 1 h after the infection and also proved to be very effective against free swimming bacteria when treatment was delayed (t = 4 h).

Even though a complete elimination of biofilm grown *P. aeruginosa* was not possible, NPs were able to decrease the bacterial load by log 6 and in this context also appear to be slightly more effective than the commercially available product Panotile®. These data underscore the potential of novel pharmaceutical formulations to deliver antibiotics across important biological barriers (e.g., mucus and biofilms) and thus, improve the therapy for CF patients in the future.

8 Summary and Outlook

Pulmonary infections with *P. aeruginosa* unfortunately occur on a daily basis in CF patients. Even today these infections are still hard to treat and sooner or later they become chronic due to biofilm formation of the pathogen [28]. The resulting pulmonary consequences of recurring lung infections and persistent inflammations are still the major cause for morbidity and mortality in CF [16]. Novel treatment approaches (e.g., with antibiotic loaded nanocarriers) raise hopes to eradicate those persistent infections. With the purpose to treat chronic infection right at the site of action, the pulmonary application of new drug delivery systems (DDSs) seems a good option. In order to evaluate the safety and efficacy of such DDSs, suitable *in vitro* models are necessary before going into pre-clinical trials.

In this work the development of an *in vitro* model of human pulmonary epithelial cells in co-culture with *P. aeruginosa* biofilms was conducted. Its applicability for safety and efficacy testing of a novel DDSs was evaluated with aerosolized ciprofloxacin-loaded NPs.

Because cell lines offer several advantages over primary cells [106], two human bronchial epithelial cell lines were evaluated for this model. During the characterization of the two cell lines at hand (i.e., Calu-3 and CFBE41io-), it became evident that the CF cell line did not produce mucus, which was in agreement with already published data [160, 161]. In addition, the measured barrier properties at ALI conditions were not sufficient for an *in vitro* model. To overcome these obstacles an alternative mucus source was utilized. Due to the addition of a human mucus layer on top of the CFBE41o- cells, barrier properties increased and moreover, an important part of a CF model, mucus, was added.

P.°aeruginosa was chosen as model pathogen for this CF co-culture model, since it becomes the predominant pathogen by late adolescence in CF patients [25, 26]. Furthermore, its ability to build biofilms *in vitro* is well documented in literature [29]. Subsequently, different growth media for *P. aeruginosa* strain PAO1 were assessed in order to find the best composition for biofilm formation. A minimal growth medium (i.e., M63) supplemented with arginine was selected.

After the two major components of the *in vitro* co-culture model were evaluated (i.e., human bronchial epithelial cell lines and the CF relevant pathogen *P. aeruginosa*), in a next step planktonic bacteria were used to infect monolayers of the model cell lines Calu-3 and CFBE41o-. In both cases, first signs of biofilm development could be

measured 4 h after the infection. However, due the rapid overgrowth and resulting death of the epithelial cells, this model could not be used to test the novel DDS. Therefore, a preformed biofilm, grown for 24 hours externally, was transferred to the apical side of the epithelial cell monolayers. The resulting model was incubated for one hour before aerosolized ciprofloxacin-loaded NPs where applied. Of note, during the whole experimental procedure ALI conditions were maintained. This is an important measure when the model is intended for application of pulmonary DDSs (e.g., dry powders for inhalation or aerosols).

During the experimental trials, it turned out that the time point of treatment (i.e., 1 h or 4 h after infection) is rather crucial. The co-culture model of Calu-3 and *P. aeruginosa* proofed to be much more vulnerable to the infectious challenge. Even with the earlier treatment time point91, barrier function and viability of the cells could not be maintained. On the contrary, the CFBE41o- cells proofed to be more robust when facing the burden of the infection of a biofilm. The epithelial cells were able to maintain their barrier function and viability until 24 h after the infection, but only when treatment was applied 1 h after the infection.

The here used aerosolized NPs showed good biocompatibility and a low cytotoxic potential in the chosen concentration. They were able to eradicate all planktonic bacteria in the co-culture model after 24 h and could even reduce the number of biofilm bound bacteria by log 6.

Even though a complete eradication of *P. aeruginosa* biofilm was not possible, further tests might shed more light on the efficacy of the novel DDS. Therefore, the application of repeated doses might be of interest. Furthermore, also the introduction of additional washing steps into the experimental procedure is possible. They could on the one hand reduce the bacterial burden of planktonic bacteria on the epithelial cells, and thus prolong the viability and applicability of the *in vitro* model. On the other hand, such repeated washing steps could clearly proof the advantage of the DDS compared to free drug, since the particles should get entrapped in the mucus biofilm mixture on top of the cells and not be rinsed away during the washing steps like the free drug.

In addition to the mentioned improvements of the model also the use of clinical isolates of *P. aeruginosa* seem of great importance and could enhance the impact of the model.

Nevertheless, the experimental set up of a CF relevant *in vitro* model mimicking the biofilm infected lung presented in this work was successfully used to test the efficacy and safety of a novel aerosolized DDS. Furthermore, the continuous cultivation of this model at ALI conditions makes it valid to be used for potential future trials of dry powder formulations together with the PADDOCC system. In such a set-up the here applied NPs could be reformulated into microparticels and applied onto the co-culture in a formulation that also later would be found in clinical trials.

List of abbreviations

3-D	Three-dimensional
AET	Antibiotic eradication therapy
AHL	*N*-acyl-*l*-homoserine lactones
ALI	Air-liquid interface
ANOVA	Analysis of variance
AO	Acridine orange
ASL	Airway surface liquid
ATCC	American Type Culture Collection
BSA	Bovine serum albumin
CAA	Casamino acids
CF	Cystic fibrosis
CFTR	Cystic fibrosis transmembrane conductance regulator
CFU	Colony forming unit
CLSM	Confocal laser scanning microscopy
CV	Crystal violet
DAPI	4',6-Diamidin-2-phenylindol
DDS	Drug delivery system
DMSO	Dimethyl sulfoxide
DPI	Dry powder for inhalation
DPPA	1,2-Dipalmitoyl-sn-glycero-3-phosphatidic acid, sodium salt
eDNA	Extracellular deoxyribonucleic acid
EE	Encapsulation efficiency
EMA	European Medicine Agency
EO	Ethylene oxide
EPS	Extracellular polymeric substances
EVOM	Epithelial voltohmmeter
FDA	(U.S.) Food and Drug Administration
FCS	Fetal calf serum
FPF	Fine particle fraction
GRAS	Generally recognized as safe
GSD	Geometric standard deviation

HBSS	Hank's Balanced Salt Solution
HEPES	4-(2-hydroxyethyl)-1-piperazineethanesulfonic acid
HMDS	Hexamethyldisilazane
IQS	Integrated quorum sensing system
JAMs	Junctional adhesion molecules
KRB	Krebs ringer buffer
LCC	Liquid-covered conditions
MAPs	Mucoadhisive particles
MCC	Mucociliary clearance
MDR-PA	Multidrug-resistant *P. aeruginosa*
MEM	Minimum Essential Medium
MJR	MicroJet Reactor
MMAD	Mass median aerodynamic diameter
MOI	Multiplicity of infection
MRSA	Methicillin-resistant Staphylococcus aureus
MTT	3-(4,5-dimethylthiazol-2-yl)-2,5-diphenyltetrazolium bromide
MW	Molecular weight
MWCO	Molecular weight cut-off
NaFluo	Sodium fluorescein
NDA	New drug application
NEAA	Non-essential amino acids
NPs	Nanoparticles
OD_{600}	Optical density at 600 nm
PADDOCC	Pharmaceutical Aerosol Deposition Device on Cell Cultures
P_{app}	Apparent permeability coefficient
PAS	Peridoc acid-Schiff
PBS	Phosphate buffered saline
PCL	Periciliary liquid layer
PdI	Poly dispersity index
PEG	Poly ethylene glycol
PFA	Paraformaldehyde
PGA	Poly glycolic acid
PI	Propidium iodide

PLA	Poly lactic acid
PLGA	Poly(lactic-co-glycolic) acid
PO	Propylene oxide
PPO	Poly propylene oxide
PQS	Pseudomonas quinolone signal
P/S	Penicillin/Streptomycin
QS	Quorum sensing
QSI	Quorum sensing inhibitors
RT	Room temperature
SDS	Sodium dodecyl sulfate
SEM	Scanning electron microscopy
SEM*	Standard error of the mean
SMG	Submucosal glands
SN	Supernatant
SV-40	Simian virus 40
TEER	Transepithelial electrical resistance
TJs	Tight junctions

References

1.	De Boeck, K. and M.D. Amaral, *Progress in therapies for cystic fibrosis.* Lancet Respir Med, 2016. **4**(8): p. 662-674.
2.	Castellani, C. and B.M. Assael, *Cystic fibrosis: a clinical view.* Cell Mol Life Sci, 2017. **74**(1): p. 129-140.
3.	Maiuri, L., V. Raia, and G. Kroemer, *Strategies for the etiological therapy of cystic fibrosis.* Cell Death Differ, 2017.
4.	Paranjape, S.M. and P.J. Mogayzel, Jr., *Cystic fibrosis in the era of precision medicine.* Paediatr Respir Rev, 2017.
5.	Andersen, D.H., *Cystic fibrosis of the pancreas and its relation to celiac disease: A clinical and pathologic study.* American Journal of Diseases of Children, 1938. **56**(2): p. 344-399.
6.	Kerem B, et al., *Identification of the cystic fibrosis gene: genetic analysis.* Science. , 1989. **245**(4922): p. 1073-80.
7.	Griesenbach, U., J.C. Davies, and E. Alton, *Cystic fibrosis gene therapy: a mutation-independent treatment.* Curr Opin Pulm Med, 2016. **22**(6): p. 602-9.
8.	Zielenski, J. and L.C. Tsui, *Cystic fibrosis: genotypic and phenotypic variations.* Annu Rev Genet, 1995. **29**: p. 777-807.
9.	Quon, B.S. and S.M. Rowe, *New and emerging targeted therapies for cystic fibrosis.* Bmj, 2016. **352**: p. i859.
10.	Prickett, M. and M. Jain, *Gene therapy in cystic fibrosis.* Transl Res, 2013. **161**(4): p. 255-64.
11.	Stanke, F. and B. Tummler, *Classification of CFTR mutation classes.* Lancet Respir Med, 2016. **4**(8): p. e36.
12.	Marson, F.A.L., C.S. Bertuzzo, and J.D. Ribeiro, *Classification of CFTR mutation classes.* Lancet Respir Med, 2016. **4**(8): p. e37-e38.
13.	De Boeck, K. and M.D. Amaral, *Classification of CFTR mutation classes - Authors' reply.* Lancet Respir Med, 2016. **4**(8): p. e39.
14.	Rowe , S.M., S. Miller , and E.J. Sorscher *Cystic Fibrosis.* New England Journal of Medicine, 2005. **352**(19): p. 1992-2001.
15.	Virant-Young, D., et al., *Cystic Fibrosis: A Novel Pharmacologic Approach to Cystic Fibrosis Transmembrane Regulator Modulation Therapy.* J Am Osteopath Assoc, 2015. **115**(9): p. 546-55.
16.	Heijerman, H., *Infection and inflammation in cystic fibrosis: a short review.* J Cyst Fibros, 2005. **4 Suppl 2**: p. 3-5.
17.	Haley, C.L., J.A. Colmer-Hamood, and A.N. Hamood, *Characterization of biofilm-like structures formed by Pseudomonas aeruginosa in a synthetic mucus medium.* BMC Microbiol, 2012. **12**(181): p. 1471-2180.
18.	Button, B., et al., *A Periciliary Brush Promotes the Lung Health by Separating the Mucus Layer from Airway Epithelia.* Science, 2012. **337**(6097): p. 937-941.
19.	Rokicki, W., et al., *The role and importance of club cells (Clara cells) in the pathogenesis of some respiratory diseases.* Kardiochir Torakochirurgia Pol, 2016. **13**(1): p. 26-30.
20.	Tarran, R., *Regulation of airway surface liquid volume and mucus transport by active ion transport.* Proc Am Thorac Soc, 2004. **1**(1): p. 42-6.
21.	Knowles, M.R. and R.C. Boucher, *Mucus clearance as a primary innate defense mechanism for mammalian airways.* J Clin Invest, 2002. **109**(5): p. 571-7.

22. Griesenbach, U., K.M. Pytel, and E.W. Alton, *Cystic Fibrosis Gene Therapy in the UK and Elsewhere.* Hum Gene Ther, 2015. **26**(5): p. 266-75.

23. Filkins, L.M. and G.A. O'Toole, *Cystic Fibrosis Lung Infections: Polymicrobial, Complex, and Hard to Treat.* PLoS Pathog, 2015. **11**(12): p. e1005258.

24. Döring, G., et al., *Treatment of lung infection in patients with cystic fibrosis: Current and future strategies.* Journal of Cystic Fibrosis, 2012. **11**(6): p. 461-479.

25. Cystic Fibrosis Foundation, *2016 Annual Data Report, ,* in *Cystic Fibrosis Foundation Patient Registry* ©2017 Cystic Fibrosis Foundation: Bethesda, Maryland.

26. Lyczak, J.B., C.L. Cannon, and G.B. Pier, *Lung infections associated with cystic fibrosis.* Clin Microbiol Rev, 2002. **15**(2): p. 194-222.

27. Moreau-Marquis, S., G.A. O'Toole, and B.A. Stanton, *Tobramycin and FDA-approved iron chelators eliminate Pseudomonas aeruginosa biofilms on cystic fibrosis cells.* Am J Respir Cell Mol Biol, 2009. **41**(3): p. 305-13.

28. Costerton, J.W., P.S. Stewart, and E.P. Greenberg, *Bacterial biofilms: a common cause of persistent infections.* Science, 1999. **284**(5418): p. 1318-22.

29. O'Toole, G.A., *To build a biofilm.* J Bacteriol, 2003. **185**(9): p. 2687-9.

30. Drenkard, E., *Antimicrobial resistance of Pseudomonas aeruginosa biofilms.* Microbes and Infection, 2003. **5**(13): p. 1213-1219.

31. Donlan, R.M. and J.W. Costerton, *Biofilms: survival mechanisms of clinically relevant microorganisms.* Clin Microbiol Rev, 2002. **15**(2): p. 167-93.

32. Flemming, H.C. and J. Wingender, *The biofilm matrix.* Nat Rev Microbiol, 2010. **8**(9): p. 623-33.

33. Flemming, H.C., *The perfect slime.* Colloids Surf B Biointerfaces, 2011. **86**(2): p. 251-9.

34. Tseng, B.S., et al., *The extracellular matrix protects Pseudomonas aeruginosa biofilms by limiting the penetration of tobramycin.* Environ Microbiol, 2013. **15**(10): p. 2865-78.

35. Stewart, P.S. and J.W. Costerton, *Antibiotic resistance of bacteria in biofilms.* Lancet, 2001. **358**(9276): p. 135-8.

36. Forier, K., et al., *Lipid and polymer nanoparticles for drug delivery to bacterial biofilms.* J Control Release, 2014. **190**(0): p. 607-23.

37. Høiby, N., et al., *Antibiotic resistance of bacterial biofilms.* International Journal of Antimicrobial Agents, 2010. **35**(4): p. 322-332.

38. Walters, M.C., 3rd, et al., *Contributions of antibiotic penetration, oxygen limitation, and low metabolic activity to tolerance of Pseudomonas aeruginosa biofilms to ciprofloxacin and tobramycin.* Antimicrob Agents Chemother, 2003. **47**(1): p. 317-23.

39. Prince, A.S., *Biofilms, antimicrobial resistance, and airway infection.* N Engl J Med, 2002. **347**(14): p. 1110-1.

40. Sauer, K., *The genomics and proteomics of biofilm formation.* Genome Biol, 2003. **4**(6): p. 219.

41. Singh PK, et al., *Quorum-sensing signals indicate that cystic fibrosis lungs are infected with bacterial biofilms.* Nature, 2000. **407**(6805): p. 762-4.

42. Bjarnsholt, T., *The role of bacterial biofilms in chronic infections.* APMIS Suppl, 2013(136): p. 1-51.

43.   Bjarnsholt T, J.P., Jakobsen TH, Phipps R, Nielsen AK, Rybtke MT, Tolker-Nielsen T, Givskov M, Høiby N, Ciofu O; Scandinavian Cystic Fibrosis Study Consortium., *Quorum sensing and virulence of Pseudomonas aeruginosa during lung infection of cystic fibrosis patients.* PLoS One, 2010. **5**(4).

44.   Diggle, S.P., et al., *The Pseudomonas aeruginosa quinolone signal molecule overcomes the cell density-dependency of the quorum sensing hierarchy, regulates rhl-dependent genes at the onset of stationary phase and can be produced in the absence of LasR.* Mol Microbiol, 2003. **50**(1): p. 29-43.

45.   Pesci, E.C., et al., *Regulation of las and rhl quorum sensing in Pseudomonas aeruginosa.* J Bacteriol, 1997. **179**(10): p. 3127-32.

46.   Cady, N.C., et al., *Inhibition of biofilm formation, quorum sensing and infection in Pseudomonas aeruginosa by natural products-inspired organosulfur compounds.* PLoS ONE, 2012. **7**(6): p. 8.

47.   Davies, D.G., et al., *The involvement of cell-to-cell signals in the development of a bacterial biofilm.* Science, 1998. **280**(5361): p. 295-8.

48.   Lee, J., et al., *A cell-cell communication signal integrates quorum sensing and stress response.* Nat Chem Biol, 2013. **9**(5): p. 339-43.

49.   Long, J., et al., *Depletion of intestinal phosphate after operative injury activates the virulence of P aeruginosa causing lethal gut-derived sepsis.* Surgery, 2008. **144**(2): p. 189-97.

50.   Lee, J. and L. Zhang, *The hierarchy quorum sensing network in Pseudomonas aeruginosa.* Protein Cell, 2015. **6**(1): p. 26-41.

51.   Hollander, F.M., N.M. de Roos, and H.G.M. Heijerman, *The optimal approach to nutrition and cystic fibrosis: latest evidence and recommendations.* Curr Opin Pulm Med, 2017. **23**(6): p. 556-561.

52.   Michl, R.K., et al., *Clinical approach to the diagnosis and treatment of cystic fibrosis and CFTR-related disorders.* Expert Rev Respir Med, 2016: p. 1-10.

53.   Cohen-Cymberknoh, M., D. Shoseyov, and E. Kerem, *Managing cystic fibrosis: strategies that increase life expectancy and improve quality of life.* Am J Respir Crit Care Med, 2011. **183**(11): p. 1463-71.

54.   Cystic Fibrosis Foundation. *Cystic Fibrosis Foundation's Drug Development Pipeline*. [cited 2018 August 15]; Available from: https://www.cff.org/Trials/Pipeline.

55.   Elkins, M.R., et al., *A controlled trial of long-term inhaled hypertonic saline in patients with cystic fibrosis.* N Engl J Med, 2006. **354**(3): p. 229-40.

56.   Robinson, M., et al., *Effect of increasing doses of hypertonic saline on mucociliary clearance in patients with cystic fibrosis.* Thorax, 1997. **52**(10): p. 900-3.

57.   Rosenfeld, M., et al., *Early pulmonary infection, inflammation, and clinical outcomes in infants with cystic fibrosis.* Pediatr Pulmonol, 2001. **32**(5): p. 356-66.

58.   Cantin, A., *Cystic fibrosis lung inflammation: early, sustained, and severe.* Am J Respir Crit Care Med, 1995. **151**(4): p. 939-41.

59.   Heijerman, H., et al., *Inhaled medication and inhalation devices for lung disease in patients with cystic fibrosis: A European consensus.* J Cyst Fibros, 2009. **8**(5): p. 295-315.

60.   Taccetti, G., et al., *Early antibiotic treatment for Pseudomonas aeruginosa eradication in patients with cystic fibrosis: a randomised multicentre study comparing two different protocols.* Thorax, 2012. **67**(10): p. 853-9.

61. Langton Hewer, S.C. and A.R. Smyth, *Antibiotic strategies for eradicating Pseudomonas aeruginosa in people with cystic fibrosis.* Cochrane Database Syst Rev, 2017. **4**: p. Cd004197.

62. Hoiby, N., B. Frederiksen, and T. Pressler, *Eradication of early Pseudomonas aeruginosa infection.* J Cyst Fibros, 2005. **4 Suppl 2**: p. 49-54.

63. Hoiby, N., O. Ciofu, and T. Bjarnsholt, *Pseudomonas aeruginosa biofilms in cystic fibrosis.* Future Microbiol, 2010. **5**(11): p. 1663-74.

64. Smyth, A.R., et al., *European Cystic Fibrosis Society Standards of Care: Best Practice guidelines.* J Cyst Fibros, 2014. **13 Suppl 1**: p. S23-42.

65. Ryan, G., M. Singh, and K. Dwan, *Inhaled antibiotics for long-term therapy in cystic fibrosis.* Cochrane Database Syst Rev, 2011. **16**(3).

66. Wolter, J., et al., *Effect of long term treatment with azithromycin on disease parameters in cystic fibrosis: a randomised trial.* Thorax, 2002. **57**(3): p. 212-6.

67. Gibson, R.L., J.L. Burns, and B.W. Ramsey, *Pathophysiology and management of pulmonary infections in cystic fibrosis.* Am J Respir Crit Care Med, 2003. **168**(8): p. 918-51.

68. Martiniano, S.L., S.D. Sagel, and E.T. Zemanick, *CYSTIC FIBROSIS: A MODEL SYSTEM FOR PRECISION MEDICINE.* Curr Opin Pediatr, 2016. **28**(3): p. 312-7.

69. Alton, E., et al., *Repeated nebulisation of non-viral CFTR gene therapy in patients with cystic fibrosis: a randomised, double-blind, placebo-controlled, phase 2b trial.* Lancet Respir Med, 2015. **3**(9): p. 684-691.

70. Zemanick, E.T., et al., *Highlights from the 2016 North American Cystic Fibrosis Conference.* Pediatr Pulmonol, 2017. **52**(8): p. 1103-1110.

71. Hadinoto, K. and W.S. Cheow, *Nano-antibiotics in chronic lung infection therapy against Pseudomonas aeruginosa.* Colloids Surf B Biointerfaces, 2014. **116**: p. 772-85.

72. Sans-Serramitjana, E., et al., *Free and Nanoencapsulated Tobramycin: Effects on Planktonic and Biofilm Forms of Pseudomonas.* Microorganisms, 2017. **5**(3).

73. Nafee, N., et al., *Antibiotic-free nanotherapeutics: Ultra-small, mucus-penetrating solid lipid nanoparticles enhance the pulmonary delivery and anti-virulence efficacy of novel quorum sensing inhibitors.* Journal of Controlled Release, 2014. **3**(14): p. 00464-7.

74. Carvalho, T.C., J.I. Peters, and R.O. Williams, 3rd, *Influence of particle size on regional lung deposition--what evidence is there?* Int J Pharm, 2011. **406**(1-2): p. 1-10.

75. Scheuch, G., et al., *Clinical perspectives on pulmonary systemic and macromolecular delivery.* Adv Drug Deliv Rev, 2006. **58**(9-10): p. 996-1008.

76. Bailey, M.M. and C.J. Berkland, *Nanoparticle formulations in pulmonary drug delivery.* Med Res Rev, 2009. **29**(1): p. 196-212.

77. Newhouse, M.T., et al., *Inhalation of a dry powder tobramycin PulmoSphere formulation in healthy volunteers.* Chest, 2003. **124**(1): p. 360-6.

78. Mitchell, J.P. and M.W. Nagel, *Cascade impactors for the size characterization of aerosols from medical inhalers: their uses and limitations.* J Aerosol Med, 2003. **16**(4): p. 341-77.

79. Allegretta G, *Evaluation of the Pseudomonas aeruginosa Quorum Sensing proteins PqsD, PqsBC and MvfR as novel anti-virulence targets*, in *Naturwissenschaftlich-Technischen Fakultät*. 2017, Saarland University: Saarbrücken.

80. Wagner, S., et al., *Novel Strategies for the Treatment of Pseudomonas aeruginosa Infections.* J Med Chem, 2016. **59**(13): p. 5929-69.

81. Pesci, E.C., et al., *Quinolone signaling in the cell-to-cell communication system of Pseudomonas aeruginosa.* Proc Natl Acad Sci U S A, 1999. **96**(20): p. 11229-34.

82. Shiley, J.R., K.K. Comfort, and J.B. Robinson, *Immunogenicity and antimicrobial effectiveness of Pseudomonas aeruginosa specific bacteriophage in a human lung in vitro model.* Appl Microbiol Biotechnol, 2017.

83. Debarbieux, L., et al., *Bacteriophages can treat and prevent Pseudomonas aeruginosa lung infections.* J Infect Dis, 2010. **201**(7): p. 1096-104.

84. Betts, A., et al., *Back to the future: evolving bacteriophages to increase their effectiveness against the pathogen Pseudomonas aeruginosa PAO1.* Evol Appl, 2013. **6**(7): p. 1054-63.

85. Rosen, B.H., et al., *Animal and model systems for studying cystic fibrosis.* J Cyst Fibros, 2017.

86. Snouwaert, J.N., et al., *An animal model for cystic fibrosis made by gene targeting.* Science, 1992. **257**(5073): p. 1083-8.

87. Dorin, J.R., et al., *Cystic fibrosis in the mouse by targeted insertional mutagenesis.* Nature, 1992. **359**(6392): p. 211-5.

88. Mall, M., et al., *Increased airway epithelial Na+ absorption produces cystic fibrosis-like lung disease in mice.* Nat Med, 2004. **10**(5): p. 487-93.

89. Zhou-Suckow, Z., et al., *Airway mucus, inflammation and remodeling: emerging links in the pathogenesis of chronic lung diseases.* Cell Tissue Res, 2017. **367**(3): p. 537-550.

90. Lebeaux, D., et al., *From in vitro to in vivo Models of Bacterial Biofilm-Related Infections.* Pathogens, 2013. **2**(2): p. 288-356.

91. Moser, C., et al., *Novel experimental Pseudomonas aeruginosa lung infection model mimicking long-term host-pathogen interactions in cystic fibrosis.* Apmis, 2009. **117**(2): p. 95-107.

92. Bragonzi, A., *Murine models of acute and chronic lung infection with cystic fibrosis pathogens.* Int J Med Microbiol, 2010. **300**(8): p. 584-93.

93. Bayes, H.K., et al., *A murine model of early Pseudomonas aeruginosa lung disease with transition to chronic infection.* Sci Rep, 2016. **6**(35838).

94. Hoffmann, N., et al., *Novel mouse model of chronic Pseudomonas aeruginosa lung infection mimicking cystic fibrosis.* Infect Immun, 2005. **73**(4): p. 2504-14.

95. Hoffmann, N., et al., *Azithromycin blocks quorum sensing and alginate polymer formation and increases the sensitivity to serum and stationary-growth-phase killing of Pseudomonas aeruginosa and attenuates chronic P. aeruginosa lung infection in Cftr(-/-) mice.* Antimicrob Agents Chemother, 2007. **51**(10): p. 3677-87.

96. Yan, Z., et al., *Ferret and pig models of cystic fibrosis: prospects and promise for gene therapy.* Hum Gene Ther Clin Dev, 2015. **26**(1): p. 38-49.

97. Russell, W.M.S. and R.L. Burch, *The Principles of Humane Experimental Technique.* . 1959: London: Methuen.

98. Bednarski, C., et al., *Targeted Integration of a Super-Exon into the CFTR Locus Leads to Functional Correction of a Cystic Fibrosis Cell Line Model.* PLoS One, 2016. **11**(8): p. e0161072.

99. Harrison, J.J., et al., *Microtiter susceptibility testing of microbes growing on peg lids: a miniaturized biofilm model for high-throughput screening.* Nat Protoc, 2010. **5**(7): p. 1236-54.

100.   O'Toole, G.A., *Microtiter dish biofilm formation assay.* J Vis Exp, 2011. **30**(47).

101.   Elkhatib, W. and A. Noreddin, *Efficacy of Ciprofloxacin-Clarithromycin Combination Against Drug-Resistant Pseudomonas aeruginosa Mature Biofilm Using In Vitro Experimental Model.* Microb Drug Resist, 2014. **22**: p. 22.

102.   Ceri, H., et al., *The Calgary Biofilm Device: new technology for rapid determination of antibiotic susceptibilities of bacterial biofilms.* J Clin Microbiol, 1999. **37**(6): p. 1771-6.

103.   Zemke, A.C., et al., *Nitrite modulates bacterial antibiotic susceptibility and biofilm formation in association with airway epithelial cells.* Free Radic Biol Med, 2014. **77**: p. 307-16.

104.   Forbes, B., *Human airway epithelial cell lines for in vitro drug transport and metabolism studies.* Pharmaceutical Science & Technology Today, 2000. **3**(1): p. 18-27.

105.   Bur, M. and C.M. Lehr, *Pulmonary cell culture models to study the safety and efficacy of innovative aerosol medicines.* Expert Opin Drug Deliv, 2008. **5**(6): p. 641-52.

106.   Gruenert, D.C., W.E. Finkbeiner, and J.H. Widdicombe, *Culture and transformation of human airway epithelial cells.* Am J Physiol, 1995. **268**(3 Pt 1): p. L347-60.

107.   Gruenert, D.C., et al., *Established cell lines used in cystic fibrosis research.* Journal of Cystic Fibrosis, 2004. **3**: p. 191-196.

108.   Ehrhardt, C., et al., *Towards an in vitro model of cystic fibrosis small airway epithelium: characterisation of the human bronchial epithelial cell line CFBE41o.* Cell Tissue Res, 2006. **323**(3): p. 405-15.

109.   National Center for Biotechnology Information, U.S.N.L.o.M. *PubMed*. 2018 [cited 2018 September 08]; Available from: https://www.ncbi.nlm.nih.gov/pubmed/?term=cfbe41o-++cystic+fibrosis.

110.   Hein S, B.M., Kolb T, Muellinger B, Schaefer UF, Lehr CM, *The Pharmaceutical Aerosol Deposition Device On Cell Cultures (PADDOCC) In Vitro System: Design and Experimental Protocol.* Altern Lab Anim, 2010. **38**(4): p. 285-95.

111.   Moreau-Marquis, S., et al., *Co-culture models of Pseudomonas aeruginosa biofilms grown on live human airway cells.* Journal of Visualized Experiments, 2010(44).

112.   Anderson, G.G., et al., *In vitro analysis of tobramycin-treated Pseudomonas aeruginosa biofilms on cystic fibrosis-derived airway epithelial cells.* Infect Immun, 2008. **76**(4): p. 1423-33.

113.   Swiatecka-Urban A, et al., *Pseudomonas aeruginosa inhibits endocytic recycling of CFTR in polarized human airway epithelial cells.* Am J Physiol Cell Physiol, 2006. **290**(3): p. 862-72.

114.   Tan, Q., et al., *Human airway organoid engineering as a step toward lung regeneration and disease modeling.* Biomaterials, 2017. **113**: p. 118-132.

115.   Carterson, A.J., et al., *A549 lung epithelial cells grown as three-dimensional aggregates: alternative tissue culture model for Pseudomonas aeruginosa pathogenesis.* Infect Immun, 2005. **73**(2): p. 1129-40.

116.   Swain, R.J., et al., *Assessment of cell line models of primary human cells by Raman spectral phenotyping.* Biophys J, 2010. **98**(8): p. 1703-11.

117.   Forbes, B. and C. Ehrhardt, *Human respiratory epithelial cell culture for drug delivery applications.* European Journal of Pharmaceutics and Biopharmaceutics, 2005. **60**(2): p. 193-205.

118. Sakagami, M., *In vivo, in vitro and ex vivo models to assess pulmonary absorption and disposition of inhaled therapeutics for systemic delivery.* Advanced Drug Delivery Reviews, 2006. **58**(9–10): p. 1030-1060.

119. Steimer, A., E. Haltner, and C.M. Lehr, *Cell culture models of the respiratory tract relevant to pulmonary drug delivery.* J Aerosol Med, 2005. **18**(2): p. 137-82.

120. Daum, N., et al., *In vitro systems for studying epithelial transport of macromolecules.* Methods Mol Biol, 2009. **480**: p. 151-64.

121. Schneider, C.A., W.S. Rasband, and K.W. Eliceiri, *NIH Image to ImageJ: 25 years of image analysis.* Nat Methods, 2012. **9**(7): p. 671-5.

122. Schindelin, J., et al., *Fiji: an open-source platform for biological-image analysis.* Nat Methods, 2012. **9**(7): p. 676-82.

123. Shumilov, D., et al., *Real-time imaging of exocytotic mucin release and swelling in Calu-3 cells using acridine orange.* Methods, 2014. **66**(2): p. 312-24.

124. Kapuscinski, J., Z. Darzynkiewicz, and M.R. Melamed, *Luminescence of the solid complexes of acridine orange with RNA.* Cytometry, 1982. **2**(4): p. 201-11.

125. Teubl, B.J., et al., *The oral cavity as a biological barrier system: Design of an advanced buccal in vitro permeability model.* European Journal of Pharmaceutics and Biopharmaceutics, 2013. **84**(2): p. 386-393.

126. Feldman, G.J., J.M. Mullin, and M.P. Ryan, *Occludin: structure, function and regulation.* Adv Drug Deliv Rev, 2005. **57**(6): p. 883-917.

127. Citi, S. and M. Cordenonsi, *Tight junction proteins1.* Biochimica et Biophysica Acta (BBA) - Molecular Cell Research, 1998. **1448**(1): p. 1-11.

128. Farquhar, M.G. and G.E. Palade, *Junctional complexes in various epithelia.* J Cell Biol, 1963. **17**(2): p. 375-412.

129. Staehelin, L.A., *Further observations on the fine structure of freeze-cleaved tight junctions.* J Cell Sci, 1973. **13**(3): p. 763-86.

130. Dorfel, M.J. and O. Huber, *Modulation of tight junction structure and function by kinases and phosphatases targeting occludin.* J Biomed Biotechnol, 2012. **2012**: p. 807356.

131. Ikenouchi, J., et al., *Tricellulin constitutes a novel barrier at tricellular contacts of epithelial cells.* J Cell Biol, 2005. **171**(6): p. 939-45.

132. Farkas, A.E., C.T. Capaldo, and A. Nusrat, *Regulation of epithelial proliferation by tight junction proteins.* Ann N Y Acad Sci, 2012. **1258**: p. 115-24.

133. Balda, M.S. and K. Matter, *Tight junctions at a glance.* J Cell Sci, 2008. **121**(Pt 22): p. 3677-82.

134. Marchiando, A.M., W.V. Graham, and J.R. Turner, *Epithelial barriers in homeostasis and disease.* Annu Rev Pathol, 2010. **5**: p. 119-44.

135. Paris, L., et al., *Structural organization of the tight junctions.* Biochim Biophys Acta, 2008. **1778**(3): p. 646-59.

136. Tang, V.W., *Proteomic and bioinformatic analysis of epithelial tight junction reveals an unexpected cluster of synaptic molecules.* Biol Direct, 2006. **1**: p. 37.

137. Deli, M.A., *Potential use of tight junction modulators to reversibly open membranous barriers and improve drug delivery.* Biochim Biophys Acta, 2009. **1788**(4): p. 892-910.

138. Gonzalez-Mariscal, L., S. Lechuga, and E. Garay, *Role of tight junctions in cell proliferation and cancer.* Prog Histochem Cytochem, 2007. **42**(1): p. 1-57.

139. Grainger, C.I., et al., *Culture of Calu-3 Cells at the Air Interface Provides a Representative Model of the Airway Epithelial Barrier.* Pharmaceutical Research, 2006. **23**(7): p. 1482-1490.

140. Stentebjerg-Andersen, A., et al., *Calu-3 cells grown under AIC and LCC conditions: implications for dipeptide uptake and transepithelial transport of substances.* Eur J Pharm Biopharm, 2011. **78**(1): p. 19-26.

141. Ehrhardt, C., et al., *Drug absorption by the respiratory mucosa: cell culture models and particulate drug carriers.* J Aerosol Med, 2002. **15**(2): p. 131-9.

142. Florea, B.I., et al., *Drug transport and metabolism characteristics of the human airway epithelial cell line Calu-3.* J Control Release, 2003. **87**(1-3): p. 131-8.

143. Foster, K.A., et al., *Characterization of the Calu-3 cell line as a tool to screen pulmonary drug delivery.* Int J Pharm, 2000. **208**(1-2): p. 1-11.

144. Fiegel, J., et al., *Large porous particle impingement on lung epithelial cell monolayers--toward improved particle characterization in the lung.* Pharm Res, 2003. **20**(5): p. 788-96.

145. Haghi, M., et al., *Time- and passage-dependent characteristics of a Calu-3 respiratory epithelial cell model.* Drug Dev Ind Pharm, 2010. **36**(10): p. 1207-14.

146. Meindl, C., et al., *Permeation of Therapeutic Drugs in Different Formulations across the Airway Epithelium In Vitro.* PLoS One, 2015. **10**(8): p. e0135690.

147. Bhat, P.G., D.R. Flanagan, and M.D. Donovan, *Drug diffusion through cystic fibrotic mucus: steady-state permeation, rheologic properties, and glycoprotein morphology.* J Pharm Sci, 1996. **85**(6): p. 624-30.

148. Cone, R.A., *Barrier properties of mucus.* Advanced Drug Delivery Reviews, 2009. **61**(2): p. 75-85.

149. Murgia, X., et al., *Size-Limited Penetration of Nanoparticles into Porcine Respiratory Mucus after Aerosol Deposition.* Biomacromolecules, 2016. **17**(4): p. 1536-42.

150. Nordgard, C.T., et al., *Alterations in mucus barrier function and matrix structure induced by guluronate oligomers.* Biomacromolecules, 2014. **15**(6): p. 2294-300.

151. Fahy, J.V. and B.F. Dickey, *Airway mucus function and dysfunction.* N Engl J Med, 2010. **363**(23): p. 2233-47.

152. Ruge, C.A., J. Kirch, and C.M. Lehr, *Pulmonary drug delivery: from generating aerosols to overcoming biological barriers-therapeutic possibilities and technological challenges.* Lancet Respir Med, 2013. **1**(5): p. 402-13.

153. Kilcoyne, M., et al., *Periodic acid-Schiff's reagent assay for carbohydrates in a microtiter plate format.* Anal Biochem, 2011. **416**(1): p. 18-26.

154. Shen, B.Q., et al., *Calu-3: a human airway epithelial cell line that shows cAMP-dependent Cl- secretion.* Am J Physiol, 1994. **266**(5 Pt 1): p. L493-501.

155. Berger, J.T., et al., *Respiratory carcinoma cell lines. MUC genes and glycoconjugates.* Am J Respir Cell Mol Biol, 1999. **20**(3): p. 500-10.

156. Marusic, M., et al., *Calu-3 model under AIC and LCC conditions and application for protein permeability studies.* Acta Chim Slov, 2014. **61**(1): p. 100-9.

157. Pezron, I., et al., *Insulin aggregation and asymmetric transport across human bronchial epithelial cell monolayers (Calu-3).* J Pharm Sci, 2002. **91**(4): p. 1135-46.

158. Patel, J., et al., *Transport of HIV-protease inhibitors across 1 alpha,25di-hydroxy vitamin D3-treated Calu-3 cell monolayers: modulation of P-glycoprotein activity.* Pharm Res, 2002. **19**(11): p. 1696-703.

159. Mathias, N.R., et al., *Permeability characteristics of calu-3 human bronchial epithelial cells: in vitro-in vivo correlation to predict lung absorption in rats* J Drug Target, 2002. **10**(1): p. 31-40.

160. Moreau-Marquis, S., et al., *The DeltaF508-CFTR mutation results in increased biofilm formation by Pseudomonas aeruginosa by increasing iron availability.* Am J Physiol Lung Cell Mol Physiol, 2008. **295**(1): p. L25-37.

161. Price, K.E., et al., *Mannitol Does Not Enhance Tobramycin Killing of Pseudomonas aeruginosa in a Cystic Fibrosis Model System of Biofilm Formation.* PLoS ONE, 2015. **10**(10).

162. Hein, S., et al., *A new Pharmaceutical Aerosol Deposition Device on Cell Cultures (PADDOCC) to evaluate pulmonary drug absorption for metered dose dry powder formulations.* European Journal of Pharmaceutics and Biopharmaceutics, 2011. **77**(1): p. 132-138.

163. Griffiths, P.C., et al., *Probing the interaction of nanoparticles with mucin for drug delivery applications using dynamic light scattering.* Eur J Pharm Biopharm, 2015. **97**(Pt A): p. 218-22.

164. Voynow, J.A. and B.K. Rubin, *Mucins, mucus, and sputum.* Chest, 2009. **135**(2): p. 505-12.

165. Groo, A.C. and F. Lagarce, *Mucus models to evaluate nanomedicines for diffusion.* Drug Discov Today, 2014. **19**(8): p. 1097-108.

166. Meyerholz, D.K., et al., *Immunohistochemical Detection of Markers for Translational Studies of Lung Disease in Pigs and Humans.* Toxicol Pathol, 2016. **44**(3): p. 434-41.

167. Aigner, B., et al., *Transgenic pigs as models for translational biomedical research.* J Mol Med (Berl), 2010. **88**(7): p. 653-64.

168. Rogers, C.S., et al., *The porcine lung as a potential model for cystic fibrosis.* Am J Physiol Lung Cell Mol Physiol, 2008. **295**(2): p. L240-63.

169. Sharma, R., et al., *Surfactant Driven Post-Deposition Spreading of Aerosols on Complex Aqueous Subphases. 2: Low Deposition Flux Representative of Aerosol Delivery to Small Airways.* J Aerosol Med Pulm Drug Deliv, 2015. **28**(5): p. 394-405.

170. Pritchard, M.F., et al., *A New Class of Safe Oligosaccharide Polymer Therapy To Modify the Mucus Barrier of Chronic Respiratory Disease.* Mol Pharm, 2016. **13**(3): p. 863-72.

171. d'Angelo, I., et al., *Overcoming barriers in Pseudomonas aeruginosa lung infections: Engineered nanoparticles for local delivery of a cationic antimicrobial peptide.* Colloids Surf B Biointerfaces, 2015. **135**: p. 717-725.

172. Kirch, J., et al., *Optical tweezers reveal relationship between microstructure and nanoparticle penetration of pulmonary mucus.* Proc Natl Acad Sci U S A, 2012. **109**(45): p. 18355-60.

173. Schuster, B.S., et al., *Nanoparticle diffusion in respiratory mucus from humans without lung disease.* Biomaterials, 2013. **34**(13): p. 3439-46.

174. Stoltz, D.A., et al., *Cystic fibrosis pigs develop lung disease and exhibit defective bacterial eradication at birth.* Sci Transl Med, 2010. **2**(29): p. 29ra31.

175. Rubin, B.K., et al., *General anesthesia does not alter the viscoelastic or transport properties of human respiratory mucus.* Chest, 1990. **98**(1): p. 101-4.

176. Rubin, B.K., et al., *Collection and analysis of respiratory mucus from subjects without lung disease.* Am Rev Respir Dis, 1990. **141**(4 Pt 1): p. 1040-3.

177. Murgia, X., et al., *Modelling the bronchial barrier in pulmonary drug delivery: A human bronchial epithelial cell line supplemented with human tracheal mucus.* Eur J Pharm Biopharm, 2017.

178. Boegh, M., et al., *Property profiling of biosimilar mucus in a novel mucus-containing in vitro model for assessment of intestinal drug absorption.* Eur J Pharm Biopharm, 2014. **87**(2): p. 227-35.

179. Semmler, A.B., C.B. Whitchurch, and J.S. Mattick, *A re-examination of twitching motility in Pseudomonas aeruginosa.* Microbiology, 1999. **145 (Pt 10)**: p. 2863-73.

180. Arora, S.K., et al., *The Pseudomonas aeruginosa flagellar cap protein, FliD, is responsible for mucin adhesion.* Infect Immun, 1998. **66**(3): p. 1000-7.

181. O'Toole, G., H.B. Kaplan, and R. Kolter, *Biofilm formation as microbial development.* Annu Rev Microbiol, 2000. **54**: p. 49-79.

182. Costerton, J.W., et al., *Microbial biofilms.* Annu Rev Microbiol, 1995. **49**: p. 711-45.

183. O'Toole, G.A. and R. Kolter, *Initiation of biofilm formation in Pseudomonas fluorescens WCS365 proceeds via multiple, convergent signalling pathways: a genetic analysis.* Mol Microbiol, 1998. **28**(3): p. 449-61.

184. Wimpenny, J.W.T. and R. Colasanti, *A unifying hypothesis for the structure of microbial biofilms based on cellular automaton models.* FEMS Microbiology Ecology, 1997. **22**(1): p. 1-16.

185. Miller, J.H., *A short course in bacterial genetics a laboratory manual and handbook for Escherichia coli and related bacteria*. Vol. Laboratory manual Handbook. 1992: Cold Spring Harbor, N.Y., Cold Spring Harbor Lab.

186. O'Toole, G.A., et al., *Genetic approaches to study of biofilms.* Methods Enzymol, 1999. **310**: p. 91-109.

187. Caiazza, N.C. and G.A. O'Toole, *SadB is required for the transition from reversible to irreversible attachment during biofilm formation by Pseudomonas aeruginosa PA14.* J Bacteriol, 2004. **186**(14): p. 4476-85.

188. Holloway, B.W., *Genetic recombination in Pseudomonas aeruginosa.* J Gen Microbiol, 1955. **13**(3): p. 572-81.

189. Stover, C.K., et al., *Complete genome sequence of Pseudomonas aeruginosa PAO1, an opportunistic pathogen.* Nature, 2000. **406**(6799): p. 959-64.

190. National Center for Biotechnology Information, U.S.N.L.o.M. *PubMed*. 2018 [cited 2018 August 20]; Available from: https://www.ncbi.nlm.nih.gov/pubmed/?term=pseudomonas+aeruginosa+pao1+cystic+fibrosis.

191. Penesyan, A., et al., *Genetically and Phenotypically Distinct Pseudomonas aeruginosa Cystic Fibrosis Isolates Share a Core Proteomic Signature.* PLoS One, 2015. **10**(10): p. e0138527.

192. Jorgensen, K.M., et al., *Diversity of metabolic profiles of cystic fibrosis Pseudomonas aeruginosa during the early stages of lung infection.* Microbiology, 2015. **161**(7): p. 1447-62.

193. Elbing, K.L. and R. Brent, *Media Preparation and Bacteriological Tools*, in *Current Protocols in Protein Science*. 2001, John Wiley & Sons, Inc.

194. Pardee, A.B., F. Jacob, and J. Monod, *The genetic control and cytoplasmic expression of "Inducibility" in the synthesis of β-galactosidase by E. coli.* Journal of Molecular Biology, 1959. **1**(2): p. 165-178.

195. Emerson, J., et al., *Pseudomonas aeruginosa and other predictors of mortality and morbidity in young children with cystic fibrosis.* Pediatr Pulmonol, 2002. **34**(2): p. 91-100.

196. Klausen, M., et al., *Biofilm formation by Pseudomonas aeruginosa wild type, flagella and type IV pili mutants.* Mol Microbiol, 2003. **48**(6): p. 1511-24.

197. Merritt, J.H., D.E. Kadouri, and G.A. O'Toole, *Growing and analyzing static biofilms.* Curr Protoc Microbiol, 2005. **Chapter 1**(1): p. Unit 1B 1.

198. Musken, M., et al., *Genetic determinants of Pseudomonas aeruginosa biofilm establishment.* Microbiology, 2010. **156**(Pt 2): p. 431-41.

199. Mura, S., et al., *Biodegradable nanoparticles meet the bronchial airway barrier: how surface properties affect their interaction with mucus and epithelial cells.* Biomacromolecules, 2011. **12**(11): p. 4136-43.

200. Caldara, M., et al., *Mucin biopolymers prevent bacterial aggregation by retaining cells in the free-swimming state.* Curr Biol, 2012. **22**(24): p. 2325-30.

201. Sadikot, R.T., et al., *Pathogen-host interactions in Pseudomonas aeruginosa pneumonia.* Am J Respir Crit Care Med, 2005. **171**(11): p. 1209-23.

202. Furukawa, S., S.L. Kuchma, and G.A. O'Toole, *Keeping Their Options Open: Acute versus Persistent Infections.* Journal of Bacteriology, 2006. **188**(4): p. 1211-1217.

203. Yang, L., et al., *Effects of iron on DNA release and biofilm development by Pseudomonas aeruginosa.* Microbiology, 2007. **153**(Pt 5): p. 1318-28.

204. Lieleg, O., et al., *Mechanical robustness of Pseudomonas aeruginosa biofilms.* Soft Matter, 2011. **7**(7): p. 3307-3314.

205. Bjarnsholt, T., et al., *Pseudomonas aeruginosabiofilms in the respiratory tract of cystic fibrosis patients.* Pediatric Pulmonology, 2009. **44**(6): p. 547-558.

206. Proesmans, M., et al., *Comparison of two treatment regimens for eradication of Pseudomonas aeruginosa infection in children with cystic fibrosis.* J Cyst Fibros, 2013. **12**(1): p. 29-34.

207. Ratjen, F., et al., *Treatment of early Pseudomonas aeruginosa infection in patients with cystic fibrosis: the ELITE trial.* Thorax, 2010. **65**(4): p. 286-91.

208. Treggiari, M.M., et al., *Comparative efficacy and safety of 4 randomized regimens to treat early Pseudomonas aeruginosa infection in children with cystic fibrosis.* Arch Pediatr Adolesc Med, 2011. **165**(9): p. 847-56.

209. Lillquist, Y.P., E. Cho, and A.G. Davidson, *Economic effects of an eradication protocol for first appearance of Pseudomonas aeruginosa in cystic fibrosis patients: 1995 vs. 2009.* J Cyst Fibros, 2011. **10**(3): p. 175-80.

210. Noah, T.L., et al., *Inhaled versus systemic antibiotics and airway inflammation in children with cystic fibrosis and Pseudomonas.* Pediatr Pulmonol, 2010. **45**(3): p. 281-90.

211. Mogayzel, P.J., Jr., et al., *Cystic fibrosis pulmonary guidelines. Chronic medications for maintenance of lung health.* Am J Respir Crit Care Med, 2013. **187**(7): p. 680-9.

212. Gunday Tureli, N., et al., *Ciprofloxacin-loaded PLGA nanoparticles against cystic fibrosis P. aeruginosa lung infections.* Eur J Pharm Biopharm, 2017. **117**: p. 363-371.

213. Suk, J.S., et al., *The penetration of fresh undiluted sputum expectorated by cystic fibrosis patients by non-adhesive polymer nanoparticles.* Biomaterials, 2009. **30**(13): p. 2591-7.

214. Frohlich, E. and E. Roblegg, *Mucus as barrier for drug delivery by nanoparticles.* J Nanosci Nanotechnol, 2014. **14**(1): p. 126-36.

215. Yamamoto, H., et al., *Surface-modified PLGA nanosphere with chitosan improved pulmonary delivery of calcitonin by mucoadhesion and opening of the intercellular tight junctions.* J Control Release, 2005. **102**(2): p. 373-81.

216. Bernkop-Schnurch, A. and S. Dunnhaupt, *Chitosan-based drug delivery systems.* Eur J Pharm Biopharm, 2012. **81**(3): p. 463-9.

217. Schneider, C.S., et al., *Nanoparticles that do not adhere to mucus provide uniform and long-lasting drug delivery to airways following inhalation.* Sci Adv, 2017. **3**(4): p. e1601556.

218. Lai, S.K., Y.Y. Wang, and J. Hanes, *Mucus-penetrating nanoparticles for drug and gene delivery to mucosal tissues.* Adv Drug Deliv Rev, 2009. **61**(2): p. 158-71.

219. Suk, J.S., et al., *PEGylation as a strategy for improving nanoparticle-based drug and gene delivery.* Adv Drug Deliv Rev, 2016. **99**(Pt A): p. 28-51.

220. Lai, S.K., et al., *Rapid transport of large polymeric nanoparticles in fresh undiluted human mucus.* Proc Natl Acad Sci U S A, 2007. **104**(5): p. 1482-7.

221. Yang, M., et al., *Biodegradable nanoparticles composed entirely of safe materials that rapidly penetrate human mucus.* Angew Chem Int Ed Engl, 2011. **50**(11): p. 2597-600.

222. Wang, Y.Y., et al., *Addressing the PEG mucoadhesivity paradox to engineer nanoparticles that "slip" through the human mucus barrier.* Angew Chem Int Ed Engl, 2008. **47**(50): p. 9726-9.

223. Wacker, M., *Nanocarriers for intravenous injection--the long hard road to the market.* Int J Pharm, 2013. **457**(1): p. 50-62.

224. Danhier, F., et al., *PLGA-based nanoparticles: an overview of biomedical applications.* J Control Release, 2012. **161**(2): p. 505-22.

225. Makadia, H.K. and S.J. Siegel, *Poly Lactic-co-Glycolic Acid (PLGA) as Biodegradable Controlled Drug Delivery Carrier.* Polymers (Basel), 2011. **3**(3): p. 1377-1397.

226. Gunday Tureli, N., A.E. Tureli, and M. Schneider, *Optimization of ciprofloxacin complex loaded PLGA nanoparticles for pulmonary treatment of cystic fibrosis infections: Design of experiments approach.* Int J Pharm, 2016. **515**(1-2): p. 343-351.

227. Kabanov, A.V., et al., *Pluronic block copolymers: novel functional molecules for gene therapy.* Adv Drug Deliv Rev, 2002. **54**(2): p. 223-33.

228. Kabanov, A.V., E.V. Batrakova, and V.Y. Alakhov, *Pluronic block copolymers as novel polymer therapeutics for drug and gene delivery.* J Control Release, 2002. **82**(2-3): p. 189-212.

229. U.S. Food and Drug Administration. *Inactive Ingredient Search for Approved Drug Products.* 2018 2018, July 12 [cited 2018 August 22]; Available from: https://www.accessdata.fda.gov/scripts/cder/iig/index.cfm.

230. Batrakova, E.V. and A.V. Kabanov, *Pluronic block copolymers: evolution of drug delivery concept from inert nanocarriers to biological response modifiers.* J Control Release, 2008. **130**(2): p. 98-106.

231. Saski, W. and S.G. Shah, *AVAILABILITY OF DRUGS IN THE PRESENCE OF SURFACE-ACTIVE AGENTS. II. EFFECTS OF SOME OXYETHYLENE OXYPROPYLENE POLYMERS ON THE BIOLOGICAL ACTIVITY OF HEXETIDINE.* J Pharm Sci, 1965. **54**: p. 277-80.

232. Grabowski, N., et al., *Toxicity of surface-modified PLGA nanoparticles toward lung alveolar epithelial cells.* Int J Pharm, 2013. **454**(2): p. 686-94.

233. Adi, H., et al., *Co-spray-dried mannitol-ciprofloxacin dry powder inhaler formulation for cystic fibrosis and chronic obstructive pulmonary disease.* Eur J Pharm Sci, 2010. **40**(3): p. 239-47.

234. Baelo, A., et al., *Disassembling bacterial extracellular matrix with DNase-coated nanoparticles to enhance antibiotic delivery in biofilm infections.* J Control Release, 2015. **209**: p. 150-8.

235. Bakker-Woudenberg, I.A., et al., *Ciprofloxacin in polyethylene glycol-coated liposomes: efficacy in rat models of acute or chronic Pseudomonas aeruginosa infection.* Antimicrob Agents Chemother, 2002. **46**(8): p. 2575-81.

236. Cipolla, D., J. Blanchard, and I. Gonda, *Development of Liposomal Ciprofloxacin to Treat Lung Infections.* Pharmaceutics, 2016. **8**(1).

237. Ong, H.X., et al., *In vitro and ex vivo methods predict the enhanced lung residence time of liposomal ciprofloxacin formulations for nebulisation.* Eur J Pharm Biopharm, 2014. **86**(1): p. 83-9.

238. Ong, H.X., et al., *Liposomal nanoparticles control the uptake of ciprofloxacin across respiratory epithelia.* Pharm Res, 2012. **29**(12): p. 3335-46.

239. Osman, R., et al., *Spray dried inhalable ciprofloxacin powder with improved aerosolisation and antimicrobial activity.* Int J Pharm, 2013. **449**(1-2): p. 44-58.

240. Serisier, D.J., et al., *Inhaled, dual release liposomal ciprofloxacin in non-cystic fibrosis bronchiectasis (ORBIT-2): a randomised, double-blind, placebo-controlled trial.* Thorax, 2013. **68**(9): p. 812-7.

241. Sweeney, L.G., et al., *Spray-freeze-dried liposomal ciprofloxacin powder for inhaled aerosol drug delivery.* International Journal of Pharmaceutics, 2005. **305**(1-2): p. 180-185.

242. Yu, H., et al., *Dry powder inhaler formulation of high-payload antibiotic nanoparticle complex intended for bronchiectasis therapy: Spray drying versus spray freeze drying preparation.* Int J Pharm, 2016. **499**(1-2): p. 38-46.

243. Aksamit, T., et al., *The RESPIRE trials: Two phase III, randomized, multicentre, placebo-controlled trials of Ciprofloxacin Dry Powder for Inhalation (Ciprofloxacin DPI) in non-cystic fibrosis bronchiectasis.* Contemp Clin Trials, 2017. **58**: p. 78-85.

244. U.S. National Library of Medicine. *ClinicalTrials.gov*. 2018 2018, July 05; Available from: https://clinicaltrials.gov/ct2/results?cond=non-cystic+fibrosis+bronchiectasis&Search=Apply&recrs=e&age_v=&gndr=&type=&rslt=.

245. MD Magazine. *FDA Advisory Committee Advises Against Ciprofloxacin DPI*. 2017, November 17 [cited 2018 August 23]; Available from: https://www.mdmag.com/medical-news/fda-advisory-committee-advises-against-ciprofloxacin-dpi.

246. Bayer AG. *Annual Report 2017 Augmented Version*. 2018 2018, February 18; Available from: http://www.annualreport2017.bayer.com/management-report-annexes/about-the-group/focus-on-innovation/pharmaceuticals.html.

247. Aradigm Corporation. *Aradigm Announces Top-Line Results from Two Phase 3 Studies Evaluating Pulmaquin for the Chronic Treatment of Non-Cystic Fibrosis Bronchiectasis Patients with Lung Infections with Pseudomonas aeruginosa*. 01. December 2016 [cited 2017 July 27]; Available from: http://investor.aradigm.com/releaseDetail.cfm?ReleaseID=1001671.

248. AdisInsight Drugs. *Ciprofloxacin inhalation - Aradigm*. 2018 2018 May 28 [cited 2018 August 30]; Available from: http://adisinsight.springer.com/drugs/800021873.

249.   Aradigm Corporation. *Aradigm Receives Complete Response Letter from the FDA for Linhaliq NDA*. 2018 2018 January 29 [cited 2018 August 29]; Available from: https://aradigm.gcs-web.com/news-releases/news-release-details/aradigm-receives-complete-response-letter-fda-linhaliq-nda.

250.   Aradigm Corporation. *Lipoquin (ARD-3100) — Inhaled Ciprofloxacin for the Management of Infections in Cystic Fibrosis (CF) Patients*. 2018   [cited 2018 September 14]; Available from: http://www.aradigm.com/products_3100.html.

251.   Gunday Tureli, N., A.E. Tureli, and M. Schneider, *Counter-ion complexes for enhanced drug loading in nanocarriers: Proof-of-concept and beyond.* Int J Pharm, 2016. **511**(2): p. 994-1001.

252.   Shive, M.S. and J.M. Anderson, *Biodegradation and biocompatibility of PLA and PLGA microspheres.* Adv Drug Deliv Rev, 1997. **28**(1): p. 5-24.

253.   Cedervall, T., et al., *Understanding the nanoparticle-protein corona using methods to quantify exchange rates and affinities of proteins for nanoparticles.* Proc Natl Acad Sci U S A, 2007. **104**(7): p. 2050-5.

Scientific output

Research papers

J. Juntke, X. Murgia[a], N. Günday Türeli, A. E. Türeli, C. Carvalho-Wodarz[a], M. Schneider[c], N. Schneider-Daum, CM Lehr, *P. aeruginosa biofilms co-cultured on top of human bronchial epithelial cells for evaluating safety and efficacy of aerosolized antibiotic nanocarriers* (in preparation)

N. Günday Türeli, A. Torge, **J. Juntke**, B. C. Schwarz, N. Schneider-Daum, A. E. Türeli, CM. Lehr, M. Schneider, *Ciprofloxacin-loaded PLGA nanoparticles against Cystic Fibrosis P. aeruginosa Lung Infections*, Eur J Pharm Biopharm. 2017

Review article

M. Hittinger*, **J. Juntke***, S. Kletting*, N. Schneider-Daum, C. de Souza Carvalho-Wodarz, C.M. Lehr, *Preclinical safety and efficacy models for pulmonary drug delivery of antimicrobials with focus on in vitro models*, Adv Drug Deliv Rev. 2015.

Oral presentations

J. Juntke, N. Günday Türeli, M. Schneider, N. Schneider-Daum and CM Lehr,
Novel cystic fibrosis in vitro model for safety and efficacy testing of new drug delivery systems against chronic Pseudomonas aeruginosa infections
17th EUSAAT 3Rs congress, August 2016, Linz, Austria

J. Juntke, N. Günday Türeli, A. Torge, C. Carvalho-Wodarz, EM Prinz, M. Schneider, N. Schneider-Daum and CM Lehr
Towards a new bacterial-epithelial cell co-culture model to test novel drug delivery systems against Pseudomonas aeruginosa biofilms
20th ISAM-Congress, May to June 2015, Munich, Germany

Poster presentations

R. Hendrix*****, **J. Juntke***, S. Kletting, C. Carvalho-Wodarz, N. Schneider-Daum, CM Lehr

Pulmonary in vitro models mimicking lung inflammation and infection

6th HIPS Symposium, June 2016, Saarbrücken, Germany

J. Juntke, N. Günday Türeli, C. Carvalho-Wodarz, M. Schneider, N. Schneider-Daum and CM Lehr

New co-culture model of human airway epithelial cells infected with Pseudomonas aeruginosa to test novel drug delivery systems

10th PBP World Meeting, April 2016, Glasgow, UK

J. Juntke, N. Günday Türeli, C. de Souza Carvalho-Wodarz, M. Schneider, N. Schneider-Daum and CM Lehr

New bacterial-epithelial cell co-culture model to test novel drug delivery systems against chronic Pseudomonas aeruginosa infections

Biological Barriers, March 2016, Saarbrücken, Germany

J. Juntke, N. Günday Türeli, C. de Souza Carvalho-Wodarz, M. Schneider, N. Schneider-Daum and CM Lehr

Towards a new bacterial-epithelial cell co-culture model to test novel drug delivery systems against Pseudomonas aeruginosa biofilms

DPhG Annual Meeting, September 2015, Düsseldorf, Germany

J. Juntke, N. Günday Türeli, A. Torge, C. Carvalho-Wodarz, EM Prinz, M. Schneider, N. Schneider-Daum and CM Lehr

Towards a new bacterial-epithelial cell co-culture model to test novel drug delivery systems against Pseudomonas aeruginosa biofilms

20th ISAM-Congress, May to June 2015, Munich, Germany

* The authors contributed equally to this work.

J. Juntke, N. Günday Türeli, C. de Souza Carvalho, EM Prinz, M. Schneider, N. Schneider-Daum and CM Lehr

Towards a new bacterial-epithelial cell co-culture model to test novel drug delivery systems against Pseudomonas aeruginosa biofilms

2. Doktorandentag der Naturwissenschaftlich-Technischen Fakultät III, November 2014, Saarbrücken, Germany

J. Juntke, N. Günday Türeli, N. Schneider C. de Souza Carvalhoz, EM Prinz, M. Schneider, and CM Lehr

Towards a new bacterial-epithelial cell co-culture model to test novel drug delivery systems against Pseudomonas aeruginosa biofilms

4th HIPS Symposium, June 2014, Saarbrücken, Germany

J. Juntke, N. Daum, C. Carvalho, CM Lehr

Establishment of an in vitro model for lung diseases using a cystic fibrosis cell line infected with Pseudomonas aeruginosa

3rd HIPS Symposium, July 2013, Saarbrücken, Germany

Curriculum vitae

Personal details

Name:	Jenny Juntke
Date of birth:	08th August 1986
Place of birth:	Greiz
Nationality:	German

PhD Thesis

04/2013 — 11/2016   **PhD student at Helmholtz Institute for Pharmaceutical Research Saarland (HIPS); Institute for Biopharmacy and Pharmaceutical Technology**
Saarland University, Germany
Supervised by Prof. Dr. Claus-Michael Lehr

Education

05/2013 — now   Professional training as **Fachapotheker for Pharm. Technology**

04/2007 — 07/2012   **Study of Pharmacy and license to practice pharmacy**
Ernst-Moritz-Arndt University Greifswald, Germany

Diploma in the department of clinical pharmacy
Titel: „Untersuchungen zur regulatorischen Aktivität des Basispromotors des Transportproteins ABCC11"

08/1997 — 07/2005   **High school**
Johann-Heinrich-Pestalozzi Gymnasium Rodewisch, Germany

Work Experience

08/2017 — now   **Junior Formulation Scientist**
Fresenius Kabi Austria, Graz, Austria

05/2013 — 05/2017   **Pharmacist (part-time job)**
Saar-Apotheke im Kaufland St. Ingbert, Germany

04/2013 — 08/2015   **Teaching for pharmacy students**
Biopharmaceutics and Pharmaceutical Technology, Department of Pharmacy, Saarland University, Germany

08/2012 — 03/2013   **Pharmacist (full time job)**
Heilig-Geist-Apotheke and Cityplus Apotheke in Rosenheim, Germany

Danksagung – Acknowledgments

Danke Mädels! Die unzähligen gemütlichen Abende in unserer Küche bei einem Gläschen Wein fehlen mir schon manchmal.

Ein herzliches Dankeschön geht auch an meine Familie. Danke für euer Vertrauen in mich und eure Unterstützung und Motivation über all die Jahre die ich an der Uni zugebracht habe. Danke, dass ihr mich einfach meinen Weg habt gehen lassen und mir immer das Gefühl gegeben habt, egal was passiert, ihr steht hinter mir.

Thomas, es fehlen die Worte um zu beschreiben wie dankbar ich dir bin. Ohne dich würde es diese Seiten wahrscheinlich nicht geben. Du warst immer für mich da, hast mich unterstützt, mir den Rücken freigehalten und meine oft nicht so gute Laune während der Schreibphase ertragen. Deine Motivation und dein Glaube an mich, auch wenn ich zum x-ten Mal alles hinschmeißen wollte, bedeuten mir so viel. Ich bin so froh dich an meiner Seite zu haben und freue mich einfach nur wahnsinnig auf unsere gemeinsame Zukunft. Danke!!!